



# FRACTURE ANALYSIS of the EASTERN WARBURTON BASIN (Early Palaeozoic) South Australia

Compiled by

Xiaowen Sun

*National Centre for Petroleum Geology and Geophysics*

REPORT BOOK 99/00014

July 1999



**PRIMARY INDUSTRIES  
AND RESOURCES SA**



**Government  
of South Australia**

# CONTENTS

EXECUTIVE SUMMARY . . . . .	6
INTRODUCTION	
Fractured reservoirs . . . . .	6
Data and methods . . . . .	8
Constraints . . . . .	8
Stratigraphy and tectonic history . . . . .	8
FRACTURE CHARACTERISATION	
Identification and classification . . . . .	8
Fracture plane morphology and porosity . . . . .	9
Lithological control . . . . .	9
Associated structural features . . . . .	10
Chronology and fills . . . . .	13
CASE STUDY - FRACTURED RESERVOIR IN LYCOSA 1 . . . . .	15
FRACTURE MAPPING	
Orientation . . . . .	22
Core measurement . . . . .	22
Dipmeter and FMS log interpretation . . . . .	22
Absolute orientations . . . . .	26
Relative orientations . . . . .	31
Orientations of open and partially open fractures . . . . .	36
Fracture density . . . . .	36
DISCUSSION	
Major fracture types and orientation . . . . .	44
Origin of fractures . . . . .	45
Fracture fairway . . . . .	47
CONCLUSIONS AND RECOMMENDATIONS . . . . .	51
REFERENCES . . . . .	51
ACKNOWLEDGMENTS . . . . .	52
FIGURES	
Fig. 1 Cooper Basin well location map, showing studied wells including economic wells Lycosa 1, Sturt 6, 7 and Moolalla 1, and major structural trends. (99-0412) . . . . .	7
Fig. 2 Simplified stratigraphic column of the Warburton and Cooper Basins. (99-0413) . . . . .	8
Fig. 3 Petal fractures (induced) in sandstone from Dullingari 1, core 28, at 9669'2". (Photo 046695) . . . . .	9
Fig. 4 (a) Permian basal conglomerate above the Warburton Basin unconformity in Pelketa 1, 7093'10"–7094'. . . . .	10
(b) Detail of clasts containing pre-existing fractures within Warburton Basin siltstone and shale. (Photo 046696, 046697) . . . . .	10
Fig. 5 Core illustrating open and partially open fractures.	
(a) Core photo, showing open fractures connecting vuggy porosity in dolomite, Gidgealpa 5, 8118'. (Photo 046698) . . . . .	11
(b) Open fracture in ignimbrite from Boxwood 1, 6154.5'. (Photo 046699) . . . . .	11
(c) Core photo, showing open fracture (middle) and other filled fractures along normal microfaults, Gidgealpa 4, 7226'8-9". (Photo 046700). . . . .	11
(d) Open fracture in core, Meranji 2, 10920'. (Photo 046701) . . . . .	11
(e) Open fracture in core, Beanbush 1, 12130'6", showing fracture plane surface with very subtle mineral fill. (Photo 046702) . . . . .	12
(f) Open to completely, calcite filled fractures in Merrimelia 6, core 5, 7442'. (Photo 046703) . . . . .	12
(g) View of fracture plane, incompletely filled early with fine quartz crystals (transparent) and late coarse calcite crystals, Merrimelia 2, 9017'. (Photo 046704) . . . . .	12
(h) Remnant fracture porosity in Lycosa 1, at 8803', where matrix porosity of 6.2 per cent and permeability of 0.019 millidarcies were measured. (Photo 046705) . . . . .	12

Fig. 6	Cores illustrating deformed fractures	
	(a) Gouge filled fracture in fine-grained sandstone, showing gouge with clasts derived from fractured walls or surrounding sandstone Innamincka 1, 7199'. (Photo 046706)	13
	(b) Detail of slickensided fracture plane combined with calcite fill. Lycosa 1, 8802'. (Photo 046707)	13
Fig. 7	Mineral filled fractures	
	(a) Calcite filled fracture in Gidgealpa 2, core 9, 7275', showing a broken fracture plane. (Photo 046708)	14
	(b) Silica-filled fractures crossed orthogonally by short vertical fractures filled with ferroan carbonate. Pando 1, 5812'. (Photo 046709)	14
	(c) Cuttings thin section, showing pyrite filled fracture in siltstone, Lycosa 1, 8670-8680'. (Photo 046710)	14
	(d) Core photo, from Tilpatee A1, 7019', showing pyrite and quartz filled fractures. (Photo 046711)	14
	(e) Photomicrograph, showing siderite and kaolinite filled fracture in Daralingie 1, 7426', cross-polarised light. (Photo 046712)	14
Fig. 8	Vuggy fractures in Coonatie 1, core slab, 10400'6". (Photo 046713)	15
Fig. 9	Microfractures in thin sections.	
	(a) Vuggy dolomite from Gidgealpa 1, 12950', showing open microfracture connecting vuggy and intercrystalline pores. Plane light. (Photo 046714)	16
	(b) Incompletely filled fracture in Lycosa 1, 8798'. Plane light. Width of view 1.65 mm. (Photo 046715)	16
	(c) Open microfracture in Moolalla 1, 8600-8610'. Plane light. Width of view 1.65 mm. (Photo 046716)	16
	(d) Possible open fracture in Sturt 8, 6382.87'. Plane light. Width of view 1.65 mm. (Photo 046717)	16
	(e) Possible open fracture in Boxwood 1, 6160'. Plane light. Width of view 1.65 mm. (Photo 046718)	16
Fig. 10	Lithological control on fractures.	
	(a) At least three phases of fractures and fills in limestone, Gidgealpa 5, 7944'4"-7". (Photo 046719)	17
	(b) Numerous fractures and brecciation in quartz-arenite in Mudrangie 1. (Photo 046720)	17
	(c) In Pelketa 1, short conjugate fractures are more numerous in softer mudstone rather than siltstone layers. (Photo 046722)	17
	(d) Fractures in weathered mudstone and fresh siltstone and shale, Narcoonowie 1. (Photo 046723)	17
Fig. 11	Associated structural features.	
	(a) Microfold and numerous fractures in Wantana 1. (Photo 046724)	18
	(b) Microfold and associated cleavage in Dullingari 1, Width of view 36 mm.. (Photo 046725)	18
	(c) Thrust fault in Packsaddle 1. (Photo 046726)	18
	(d) Thrust fault in Gidgealpa 1. (Photo 046727)	18
	(e) Restoration of thrust fault in Gidgealpa 1, 12605.5'. (Photo 046728)	18
	(f) Reverse fault in Wantana 1, 9628', with 0.8-0.9 cm displacement. (Photo 046729)	19
	(g) Lycosa 1, a low-angle reverse fault displaced bedding at 8794'. (Photo 046730)	19
	(h) Coongie 1, micro-normal fault. (Photo 046731)	19
	(i) Gidgealpa 7, 9069', showing a fault zone breccia and associated gouge fill. (Photo 046732)	20
	(j) Gidgealpa 1, 11678', showing vertical stylolites. (Photo 046733)	20
	(k) Lycosa 1, 8793', showing an orthogonal set of fractures dipping towards SW (blue) and SE (red) respectively, the SW dipping fracture is still partially open. (Photo 046324)	20
	(l) Lycosa 1, showing a conjugate set of fractures with slickensides on fracture planes, one dips SE, the other dips N to NNW (similar to bedding), apparently SE fracture crosscut the latter at 8802'. (Photo 046734)	20
Fig. 12	Chronology of fractures and fills.	
	(a) Pyrite filled fracture has cut and displaced silica-filled fracture in Tilpatee A1, 7021.65'. (Photo 046735)	21

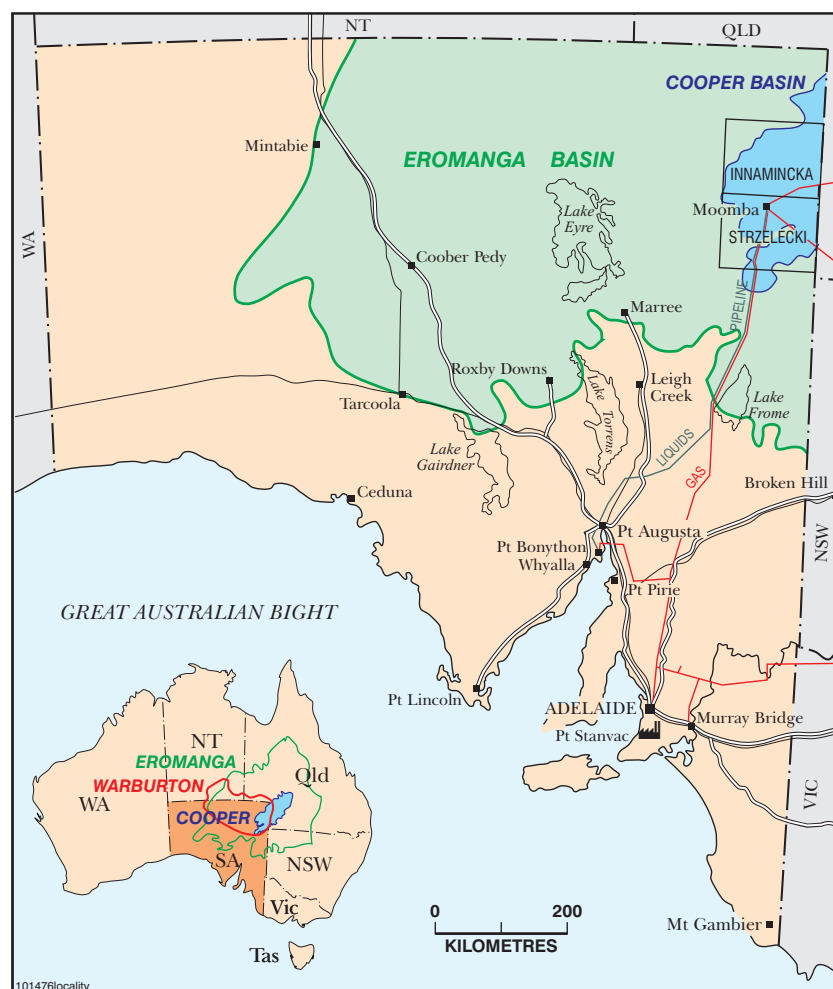
(b) Narcoonowie 1, core 2, 6542'5", showing crosscut relationship as marked by numbers in ascending chronology (I-IV). (Photo 046736) . . . . .	21
(c) Photomicrograph, Gidgealpa 7, 9062', showing calcite filled fracture and vertical stylolite crosscutting gouge-filled fracture. (Photo 046737) . . . . .	21
Fig. 13 Core 1, Lycosa 1, 8792-8814', showing main fractures on slab surface; fracture density is not even, and varies from low over the intervals 8799-8801' and 8807-8809'10", high to very high over the interval 8794-8797'. Density variations are marked to the left of the core intervals. . . . .	23
Fig. 14 Rose diagrams of fractures in core 1, Lycosa 1: (a) high angle fractures; (b) main fractures; (c) slickensided fractures and lineations; (d) fault planes and tension gashes. (e) FMS over interval of core 1, Lycosa 1 showing fractures (red and orange) interpreted by Schlumberger. Bedding is shown in green. (99-0486) . . . . .	24
Fig. 15 Stereographic projections of poles to and great circle for bedding, density and rose diagram of fractures measured from core 1, 8793', Lycosa 1. . . . .	25
Fig. 16 FMS (fracture analysis) in Lycosa 1, showing SW dipping open fractures (orange). . . . .	26
Fig. 17 Dipmeter in Lycosa 1. . . . .	27
Fig. 18 Composite log in Lycosa 1. . . . .	28
Fig. 19 Fracture orientations in cores, (a) circumferential surface in Innamincka 1, (b) right angle to core axis, Gidgealpa 3. (Photos 046738, 046739) . . . . .	29
Fig. 20 Strzelecki 3 dipmeter and core illustrations of angular unconformity between Toolachee Formation (Permian) and Dulligari Group (Ordovician). (Photo 046740) (99-0505) . . . . .	30
Fig. 21 Mudlalee 1 core, illustration of fracture sets. (Photo 046741) . . . . .	31
Fig. 22 Variation of fracture orientation with depth in Gidgealpa 1. (99-0408) . . . . .	32
Fig. 23 Map of Cooper Basin showing absolute orientations of strike directions. (99-0414) . . . . .	33
Fig. 24 Four groups of strike azimuths stand out from mean high angle fracture strike azimuths as shown in two histograms (n=45): (a) mean strike azimuths plot, with four average directions: 22°, 61°, 114°, 148°; (b) frequency of mean strike azimuths in four groups. (99-0415) . . . . .	34
Fig. 25 Map showing two sets of orthogonal fractures which are independent of local structure. (99-0504) . . . . .	35
Fig. 26 Map of Cooper Basin showing absolute orientations of dip azimuths. (99-0417) . . . . .	39
Fig. 27 Map of Cooper Basin showing those relative orientation data which fit within system I or II, or both orthogonal sets (possibility 1). (99-0418) . . . . .	40
Fig. 28 Map of Cooper Basin showing those relative orientation data which fit within system I or II, or both orthogonal sets (possibility 2). (99-0419) . . . . .	41
Fig. 29 Map of Cooper Basin showing combination of absolute and relative data (strike only). (99-0420) . . . . .	42
Fig. 30 Map of Cooper Basin showing absolute strike orientations of steep fractures (circled) to low frequency lineaments (LFL), NNE8, WNW9 and NE1 identified by Boucher (1998). (99-0421) . . . . .	43
Fig. 31 Core photo in Jennet 1, showing possible open fractures in brittle coarse sandstone. . . . .	44
Fig. 32 Core photo in Kalanna 1, showing high to very high grades of fracture density. . . . .	45
Fig. 33 Core photo in Titan 1, showing moderate grade of fracture density. . . . .	45
Fig. 34 Core photo in Meranji 2, showing low grade of fracture density. . . . .	47
Fig. 35 Core photo in Dunoon 1, showing nil grade of fracture density. . . . .	48
Fig. 36 Fracture density map of the Cooper Basin with main lithologies. (99-0422) . . . . .	49
Fig. 37 High angle fractures in Lycosa 1, including those interpreted from FMS (symbol +), (a) rose diagram, (b) lower hemisphere, stereographic projections of poles to, open fractures are within red circle and dip SW. (99-0423) . . . . .	50
Fig. 38 Well deviation plot – Palm Valley 6, 6a, 6b – showing location of drill breaks and cumulative gas flows. (from Aguilera, 1997). (99-0424) . . . . .	50

## TABLES

Table 1	Four generations of fracture fill in Tilpatee A1 (bedding arbitrarily north). . . . .	15
Table 2	Lycosa 1 directional and fill data for depth 8793'. . . . .	19
Table 3	Dipmeter, FMS fracture analysis with corresponding gas show and pay zone as shown on composite log. . . . .	22
Table 4	Dip and strike azimuths of fractures interpreted from dipmeters. . . . .	26
Table 5	Absolute orientations of mean strike direction of fractures, including those interpreted from FMS by Hillis et al., 1997 (*) and in (Rayner and Chin, 1990; Chin, 1991) ( <sup>1</sup> ) (o = open fractures, po = partially open fractures). . . . .	29
Table 6	Absolute dip azimuths and dip angles (e.g. 120/60) of steep fractures, including those interpreted from FMS by Hillis et al., 1997 (*) and in (Rayner and Chin, 1990; Chin, 1991) ( <sup>1</sup> ) . . . . .	31
Table 7	Strike orientations of fractures rotated in azimuth to fit within regional fracture systems . . . . .	36
Table 8	Case by case selection of more likely fracture strike orientation. . . . .	36
Table 9	Orientations, aperture, lithology of open and partially open fractures. . . . .	37
Table 10	Fracture density and main lithology from 91 studied wells.. . . .	37
Table 11	Fracture density change with depth in Merrimelia 2. Core recovery is 100%, except core 11 (92%) and cores 7, 15, 17 (85%). . . . .	38
Table 12	Orientations of fault-related tectonic fractures. . . . .	46

## APPENDICES (on 3.5" floppy disc included with this report)

- 1 Orientation data measured from cores.
- 2 Orientation data measured from cores in stereonet format. Part I. – Absolute orientations. Part II. – Relative orientations
- 3 Brief descriptions of fractures and associated data.
- 4 Selected mean strike azimuths from 23 wells.



Frontispiece: Locality map.

## EXECUTIVE SUMMARY

Cambro-Ordovician Warburton Basin strata and intrusive granites are conventionally regarded as economic basement beneath the Cooper-Eromanga oil and gas province in northeast South Australia and southwest Queensland. This study, the first of its kind, has identified and mapped a regional fracture system through upper levels of the Warburton Basin and because the fractures contain oil and gas from Cooper Basin source rocks, effective secondary hydrocarbon migration into fractured 'basement' traps is confirmed. Oil has flowed in commercial volumes from fractured Cambrian tuffs in Sturt 6 and 7, gas has been tested in Moolalla 1 and Lycosa 1 in Ordovician sandstone and fractured siltstone lithologies respectively (Baily, 1991a, Taylor *et al.*, 1991).

Considerable information has been gathered from a detailed core study of 91 wells in conjunction with the use of dipmeters, formation micro-scanner (FMS) logs from 27 wells. Absolute orientation data are obtained from measurements of cores and logs from 23 wells and additional relative orientation data are collected from 24 wells. Two systems of orthogonal fracture sets have been identified for the first time across local structures, and extend beneath the Cooper Basin in South Australia. System I has a pair of orthogonal fractures, striking NNE-SSW (20-200°) and ESE-WNW (110-290°). This system is similar in direction to low frequency lineaments NNE8 and WNW9 (Boucher, 1998b). System II has a pair of orthogonal fracture sets, striking NE-SW (60-240°) and NW-SE (150-330°). The NE-SW strike orientation is similar to lineament NE1 (Boucher, 1998b). Open fractures in Lycosa 1 have azimuths striking WNW and NW within systems I and II, and dip SW. Open, steeply dipping SW fractures are interpreted from FMS in the production zone over the interval 8653-8670 feet, and incompletely filled fractures are observed in core 1. Open fractures striking NNE and NW are interpreted from FMS in Malgoona 4. Based on data from Lycosa 1, Gidgealpa 5 and Tilpatee A1, system I is possibly younger than system II. The results indicate that an optimum well trajectory designed to maximise intersection with open natural fractures should be 200-210° and 240-250°, and possibly 270-290°. The deviation angle should be approximately 30° from horizontal in the fracture zone due to the high angle and subvertical fracture dips.

A semi-quantitative estimate of fracture density has been determined for 91 wells and summarised in the form of an interpretive map. The greatest fracture density is located in major fault zones or structural culminations as expected. Generally speaking, fractures are mainly developed within brittle rather than ductile rock types if they are frequently interbedded. Open fractures or incompletely filled fractures are associated with brittle dolomite such as in Gidgealpa 1, 5, 7, and also in brittle sandstones such as in Beanbush 1, Meranji 2, Jennet 1, Merrimelia 6, 7, or brittle ignimbrite and tuffaceous sandstone such as in Boxwood 1, Gidgealpa 4, and Sturt 7, 8. These fractures are mostly at a high angle. Microfractures have been found and are believed to connect secondary porosity in ignimbrite of Sturt 7, 8. Fracture fairways exist in brittle sandstone, dolomite and volcanics, and any rock types with the above suggested orientations of the two systems of orthogonal fracture sets.

## INTRODUCTION

### Fractured reservoirs

The eastern Warburton Basin unconformably underlies the Cooper and Eromanga Basins in northern South Australia. Since the discovery of gas in Gidgealpa 2 in the Cooper Basin in 1963, the Warburton Basin has been regarded as economic basement and thus not explored seriously. Its Early Palaeozoic age, limited drilling, poor seismic data below thick Permian coal beds, and tectonic deformation make the Warburton Basin a high-risk exploration target. Although, to now, more than 600 wells have partly intersected the Warburton Basin, most of them are "ratholes" with less than 40 m of penetration. Four wells (gas in Lycosa 1 and Moolalla 1, and oil in Sturt 6 and 7) (Fig. 1) have produced commercial volumes of hydrocarbons which are considered to have migrated from Cooper Basin source rocks (Taylor *et al.*, 1991). The reservoir rocks comprise: fractured siltstone (Lycosa 1), sandstone and siltstone with fracture-enhanced matrix porosity (Moolalla 1), and tuff with fracture porosity (Sturt 6 and 7) (Taylor *et al.*, 1991). The fractured siltstone in Lycosa 1 has a maximum gas flow of 5.0 MMCFD (million cubic feet per day) (0.14 Mm<sup>3</sup>/d), while the fracture enhanced sandstone reservoir in Moolalla 1 has maximum gas flow of 9.6 MMCFD (0.27 Mm<sup>3</sup>/d) (Taylor *et al.*, 1991).

The fractured tuff flowed at a rate of 1250 BOPD in Sturt 6 (Baily, 1991b). In Sturt 7, a small oil recovery from DST 4 (17.8 bbls oil + 0.7 bbls oil cut mud) demonstrated that the fractured volcanics contain oil (Nugent, 1991) and the well was subsequently completed using artificial lift. These Warburton Basin reservoirs are likely related to fractures or in fault contact with mature Permian source rocks. The relatively high porosity but very low permeability values in Warburton Basin sandstone, volcanics and dolomite (Taylor *et al.*, 1991; ACS Laboratories report in Sun and Gravestock, 1999) highlight the importance of having open fractures to connect the pore spaces.

This is the first detailed study of fracture systems in Warburton Basin cores. It aims to characterise fractured reservoirs and to delineate fracture patterns in order to predict the orientation of open fractures and thus potential reservoirs. A similar study has been carried out in the Palm Valley gas field (Berry *et al.*, 1996 and references therein), where fracture analysis was based on study of outcrops, several unoriented cores and one oriented core. Palm Valley is a relatively simple anticline, and bedding dip angles are low. However, the Warburton Basin is orders of magnitude larger, lacks outcrop and has a large number of predominantly random cores. With a range of dips, commonly exceeding 30°, a major task is to determine the orientations of bedding, fractures and other vector properties based on integration of a minimal amount of directional data.

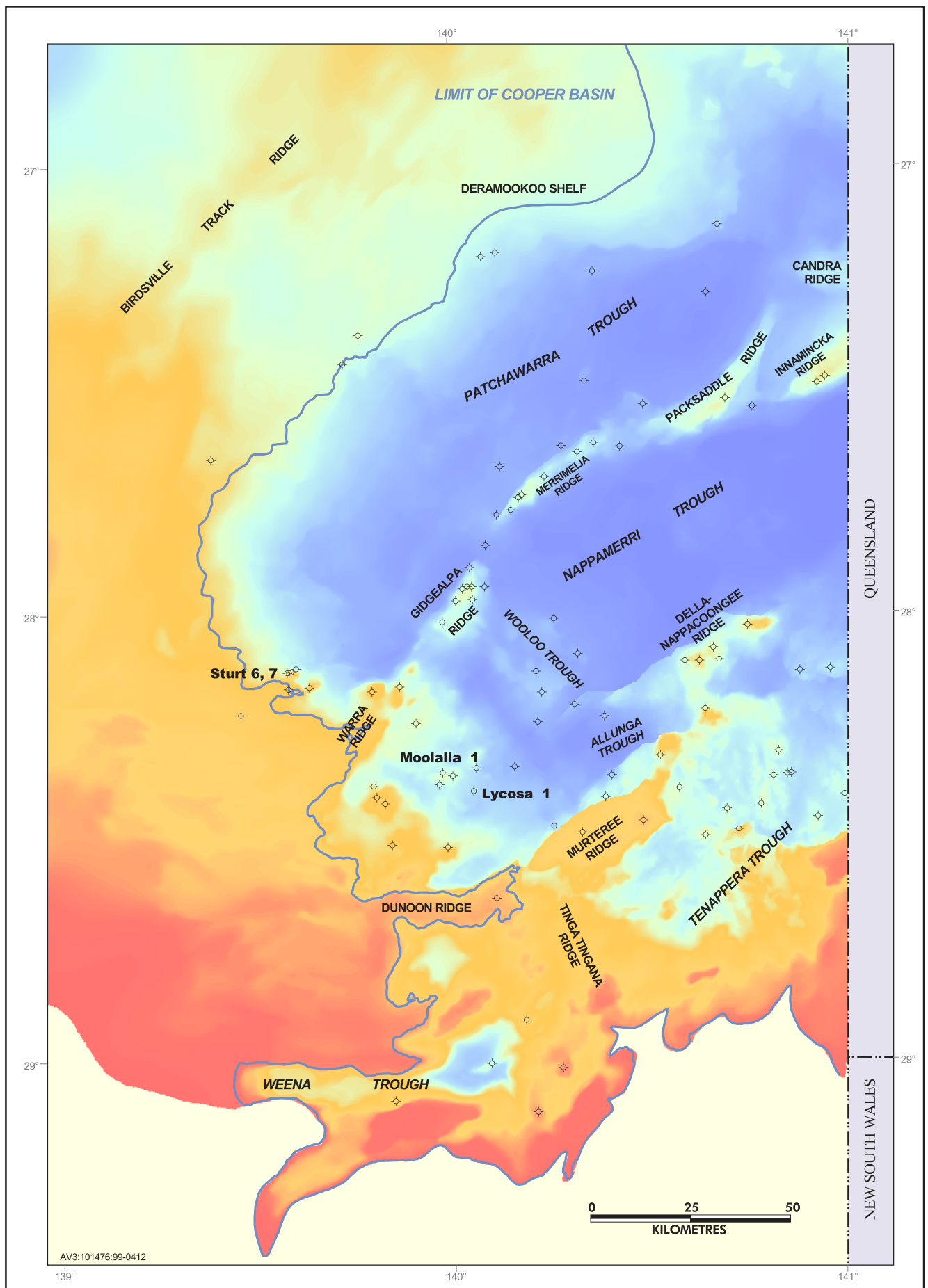


**Fig. 1** Well location map, showing studied wells including economic wells Lycosa 1, Sturt 6, 7 and Moolalla 1, and major structural trends.

## Data and methods

The study concentrates on the eastern Warburton Basin underlying the Cooper Basin (STRZELECKI and INNAMINCKA 1:250 000 map sheets).

Fractures in cores provide relative spatial information on fracture development. About 199 cores from 93 wells, which cover more than 98% of cores in the basin, have been studied in detail (Fig. 1). After washing and scrubbing cores clean, I have measured orientations of structural attributes particularly fractures and fault planes from cores. This stage of work resulted in about 135 measured orientation values at different depths from 22 oriented wells and 24 unoriented wells (Appendix 1, 2). The remaining wells studied have only core slabs, in most cases there are only 1/3 or less of the original core left. For these wells, I recorded fracture dip angles, types, chronology and fills (Appendix 3). 80% of the cores examined have been video recorded, and various kinds of fractures and fault planes have been photographed. In this study, I exclude granite (Big Lake Suite) intersected in wells such as McLeod 1, Moomba 1, and some metamorphic rocks of Willyama Supergroup, such as those cored in Mulga 1. Depths used in this study are in feet, normally KB driller depths.

## Constraints

There are many wells with dipmeters recorded over Warburton Basin intervals, but in many cases, there are only unprocessed logs available at PIRSA, thus only 23 interpreted dipmeters are used for this study. Most of these dipmeter logs are old (pre-1980), cannot pick high angle data, and some are not suitable for meaningful interpretation due to random orientations of dip azimuths.

No azimuth data of deviated drilling axes are recorded in the studied Warburton Basin wells except Lycosa 1, although younger wells mostly after 1992 have azimuth data of deviation. Therefore, correction for deviation can be done only in Lycosa 1. Fortunately, most deviation angles are less than 5 degrees except Dullingari 1 (max. 32°), Merrimelia 2 (max. 10°) and Lycosa 1 (max. 17.9°). This error is not significant considering error in measurements by hand. Most strikes and dips calculated from seismic surveys are from the overlying Cooper Basin, rather than the Warburton Basin. In most cases, bedding dips change dramatically between the Warburton Basin and the overlying Cooper Basin. This reduces the accuracy of interpretation of bedding dip azimuth from seismic data. Lacking dipmeters, the orientations of open fractures from Gidgealpa 4, Meranji 4 and Jennet 1 have been assumed relatively or by considering the bedding dips of the adjacent wells or the regional fracture patterns.

## Stratigraphy and tectonic history

The Cambro-Ordovician Warburton Basin unconformably underlies the Cooper and Eromanga Basins. Stratigraphy of the Warburton Basin has been discussed in Sun (1996, 1998), and is simplified in Fig. 2 which also shows the overlying Cooper Basin. The Warburton Basin has a complex tectonic history, which is largely speculative owing to a lack of reliable data and detailed study. Early work interpreted thrust fault-repeated sections in the Gidgealpa area (Daily, 1964; Carroll, 1990) and also in the

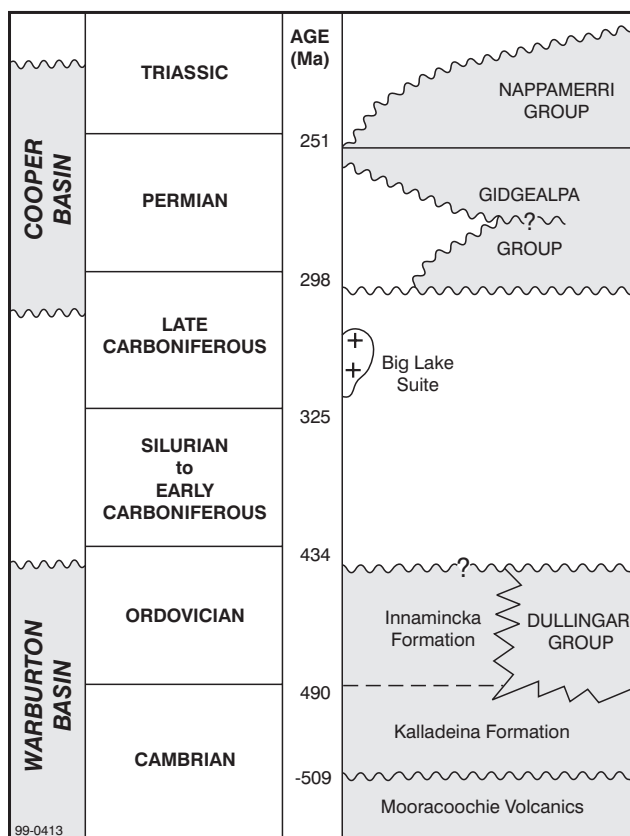


**Fig. 2** Simplified stratigraphic column of the Warburton and Cooper Basins

Merrimelia, Wantana, Packsaddle and Innamincka areas (Sun, 1996, 1997), indicating a convergent tectonic regime. Compression has been attributed to several orogenic movements: Benambran Orogeny (Gatehouse, 1986), a late stage of the Delamerian Orogeny (arc setting of Roberts *et al.*, 1990), and the much younger Alice Springs Orogeny (Gravestock and Flint, 1995).

Using seismic sequence stratigraphic and biostratigraphic data, Sun (1996, 1997) has demonstrated mild compressive NW-SE fault reactivation as young as early Mesozoic in the Packsaddle area, while other seismic interpretations (e.g. Kuang, 1985), suggest Mesozoic wrench fault activity and Tertiary east-west compression. Wopfner (1985) suggested that a general state of compression existed during the Permian and early Triassic, and in the late Cretaceous and Tertiary.

## FRACTURE CHARACTERISATION

### Identification and classification

This report discusses only natural fractures and excludes those induced by drilling, coring and handling. It is the most difficult task to distinguish natural fractures from induced fractures when both types are open in cores. A comprehensive review of the physical characteristics of natural and induced fractures and how to distinguish them have been discussed by Kulander *et al.* (1990). One kind of induced fracture is petal fractures that have been observed in Coonatie 1, and Dullingari 1 (Fig. 3).

Numerous natural fractures have been identified from cores, wireline logs, and from indirect evidence during drilling. Poor core recovery and broken pieces in cores 25-29 in Gidgealpa 1 and core 16 in Gidgealpa 7 imply the presence of highly fractured zones in both wells. In Coongie 1, minor losses of drilling fluid may be caused by fractures or a breccia at 11150-11304', which is permeable but contains salt water (Pemberton, 1970). In Toolachee 51, a gas anomaly was encountered 34' into Warburton Basin siltstone, which was interpreted as a fractured zone that was also responsible for constant mud losses. DST 1 tested this zone, but flowed gas at a rate too small to measure, the gas peak over the zone was 600U (85/12/3/tr) (Ostler, 1996). In Gahnia 1, gas peaks of 60-320 units were recorded from siltstone of the Warburton Basin, which was assumed to be related to fracturing (Baily, 1996). In Cherri 1, cycle skipping on sonic over 4569-79' was suggested to indicate fracturing (Pexa Oil N.L., 1970).

A geological classification of natural fractures has been suggested by Nelson (1985), and is followed herein.

1. tectonic fractures – associated with local tectonic events.
2. regional fractures – developed over large areas of the earth's crust with relatively little change in orientation, show no evidence of offset across the fracture plane, and always perpendicular to major bedding surfaces.
3. contractional fractures – tension or extension fractures resulting from a general bulk volume reduction through the rock.
4. surface-related fractures – developed during unloading, release of stored stress and strain, creation of free surfaces or unsupported boundaries and weathering in general.

Basically, most fractures examined in this study are either tectonic or regional except a few possible contractional fractures in rhyodacite in Gidgealpa 2, 3 and 11, and numerous fractures in basalt from Murteree A1. Here, I have concentrated on tectonic and regional fractures, which most likely contribute to the generation of fracture porosity.



**Fig. 3** Petal fractures (induced) in sandstone from Dullingari 1, core 28, at 9669'2". (Photo 046695)

Generally speaking, the majority of studied natural fractures are only observed in Warburton Basin strata, in other words, they were caused by pre-Cooper Basin events. In several wells including Pelketa 1 (Fig. 4), Big Lake 52 and Gidgealpa 8, angular clasts with pre-existing and filled-fractures from Warburton Basin strata were redeposited in basal conglomerates of the immediately overlying Cooper Basin succession. Few fractures have been observed in the overlying Cooper Basin strata in most of the studied wells except Gidgealpa 5 in which vertical joints have been recorded in the Merrimelia Formation.

However, natural fractures do exist in the immediately overlying Cooper Basin strata though they do not commonly propagate above the Permian Tirrawarra Sandstone. An exception is in the Telopea field where Triassic sedimentary rocks overlie the Mooracoochie Volcanics of the Warburton Basin directly, and have been fractured. From FMS data, Hillis *et al.* (1997) interpreted natural fractures from the lower Patchawarra Formation and the Big Lake Suite of Moomba 73.

## Fracture plane morphology and porosity

According to Nelson (1985, p.29), morphology of the fracture planes is an important attribute of fracture porosity and permeability. Four basic types of natural fracture plane morphology include:

1. open fractures,
2. deformed fractures: (a) gouge-filled fractures, (b) slickensided fractures,
3. mineral-filled fractures,
4. vuggy fractures.

These four basic types are all present, and some representatives are illustrated in Figs. 5-8. Porosity and permeability in the studied wells mainly exist in open fractures, partially open fractures or incompletely mineral-filled, slickensided, and rarely vuggy fractures.

Moolalla 1, Sturt 6 and Lycosa 1 exhibit fracture porosity, but no porosity values (as functions of the computed aperture (fracture width), Schlumberger, 1997) have been computed. Cuttings thin sections of these wells show some microfractures, but cuttings generally break along rather than across open fractures. Various microfractures are found in these and other wells, and are illustrated mainly from core samples in Figure 9.

## Lithological control

Mechanically, different rock materials react to stress differently. In more brittle rocks such as dolomite and quartz-arenite, fractures are more irregular and intensive. Examples include well fractured dolomite in Gidgealpa 5 (Fig. 5a), fractured limestone (bioclastic wackestone and packstone) (Fig. 10a), severely fractured quartz-arenite in Mudrangie 1 (Fig. 10b), and ignimbrite in Sturt 7, 8 (Nugent, 1991). In softer rock such as mudstone and shale, as in Pelketa 1, short conjugate fractures are better developed in mudstone than siltstone layers (Fig. 10c). Weathered mudstone has irregular and short fractures, in contrast to fresh siltstone and shale which have long and regular fractures, as shown in Narcoonowie 1 (Fig. 10d). Mudstone in the altered zone at the top of the Warburton Basin (Boucher, 1998a) may thus form a top seal to fractures in the underlying fresh sequence (Gravestock *et al.*, 1998).

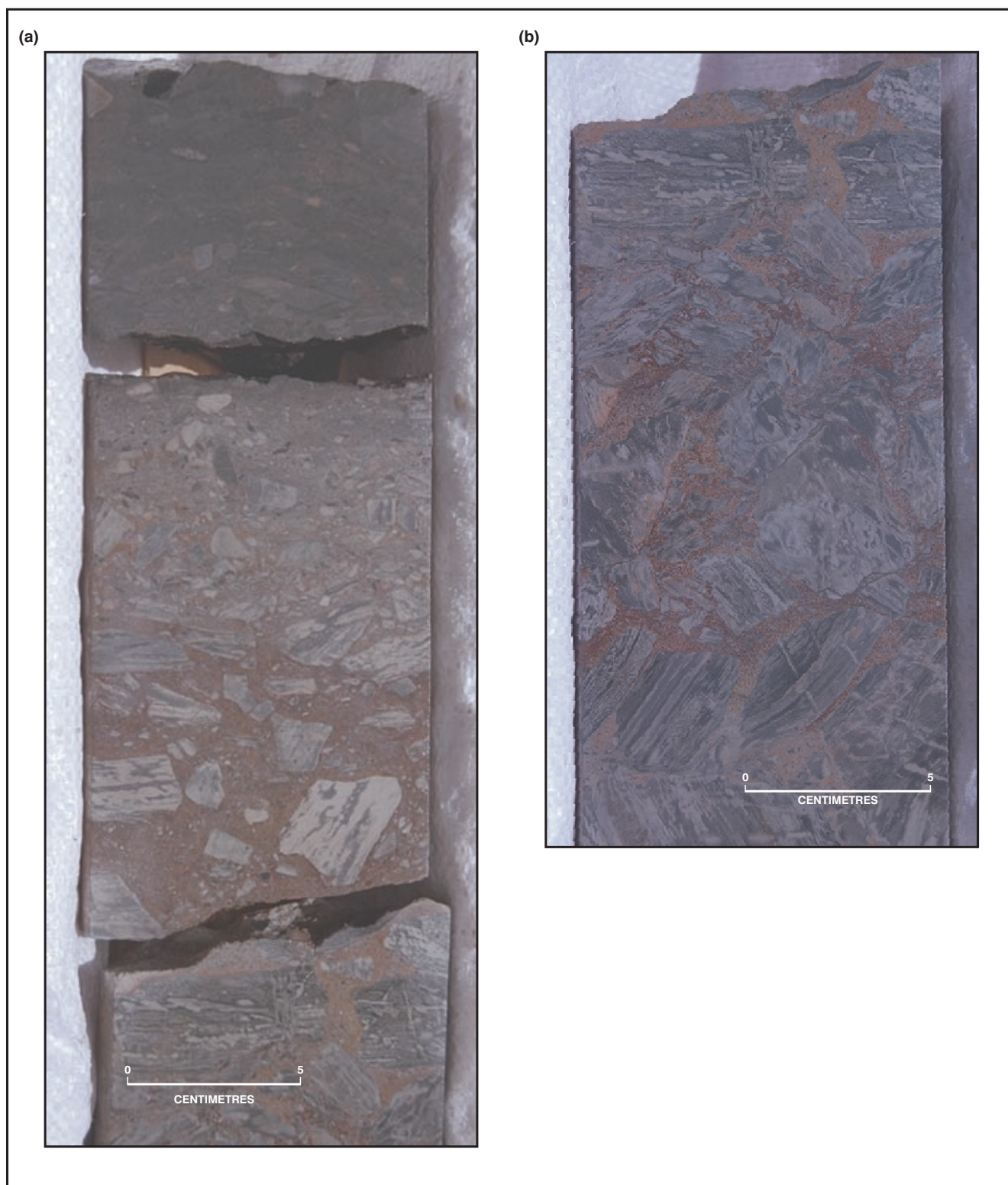


**Fig. 4** (a) Permian basal conglomerate above the Warburton Basin unconformity in Pelketa 1, 7093'10''–7094'.  
 (b) Detail of clasts containing pre-existing fractures within Warburton Basin siltstone and shale. (Photo 046696, 046697)

### Associated structural features

Many microstructures are observed in the studied cores. There are few normal microfaults whereas folds, reverse and thrust faults are common (Appendix 3), indicating deformation in a compressive tectonic regime. Most are unoriented and orientations of slickenside surfaces, lineations and fault planes can only be determined in a small number of wells with dipmeters. These structures are described briefly.

### Folds

Microfolds are observed in several cores in Warburton wells, such as in Wantana 1. A microfold is associated with numerous short fractures (Fig.11a). In Dullingari 1, cleavage is developed along an axial plane, and some subparallel fractures also occur (Fig. 11b).



**Fig. 5** (a) Core photo, showing open fractures connecting vuggy porosity in dolomite, Gidgealpa 5, 8118'.  
 (b) Open fracture in ignimbrite from Boxwood 1, 6154.5'.  
 (c) Core photo, showing open fracture and other filled fractures along normal microfaults, Gidgealpa 4, 7226'8-9".  
 (d) Open fracture in core, Meranji 2, 10920'. (Photo 046698, 046699, 046700 and 046701).

### Thrust faults

Thrust faults are observed in Packsaddle 1, (Fig. 11c). There is a thrust fault plane at 12605' in Gidgealpa 1 (Fig. 11d), at an angle of about 35°, and its azimuth is similar to that of the bedding plane, which is 67° (NE). Restoration across the fault is illustrated in Figure 11e.

### Reverse faults

A reverse fault is observed in cored *Nuia*-rich limestone in Wantana 1 (Fig. 11f), and has less than 1 cm displacement. There is a reverse fault dipping about 65° to the core axis in Boxwood 1 at 6154.5' (Fig. 5b), but its azimuth is not certain as there is no definite bedding in ignimbrite. In *Lycosa* 1, a low-angle fault has displaced bedding at 8794' in a reverse mode (Fig. 11g).

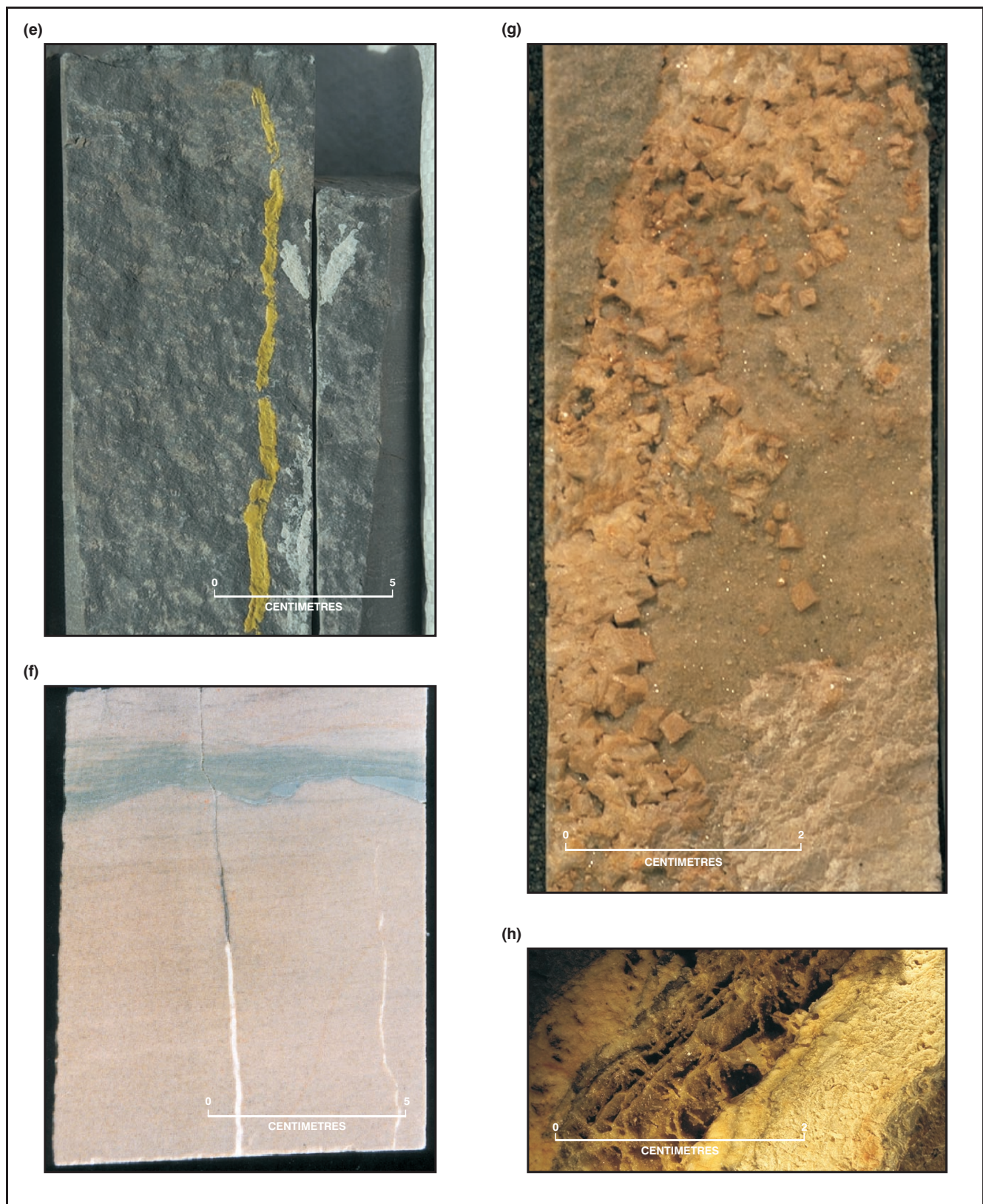


**Fig. 5** (e) Open fracture in core, Beanbush 1, 12130'6", showing fracture plane surface with very subtle mineral fill.  
 (f) Open to completely, calcite filled fractures in Merrimelia 6, core 5, 7442'.  
 (g) View of fracture plane, incompletely filled early with fine quartz crystals (transparent) and late coarse calcite crystals, Merrimelia 2, 9017'.  
 (h) Remnant fracture porosity in Lycosa 1, at 8803', where matrix porosity of 6.2 per cent and permeability of 0.019 millidarcies were measured. (Photo 046702, 046703, 046704 and 046705)

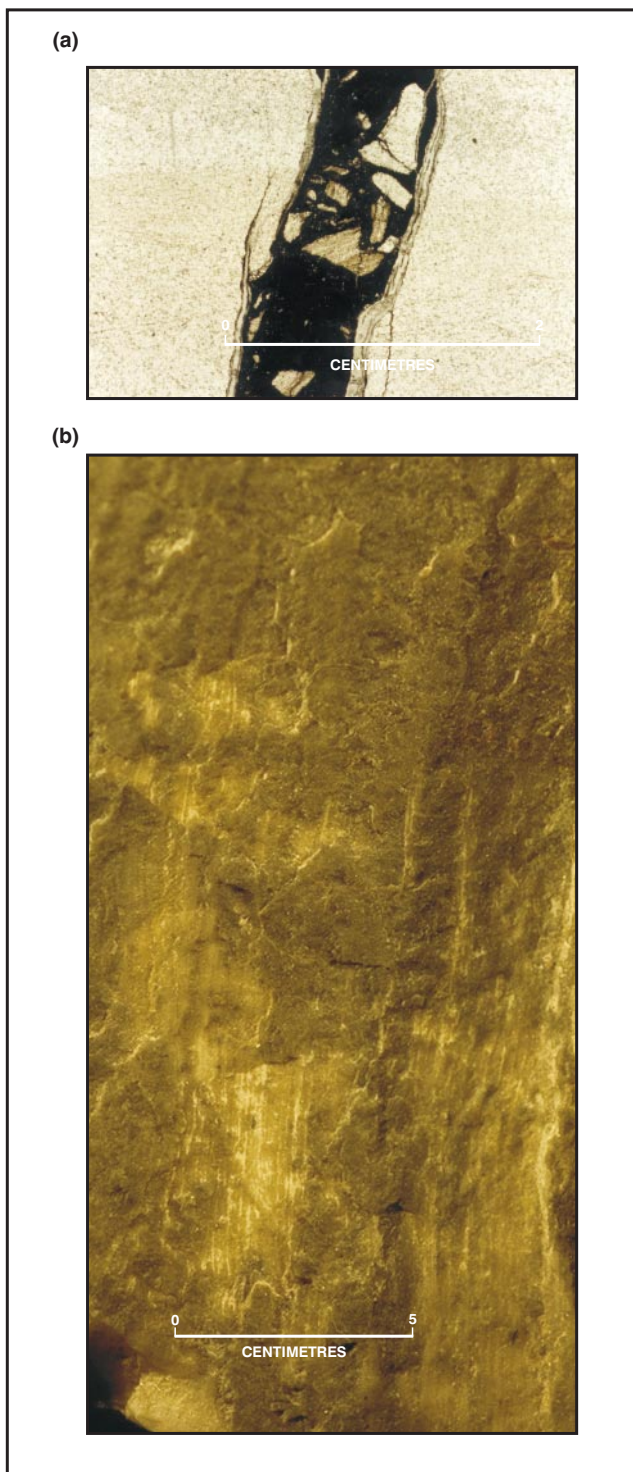


**Fig. 6** (a) Gouge filled fracture in fine-grained sandstone, showing gouge with clasts derived from fractured walls or surrounding sandstone Innamincka 1, 7199'. (b) Detail of slickensided fracture plane combined with calcite fill. Lycosa 1, 8802'. (Photo 046706, 046707)

## Normal faults

A normal microfault in Gidgealpa 4 (Fig. 5c), is open and partially open. In Coongie 1, normal microfaults are found in thin section, and fractures have been filled with calcite (Fig. 11h).

## Fault zone, gouge fill, shale smear

There is a major fault zone and associated gouge fill in limestone of Gidgealpa 7 (Fig. 11i). Carroll (1990) interpreted a thrust fault in this well but below this depth. There is another major fault zones and associated gouge fill in volcanics of Gidgealpa 8. Relatively smaller-scaled fault zones associated with little cataclasis and shale smear have been found in several wells such as Boxwood 1, Murteree 1 and Snake Hole 1 (Appendix 3).

## Slickensides

Many slickensides are observed along bedding, fracture or fault planes. Those along fault planes have good lineations indicating movement of faults. In wells Lycosa 1, Gidgealpa 1, Snake Hole 1, Pelketa 1, slickenside surfaces are mainly SE dipping. Slickenside lineation is predominantly SE-NW, and subordinately NE-SW, such as in Lycosa 1 (Figs. 6b; 11l).

## Stylolites

There are basically two kinds of stylolites; one is the common horizontal type due to burial compaction from loading, the other is vertical such as in Gidgealpa 1 (Fig. 11j) due to lateral compressional stress. Most of the stylolites are found in limestone rocks, seldom in siliciclastics, which is unusual since a number of sandstones in the overlying Cooper Basin do possess stylolites.

## Conjugate fractures

Conjugate fractures are common, such as observed in cores of Nappacoongee 1, Lycosa 1 (Fig. 11l), Mudlalee 1, Tinga Tingana 1, Pelketa and Wantana 1. They have also been interpreted from dipmeters of Mudlalee 1, 2, Coochilara 1 and Strzelecki 3.

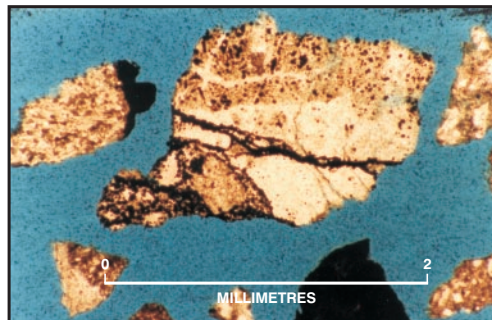
## Chronology and fills

Chronology of fractures and fracture fills in each individual well is determined by crosscut relationships and recorded in Appendix 3. Although limited coring and intersection of fractures prevent positive fracture chronology determined by crosscutting of fractures in most wells, two general patterns are recognised: (1) High angle, fine fractures cross-cut low angle fault planes associated with fault breccia. They possibly also postdate high angle coarse fractures filled with calcite such as in Lycosa 1 and Gidgealpa 5. (2) At least four phases of fracture fill are found in several wells. Typical examples are in Murteree 1 and Tilpatee A1 (Fig. 12a), Narcoonowie 1 (Fig. 12b), Gidgealpa 5 (Fig. 10a) and Gidgealpa 7 (Fig. 12c). Tilpatee A1 is a typical example. Tilpatee A1, particularly measured in core 3, 7019' 1" has the following relative orientation data (Table 1): (1) Fine fracture or joint, with dip angle of 85-90°, and dipping to the NW (300° dip azimuth); (2) fault plane, with dip angle of 60°, parallel to bedding (arbitrarily assigned to the north); (3) with dip angle of 70-90°, dipping SW (240°); (4) with dip angle of 60-80°, and dipping to the SE (140°). Table 1 also shows four generations of fracture and vein systems in ascending order.

(a)



(c)



(b)



(d)



(e)

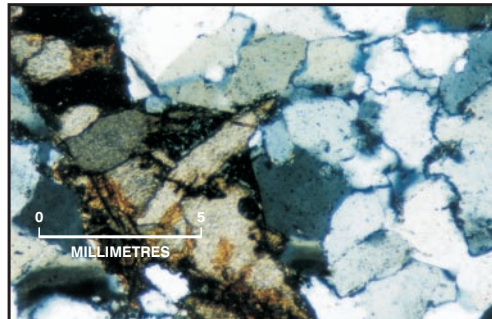


**Fig. 7** (a) Calcite filled fracture in Gidgealpa 2, core 9, 7275', showing a broken fracture plane.  
(b) Silica-filled fractures crossed orthogonally by short vertical fractures filled with ferroan carbonate. Pando 1, 5812'.  
(c) Cuttings thin section, showing pyrite filled fracture in siltstone, Lycosa 1, 8670-8680'.  
(d) Core photo, from Tilpatee A1, 7019', showing pyrite and quartz filled fractures.  
(e) Photomicrograph, showing siderite and kaolinite filled fracture in Daralingie 1, 7426', cross-polarised light.  
(Photo 046708, 046709, 046710, 046711 and 046712)



**Fig. 8** Vuggy fractures in Coonatie 1, core slab, 10400'6".  
(Photo 046713)

**Table 1** Four generations of fracture fill in Tilpatee A1 (bedding arbitrarily north).

Type	Dip azimuth angle	Dip angle	Colour code	Comments	Generation (ascending)	Fills
bedding	0	60-70	green	bedding, against folding	-	-
frac (1)	300	85-90	blue	high angle, fracture	1	quartz
frac (2)	0	60	yellow	parallel to bedding, ? fault plane	2	quartz
frac (3)	240	70-90	brown	vein 2 (1-2 mm)	3	pyrite, quartz
frac (4)	140	60-80	black	vein 1, (1-8 mm) associated with slickensides	4	quartz, pyrite

The four generations of fracture fill and mineralogy is more or less consistent with the fracture fill phases recognised by Rezaee (1997). He studied fracture filling cements of core samples from 5 wells by analysing their petrography, electron microprobe, fluid inclusions and oxygen and carbon stable isotopes. He deduced that the fracture fill phases in ascending order are: quartz in the form of chalcedony, pyrite, mega-quartz, siderite and ankerite, and kaolinite. However, he did not come across calcite and dolomite cement in his data. Rezaee (1997) also concluded, quite incorrectly in the face of evidence to the contrary, that the Warburton Basin 'cannot be a fractured reservoir'. Phillips (1997) found that the carbonate spar and dusty micrite postdate kaolinite in Narcoonowie 1. Calcite and dolomite fracture filling cements occur in many other wells especially in the region where the Kalladeina Formation subcrops, basically extending from the eastern flank of the Birdsville Track Ridge to the eastern flank of GMI Ridge. For example, subvertical fractures filled with calcite are common in various rock types in Coongie 1, (as only middle slabs of cores are available in Coongie 1, the orientations of these fractures cannot be determined). Low angle fractures filled with calcite are also observed in Daer 1 and other

wells. At least four phases of calcite fill can be observed in Gidgealpa 5 (Fig. 10a) in ascending order: (1) coarse calcite vein fill (1cm width max.) and minor gouge fill, dip angle 65°, (2) fine (1-3mm max.), filled with calcite, 65°, surrounded by stylolite, (3) fine fracture (1mm), filled with calcite, steep to subvertical, 60°-85°, (4) slickenside fracture surface, undulating, slightly steeper than bedding.

## CASE STUDY - FRACTURED RESERVOIR IN LYCOSA 1

Three drillstem tests in Lycosa 1 had some decline in flow with a maximum rate of 5.0 MMCFD (0.14 Mm<sup>3</sup>/d) (Baily, 1990a; Taylor *et al.*, 1991). Mean porosity calculated from the neutron-density log is 3-4 per cent within the pay zones. These indicate that Lycosa 1 has the behaviour of a fractured reservoir. The aim is to understand which fractures contributed in producing gas.

Among the Warburton Basin discovery wells, only Lycosa 1 has a relatively complete data set including dipmeter, FMS logs, and 6.7 m core (core 1, 8792-8814') which was cut immediately below the gross pay zone. A comprehensive account of this well is provided by Taylor *et al.* (1991). However, a detailed fracture study via integration of core and logs is given here. The composite log is shown on Figure 18.

### Core data

At least five types of fracture have been measured in core 1, as listed below and can be more or less seen in core slabs (Fig. 13).

1. high angle, 78-80°, SE dipping, at 8793': dip azimuth 115-120°, hairline width, filled with calcite. At 8810', the fracture has displaced bedding plane slightly, and is associated with tension gashes and slickensides. At 8802', it is associated with slickensides as well, after being filled with calcite.
2. high angle, 60-70°, SW dipping, at 8793': dip azimuth 217-240°, hairline width, partially filled by calcite, and possibly partially filled with brown clay (?drilling mud) and white quartz at 8794';
3. Low angle fractures dipping south, displaced bedding, thus could be part of a fault system; they have similar azimuths to mineralisation and brecciated zone over the intervals of 8795-8796', and other common low angle calcite filled fractures.
4. High angle veins, up to 25 mm calcite fill at 8802'6"-8803'5", and possibly the same cement in a veinlet at 8798' (2-5 mm), more or less parallel to bedding.
5. Some nearly vertical fractures filled by calcite, curved (changing dip direction) at 8803'5" (SE), 8806-8807' (SW).

All fractures measured from, Lycosa 1 (Fig. 13) are divided into three groups and illustrated in stereonet and rose plots (Fig. 14) including (1) high angle fractures; (2) slickensided fractures; (3) other structure-related fractures. The dip azimuths and dip angles of major fractures, bedding and fault plane (after being corrected for deviation) fractures are summarised in Table 2 for the depth 8793' and illustrated in Fig. 11k and Fig. 15. They have not been picked via FMS data over the cored interval by Schlumberger (Fig. 14e).

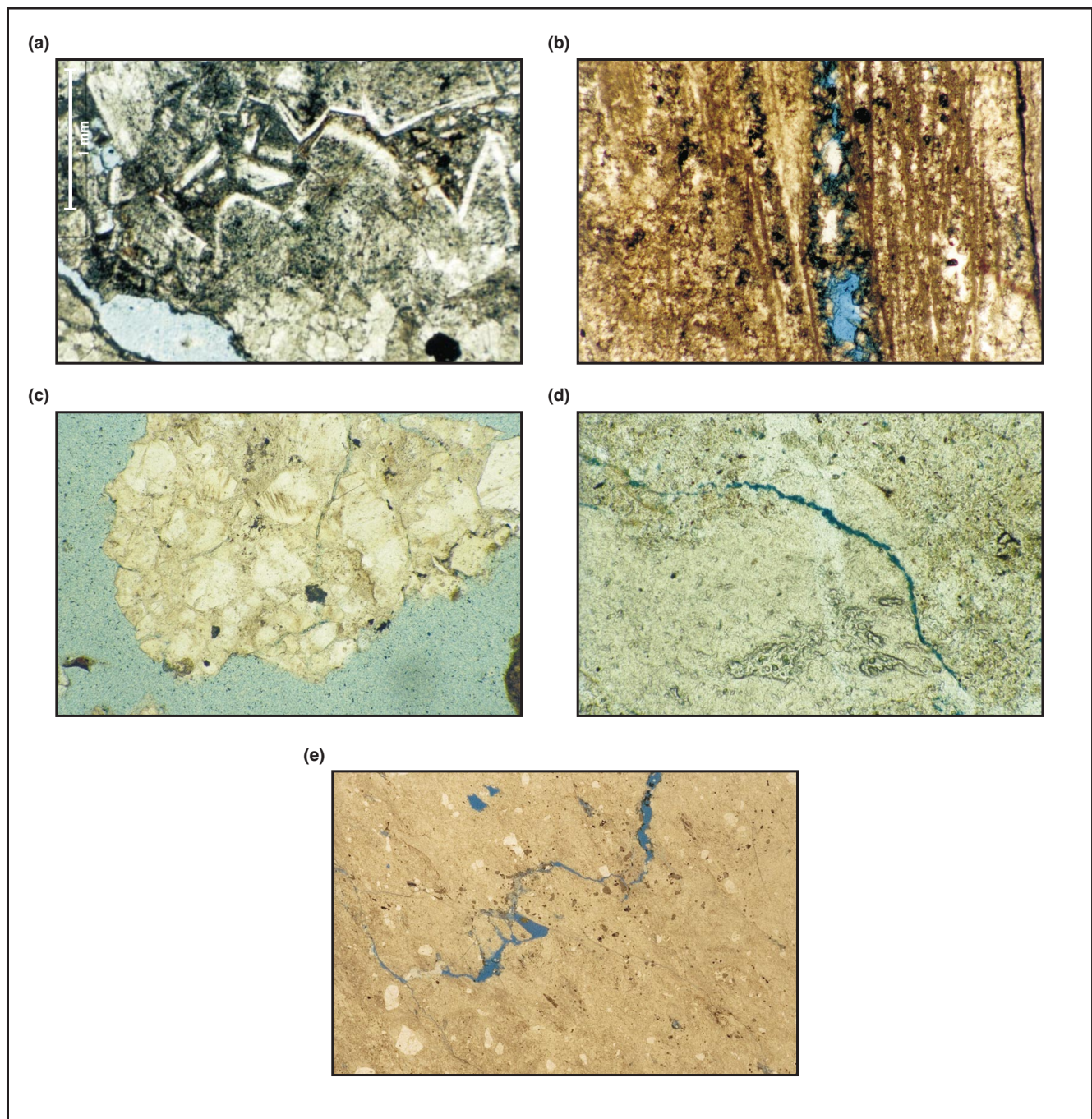


**Fig 9** (a) Vuggy dolomite from Gidgealpa 1, 12950', showing open microfracture connecting vuggy and intercrystalline pores. Plane light. (b) Incompletely filled fracture in Lycosa 1, 8798'. Plane light. Width of view 1.65 mm. (c) Open microfracture in Moolalla 1, 8600-8610'. Plane light. Width of view 1.65 mm. (d) Possible open fracture in Sturt 8, 6382.87'. Plane light. Width of view 1.65 mm. (e) Possible open fracture in Boxwood 1, 6160'. Plane light. Width of view 1.65 mm. (Photo 046714, 046715, 046717, 046716 and 046718)

## Chronology of fractures and fills

Four generations (I-IV) of fracture systems are recognised. First, as mentioned in Table 2, high angle fractures (SE and SW dipping) cross-cut the fault plane at 8793' and 8794'. Second, a high angle fracture (NNW dipping, subparallel to bedding, filled by calcite) has offset fault plane at 8798' and 8803'. Therefore, fault plane fracture is earlier than the latter two fractures. No direct crosscut relationship of the two later fractures can be observed. Movement on the NNW dipping fracture is evidenced by having a slickensided surface at 8803'. At

8802', a SE dipping slickensided fracture seems to crosscut a NNW dipping slickensided fracture (Fig. 111; Fig. 13).

Thus, at least four generations can be determined: (1) relatively low angle fault plane, associated with mineralised zone and breccia, (2) calcite-filled fracture subparallel to the bedding (NNE dip), (3) slickenside surface developed on the fracture orientation ranging from NNE to NNW, (4) SE dipping slickensided fracture. The high angle fractures (SE and SW dipping) therefore occur between generation 1 and 4.

Since high angle fractures (SE and SW dipping) belong to the system I orthogonal fracture set whereas SE and NW slickenside fractures belong to system II orthogonal fracture

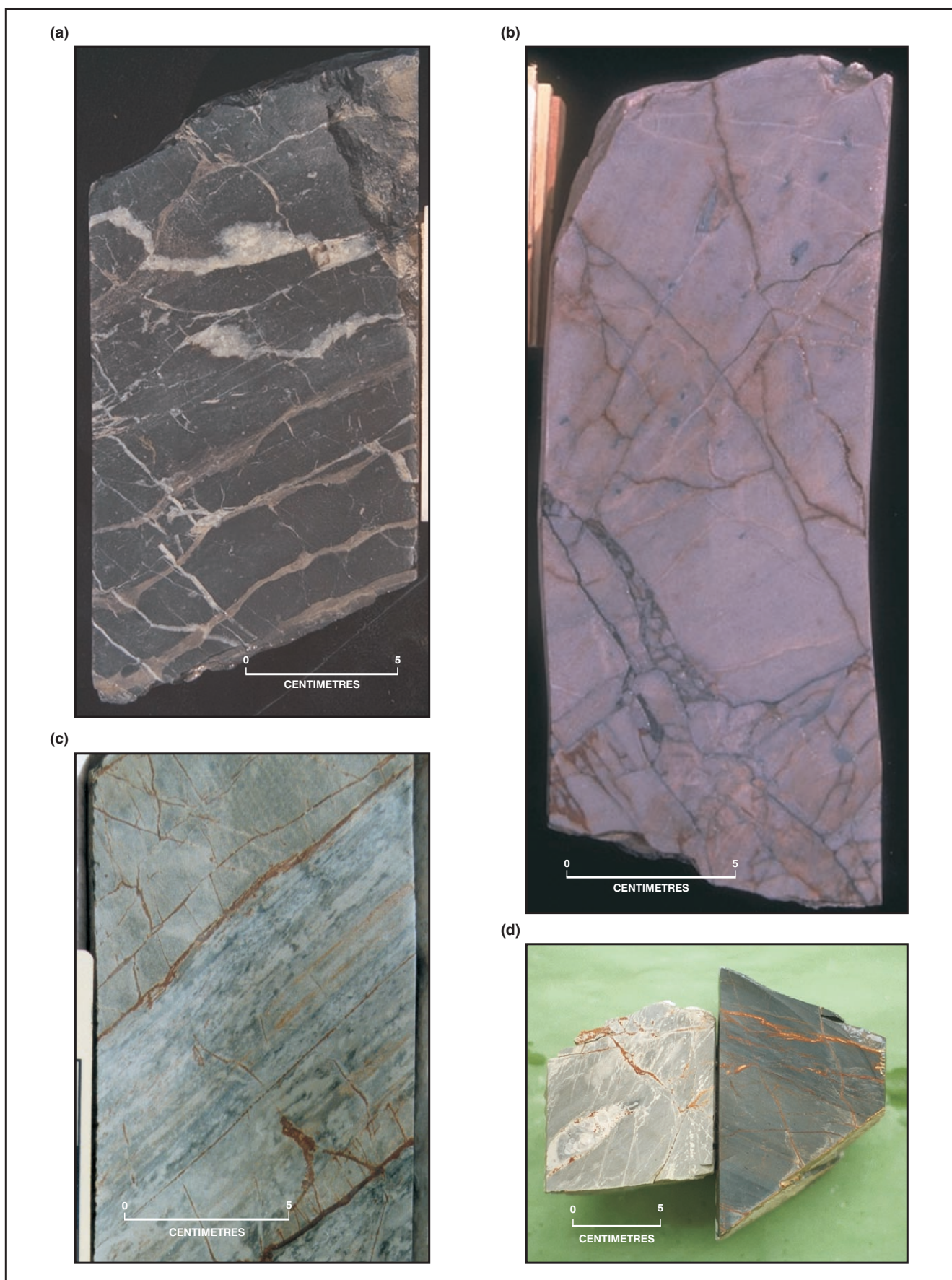


**Fig. 10** (a) At least three phases of fractures and fills in limestone, Gidgealpa 5, 7944'4"-7".  
 (b) Numerous fractures and brecciation in quartz-arenite in Mudrangie 1.  
 (c) In Pelketa 1, short conjugate fractures are more numerous in softer mudstone rather than siltstone layers.  
 (d) Fractures in weathered mudstone and fresh siltstone and shale, Narcoonowie 1. (Photo 046719, 046720, 046722 and 046723)

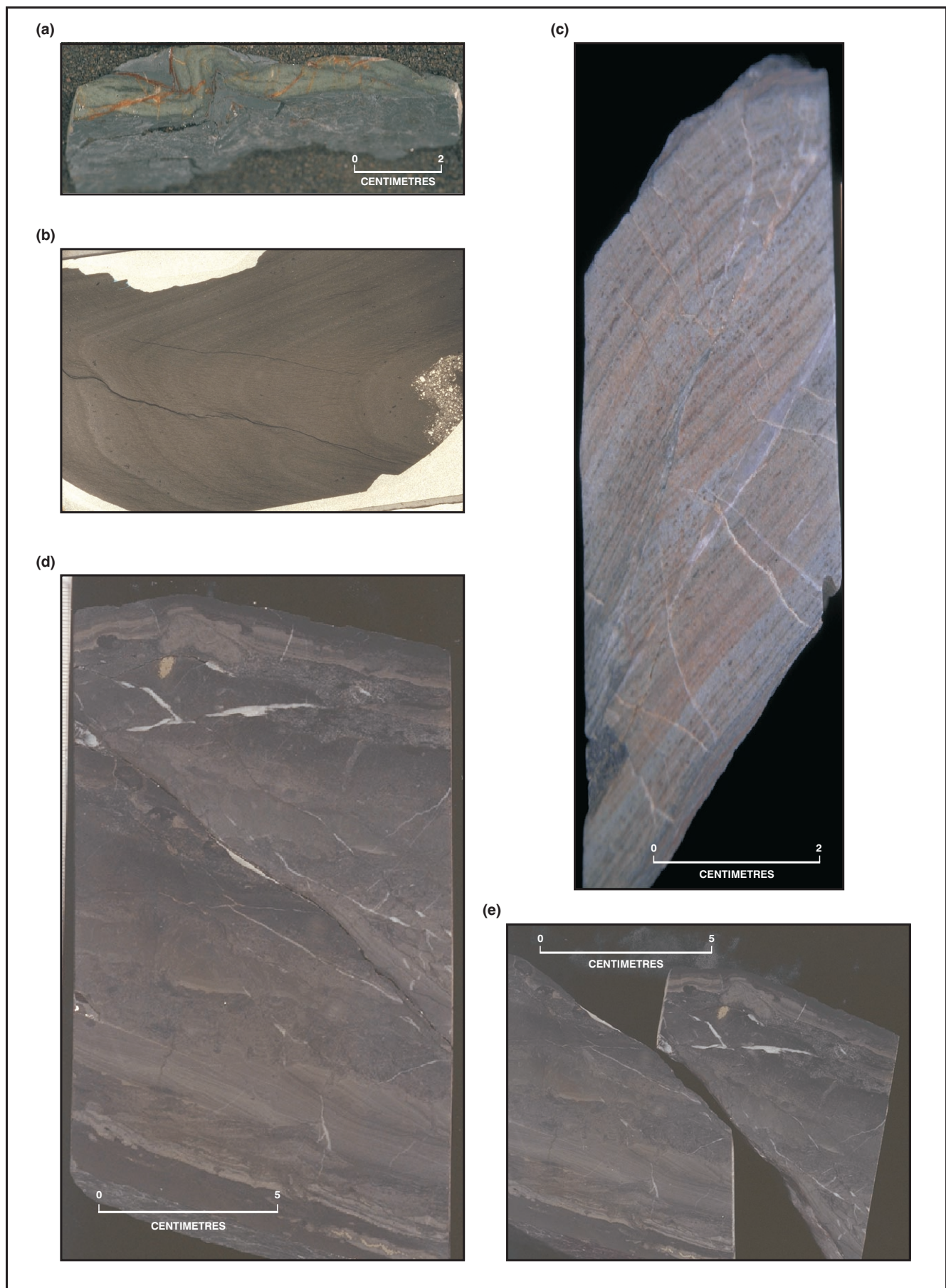
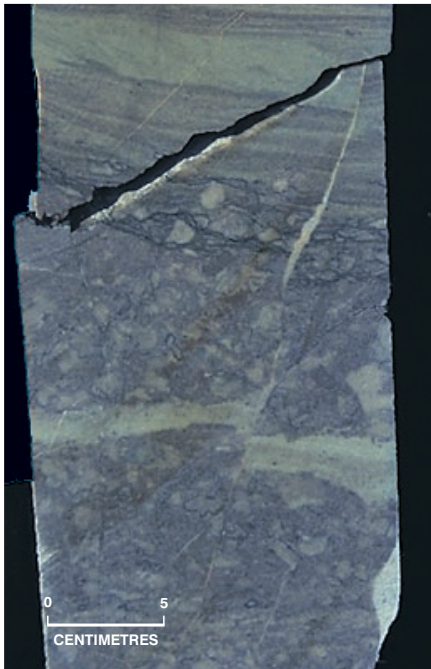


**Fig. 11** (a) Microfold and numerous fractures in Wantana 1.  
 (b) Microfold and associated cleavage in Dullingari 1, width of view 36 mm.  
 (c) Thrust fault in Packsaddle 1.  
 (d) Thrust fault in Gidgealpa 1.  
 (e) Restoration of thrust fault in Gidgealpa 1, 12605.5'. (Photo 046724, 046725, 046726, 046727 and 046728)

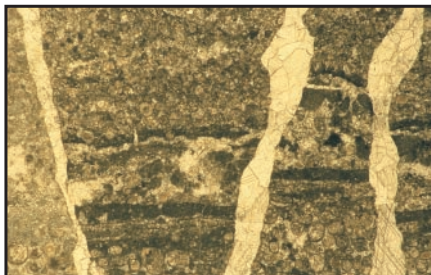
(f)



(g)



(h)

**Table 2** *Lycosa 1 directional and fill data for depth 8793'.*

Type	Dip azimuth	Dip angle	Colour code	Comments	Generation (ascending)	Fills
bedding	328.3°	20.8°	green	bedding		-
frac (1)	194.5°	81.5°	blue	high angle fracture	2	partially calcite
frac (1)	96.3°	82.7°	orange	high angle fracture	2	calcite
frac (2)	197.0°	79.2°	orange	high angle fracture	2	partially calcite
frac (1)	215.4°	76.4°	blue	high angle fracture	2	partially calcite
frac (2)	101.1°	84.0°	orange	high angle fracture	2	calcite
frac (3)	171.0°	20.3°	red	opposite bedding, fault plane	1	?dolomite

set, it is important to know which fracture set occurred first. Because the NW-SW oriented slickenside lineation is more dominant than others, the SE dipping slickensided fracture plane is interpreted to be the younger event.

### Formation Micro Scanner (FMS) interpretation

Rayner and Chin (1990) have interpreted FMS images from Lycosa 1. A total of 47 fractures were identified in the logged interval which is 8549' to 8850', with moderate scatter (Rayner and Chin, 1990, Figure 2), dominated by azimuths: 14°, 163°, 214°, 270-289°. Compared with the fractures interpreted from FMS over the cored interval in Lycosa 1, my measurements have much higher resolution, recognising SW fractures which they did not. Rayner and Chin pointed out that "The shear energy profile [from the array sonic log] indicates that the fractures over the interval 8670 – 8651' extend away from the borehole and have the most potential for production". Although SW dipping fractures such as over the interval 8650-8662' (Fig. 16) were interpreted by Rayner and Chin as having a low confidence in interpretation because the microresistivity effect may be related to conductive minerals rather than open fractures, they concluded that most of these fractures are open and dip steeply towards the southwest. The average dip azimuth over this interval is similar to the high angle SW dipping, partially open fracture observed in core at depth 8793' (Table 2, Fig. 15). I have added representative, high-angle fractures interpreted from FMS to those measured from cores, and they are plotted on a stereonet. As can be seen, the open fractures dip SW (Fig. 37).

### Dipmeter interpretation

I interpreted only the MSD 4 ft x 2 ft – 35 degree x 2 which is a non-optimum option (Fig. 17), bad for detection of high angle dips. As a result, dip azimuth is right, but dip angle value is usually too low. Most dip azimuths range

**Fig. 11** (f) *Reverse fault in Wantana 1, 9628', with 8-9 mm displacement.*  
 (g) *Lycosa 1, a low-angle reverse fault displaced bedding at 8794'.*  
 (h) *Coongie 1, micro-normal fault.*  
 (Photo 046729, 046730 and 046731)

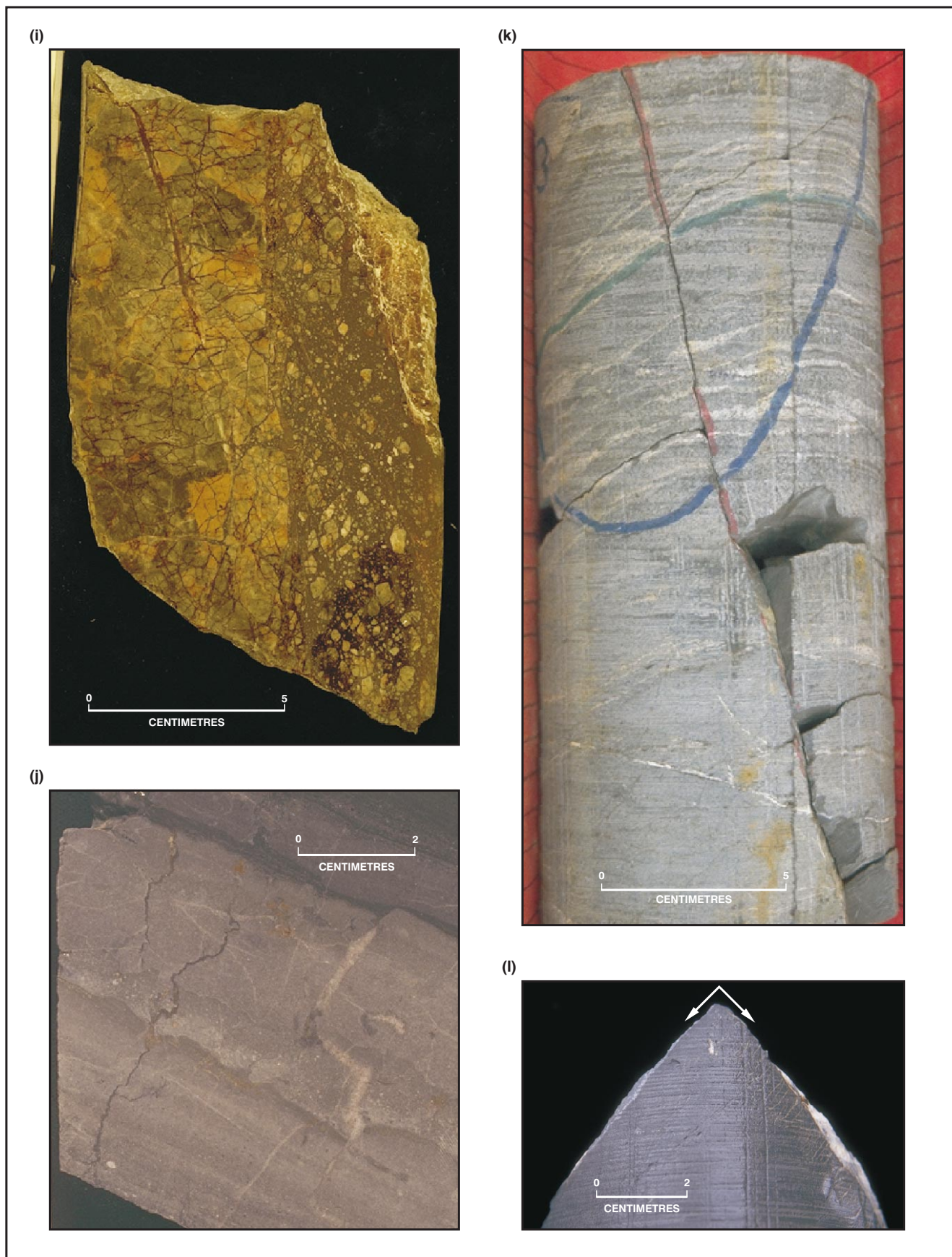


**Fig. 11** (i) Gidgealpa 7, 9069', showing a fault zone breccia and associated gouge fill.  
 (j) Gidgealpa 1, 11678', showing vertical stylolites.  
 (k) Lycosa 1, 8793', showing an orthogonal set of fractures dipping towards SW (blue) and SE (red) respectively, the SW dipping fracture is still partially open.  
 (l) Lycosa 1, showing a conjugate set of fractures with slickensides on fracture planes, one dips SE, the other dips N to NNW (similar to bedding), apparently SE fracture crosscut the latter at 8802'. (Photo 046732, 046733, 046324 and 046734)

from N (0°) to NNE (18°), dip angles range from 34° to 60° over the interval 8330 to 8940', except 8840-70': NNE (30°), dip angle 65-70°.

All the dipmeter recordings are listed in Table 3 and compared with FMS interpretation against corresponding gas shows and log calculated or test calculated pay.

## Slickensides

Several slickensides are observed in core 1, at 8803', 8810', 8813' and 8814' (Figs. 14, 15). Slickensides are also observed in cuttings samples which display calcite mineralisation over intervals with relatively low gamma values. Vague slickensides occur on the subhorizontal fracture just above 8797'.

## Fracture density

Spacing between fractures along the core axis is not even, varying from 2.5 to 15 cm (Fig. 13). Very high fracture density (greater than 10 fractures per inch) occurs over the interval 8794-8796', in which numerous filled fractures are associated with cataclasis zone containing metallic and ore minerals (e.g. galena, Taylor *et al.*, 1991).

## Creation of porosity

Open fractures (Figs. 9b; 11k), fracture surfaces parallel to slickensides (Fig. 6b), and remnant pores due to incomplete fill of original open fractures (Fig. 5h) all contribute to fracture porosity. Vuggy porosity, which more or less relates to calcite dissolution generated along cleavage of calcite crystals is also observed (Fig. 11k). Several calcite-rich intervals recognised by their low gamma log values, correspond to high gas shows, e.g. the intervals 8650-8666' and 8682-8680' with two gas peaks (Fig. 18). This indicates the possibility that calcite-rich intervals have better reservoir quality either due to incompletely filled pores or secondary dissolution. Alternatively, they correspond to open fractures due to parallel reactivation or slickensided after calcite fill such as in the interval 8650-60', where SW dipping open fractures dominate. Open space parallel to slickenside surfaces may be generated during several reactivation events of compressional tectonism. The dominant NW-SE orientation of the slickenside lineation further supports this assumption.

## Fractures which contribute to production

Most fractures in core 1 are filled by calcite, dolomite or clay, this is why no gas was circulated over the interval. Only one partially open fracture is measured from core 1 at 8793', and dips steeply SW. This category of fracture may

**Fig. 12** (a) Pyrite filled fracture has cut and displaced silica-filled fracture in Tilpatee A1, 7021.65'.  
 (b) Narcoonowie 1, core 2, 6542'5", showing crosscut relationship as marked by numbers in ascending chronology (I-IV).  
 (c) Photomicrograph, Gidgealpa 7, 9062', showing calcite filled fracture and vertical stylolite crosscutting gouge-filled fracture.  
 (Photo 046735, 046736 and 046737)

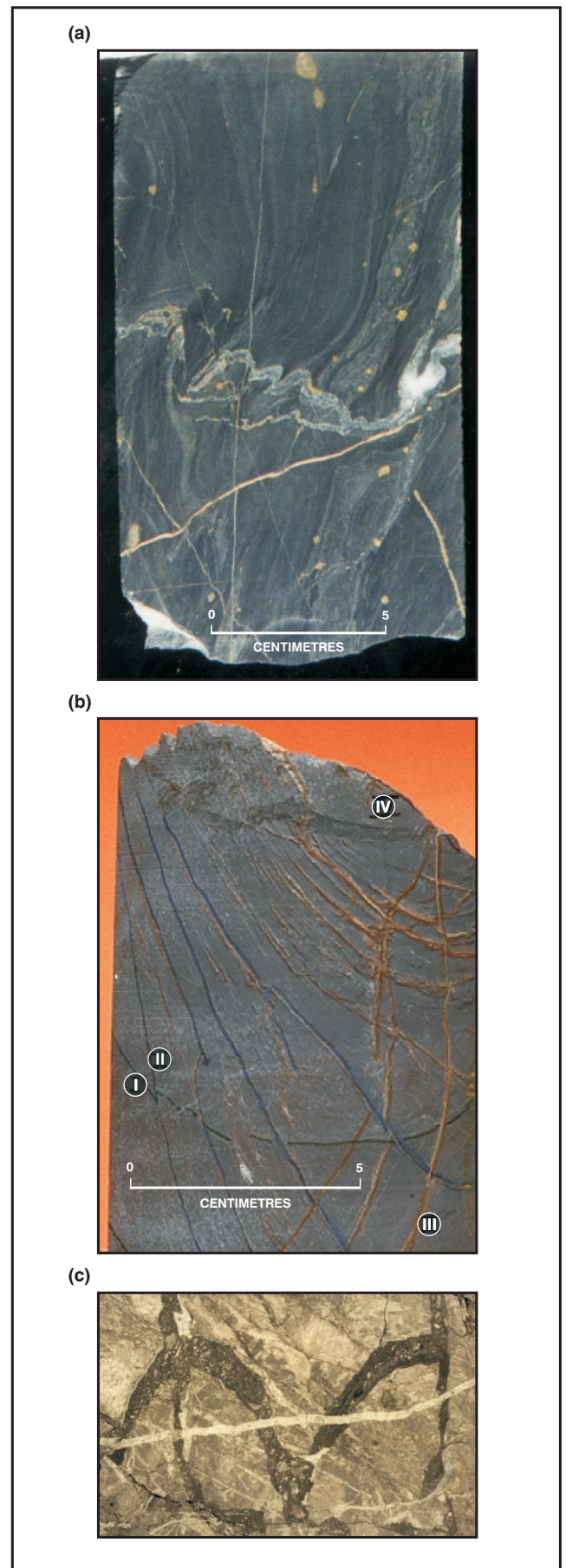


**Table 3** Dipmeter, FMS fracture analysis with corresponding gas show and pay zone as shown on composite log.

Depth (feet)	Azimuth (dipmeter)	Dip angle	Interpretation confidence	FMS depth (feet)	Gas show depth (feet)	Pay zone net pay (feet)
8300-01	S (181)	8°	Not good (NG)		8314	No pay
8318	SW (240)	6°	NG		8345-6	
8470	NW (336)	6°	NG			
8484	SW (202)	4°	NG			
8525	SW (210)	18°	G (Good)		8500, 8514	8514-8594: 17.5 Net pay
8560	NW (300)	34°	G			
8562	W (270)	32°	G	8562: near vertical, open fracture in NW and SE sectors. 8578: low planarity, open fracture in SE and NW.	8572	
8600	NW (330)	30°	G			8594-8610: 1.5 Net pay
8605	SE (120)	2°	G		8602-06	8610-8634: 0.5 net pay
8606	SE (160)	1°	G	8611-8661: SW dipping fractures.		
8653	SW (260)	38°	NG	8653-8670: SW dipping open fracture (WCR)		8634-8672: 30.5 net pay
8663	E-ENE (73)	30°	NG	8657: W dipping fracture low confid.		
8670	SW (240)	20°	NG	8678.5: healed fracture	8688-8689	
8786	SE (157)	36°	NSG	8710: mineralised, non-planar fracture In S and W sectors. 8732: mineralised fracture 8734: numerous small fracture in SW sector. 8779: sub-ver., open fracture in E sector. 8792: sub-ver. open fracture in N sector.	8729, 8732-34; 8740	8672-8800: 59.0 net pay
8805	NW (330)	18°	G	8831: south dipping mineralised fractures. 8839: NNE dipping bed.	8784 no gas circulated below 8800'	
8910	NW (345)	64°	NG			
8918	NW (333)	47°	NG			
8936	NW (348)	56°	G			

contribute to production. Supporting evidence comes from the FMS, where this fracture type dominates the interval 8622 to 8661' within which there is a good gas show (Rayner and Chin, 1990). Fractures steeply dipping SE may be a conjugate set because they have similar dipping angles and fracture apertures and also either partially or completely filled by calcite (Fig. 111). However, I am not sure why dip angles of the SW dipping fractures observed in core 1 are above 75°, being much higher angle than those recorded by either dipmeter or from FMS interpretation (Rayner and Chin, 1990), and despite correction for hole deviation.

In conclusion, detailed measurements of fractures in core 1 of Lycosa 1 and FMS interpretation indicate open or partially open fractures tend to be high angle and SW dipping. Rayner and Chin (1990) also pointed out that the shear energy profile indicates that the fractures over the interval 8670 – 8653' extend away from the borehole and have the most potential for production. With similar dip azimuths, slickensided fractures associated with pre-existing calcite fill also contribute to production. Taylor *et al.* (1991) interpreted faults dipping SW and NE from seismic sections, and these faults were propagated into the overlying Permian Patchawarra Formation. If their interpretation is right, these faults including SW dipping fractures have been reactivated in the Permian and may re-open older fractures.

## FRACTURE MAPPING

### Orientation

#### Core measurement

I have measured dips of bedding planes, fractures and fault planes from cylindrical surfaces of cleaned, normally facing cores by using a flexible ruler. Azimuths of dips were measured from a face cut perpendicular to core axis by tracing their strikes in plan view (Fig. 19a, b). If a vertical fracture occurred (90°), I recorded its strike azimuth. I initially arbitrarily assumed bedding dip to north, with other fractures measured relative to the bedding. If there is no bedding plane such as in volcanics and weathered mudstone, I used a predominant fracture to north. I entered these orientation data into a StereoNett program created by Dr Johannes Duyster in Germany. After determination of orientations of bedding planes from dipmeters, I rotated bedding planes or predominant fractures with similar dip angle as recorded in dipmeter, and others into corrected orientations. A lower hemisphere stereonet projection has been used.

#### Dipmeter and FMS log interpretation

There are 33 wells with both dipmeters and cores within Warburton Basin intervals, but only 23 wells have both full-diameter cores for measurement and available



**Fig. 13** Core 1, Lycosa 1, 8792-8814', showing main fractures on slab surface; fracture density is not even, and varies from low over the intervals 8799-8801' and 8807-8809'10", high to very high over the interval 8794-8797'. Density variations are marked to the left of the core intervals.

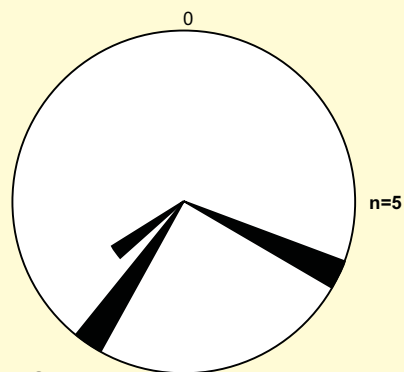
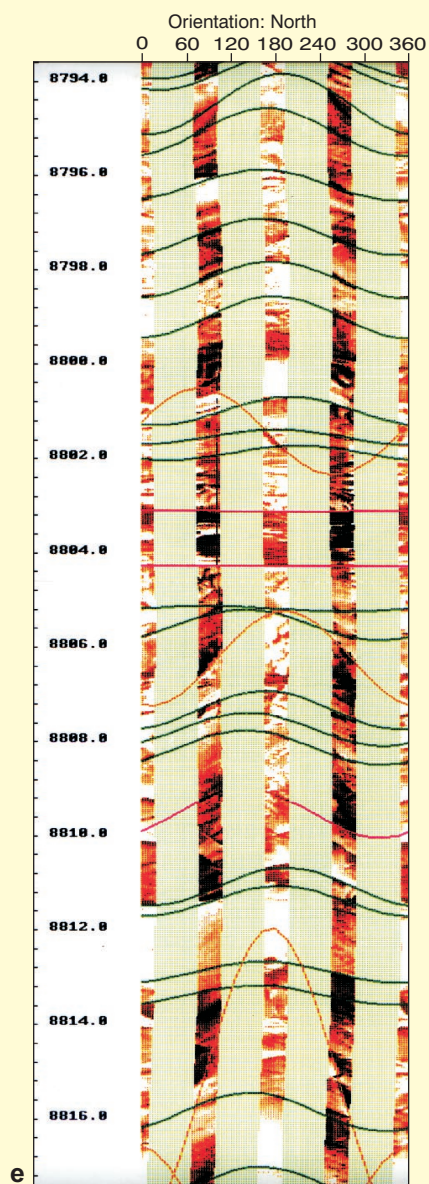
dipmeters (remaining cores have been slabbed). There are seven wells with FMS: Dullingari 44, Gidgealpa 47, Lycosa 1, Malgoona 4, Merrimelia 29, Moomba 73 and 75, but only Lycosa 1 has core material. Only three wells — Lycosa 1, Malgoona 4 and Yalchirrie 1 — have interpreted FMS logs available for this study.

Dipmeter is very useful at picking unconformities between the Warburton and Cooper or Eromanga Basins, and is normally recognised by abrupt change of azimuth or dip. The angular unconformity between the Dullingari Group and overlying Late Permian Toolachee Formation has been recognised in both core and dipmeter in Strzelecki 3 (Fig. 20).

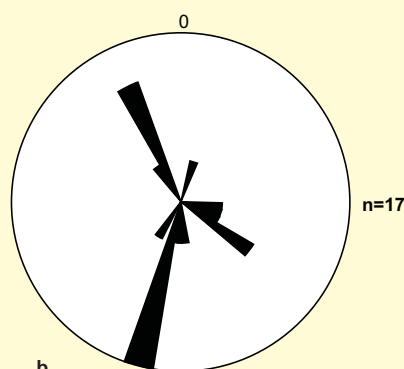
Dipmeters are fairly good at picking dips of bedding planes or structural dips, but they are not sensitive for detecting high angle bedding planes or fractures because of non-optimal processing algorithms, even in relatively modern data as in Lycosa 1 (Fig. 17). In the cases where dipmeters pick several fractures, I analysed how many groups of orientations, compare with dip azimuth of fracture sets observed in core, and decided which represents bedding dips or fracture dips. One example is in Mudlalee 1, although only the centre core slab is available for study, bedding dips are higher than fractures (Fig. 21), fracture set 1 has opposite orientation from the bedding, and fracture set 2 is at an oblique angle to the bedding.

## FMS fracture analysis

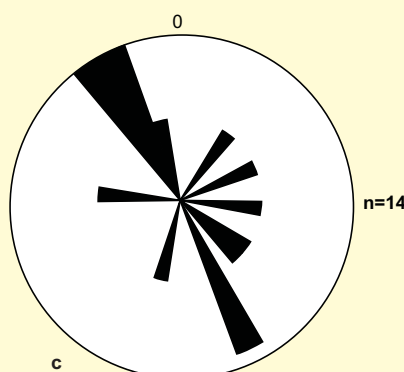
(Baily, 1991)



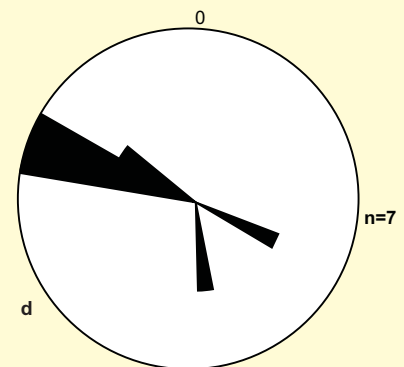
high angle fractures



major fractures



slickensides

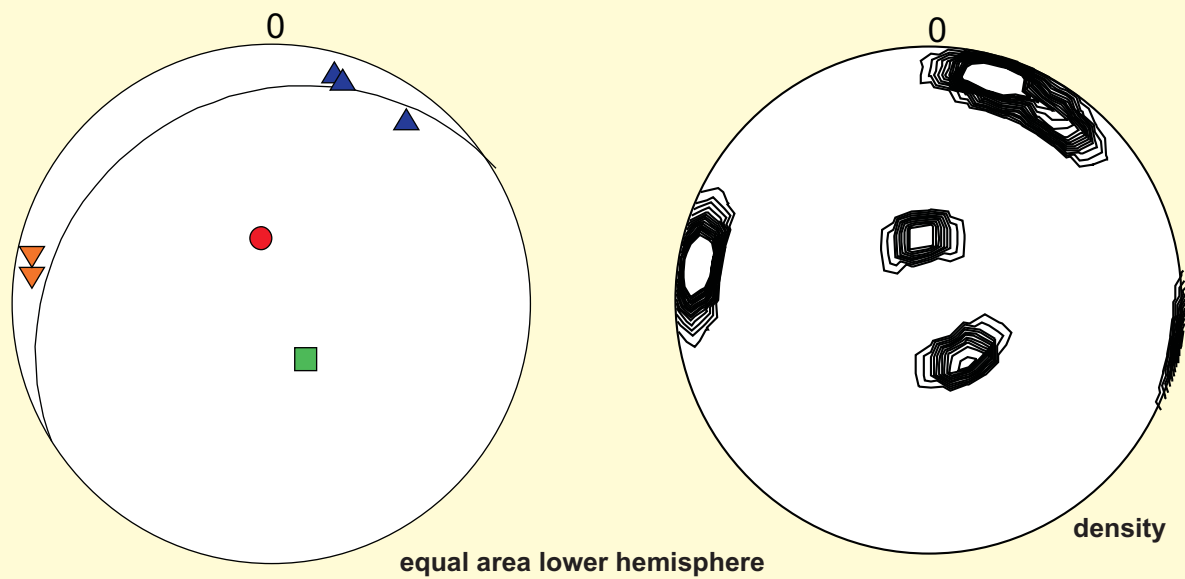


fault plane and tension gashes

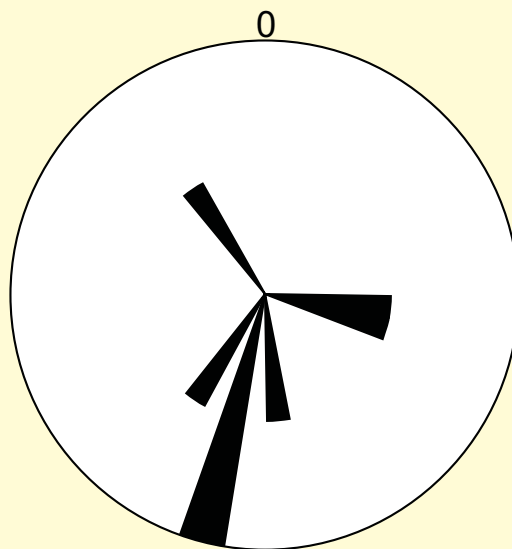
99-0486

**Fig. 14** Rose diagrams of fractures in core 1, Lycosa 1:

- (a) high angle fractures; (b) main fractures; (c) slickensided fractures and lineations; (d) fault planes and tension gashes.
- (e) FMS over interval of core 1, Lycosa 1 showing fractures (red and orange) interpreted by Schlumberger. Bedding is shown in green.



dip azimuth	dip angle	type	symbols
328	20	bedding	■
194	81	fracture 1	▲
96	82	fracture 2	▼
197	79	fracture 1	▲
215	76	fracture 1	▲
101	84	fracture 2	▼
171	20	microfault plane	●



99-0487

**Fig. 15** Stereographic projections of poles to and great circle for bedding, density and rose diagram of fractures measured from core 1, 8793', Lycosa 1.

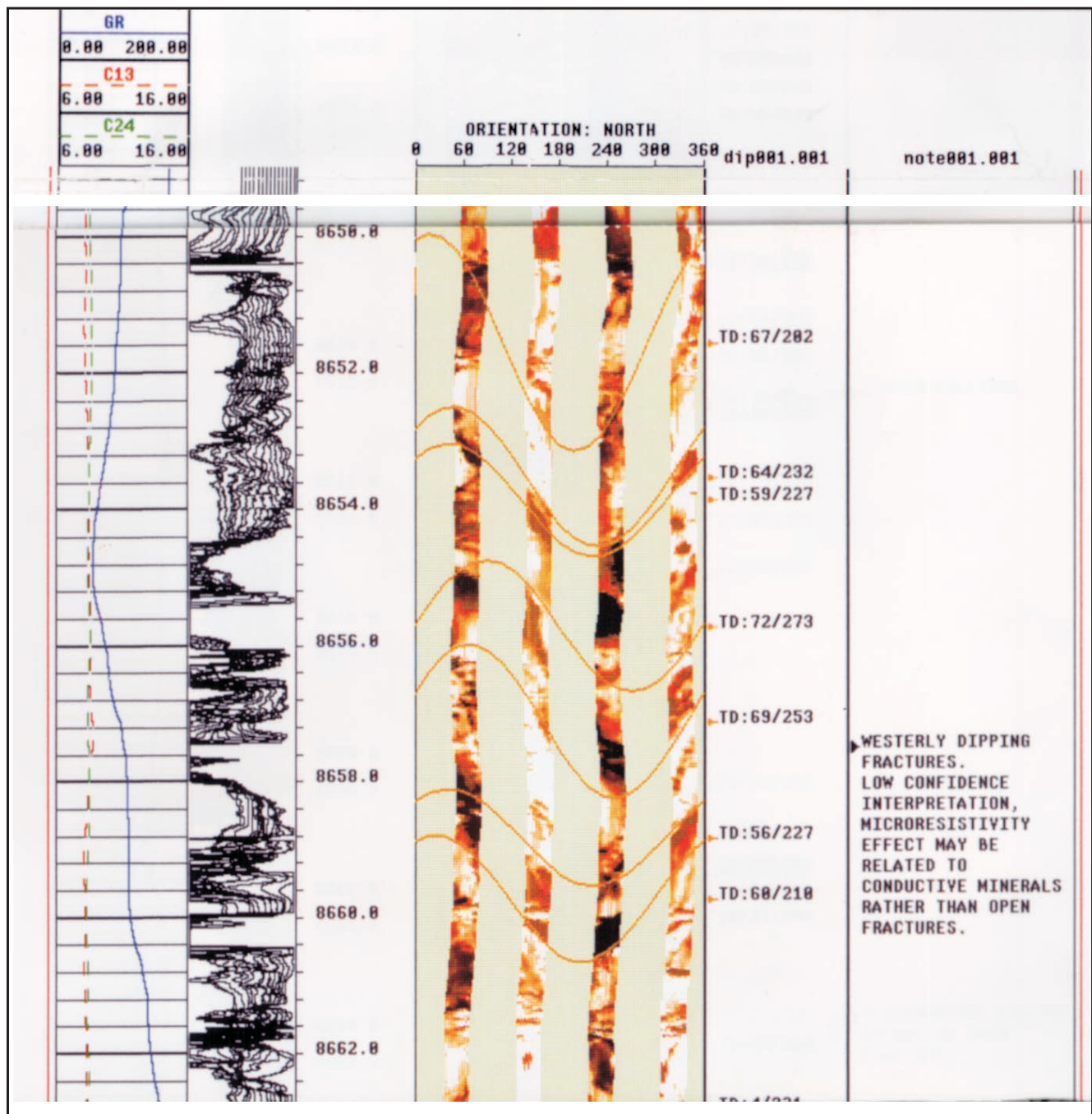


Fig. 16 FMS (fracture analysis) in Lycosa 1, showing SW dipping open fractures (orange). (From Rayner and Chin, 1990).

The wells listed in Table 4 have only core slabs except Coochilara 1 and Mudlalee 2 which lack cores. Their dipmeters can be interpreted by recognising conjugate fracture sets which cannot be confused with subvertical bedding dips as mentioned above for Mudlalee 1. With confidence, they can contribute to absolute orientation data (Figs. 23-24). The azimuths are averaged from dipmeter values, and are listed in the order of decreasing frequency of occurrence (Table 4).

Table 4 Dip and strike azimuths of fractures interpreted from dipmeters.

Well name	Dip azimuth	Strike azimuth
Coochilara 1	157°, 335°	67°, 245°
Mudlalee 1	240°, 330°	150°, 60°
Mudlalee 2	73°, 215°, 297°	163°, 125°, 27°
Strzelecki 3	52°, 335°	142°, 65°

### Absolute orientations

From almost 100 measured depths in 22 wells, Table 5 lists absolute strike orientations of mostly high angle fractures. Low angle fractures have also been measured (Appendix 1, 2). Warburton Basin intervals in most wells have only one or two cores, each core is normally 10 feet long. However some old wells such as Gidgealpa 1, 2, 3, 4, 5, 7, 8, 9, 11, Merrimelia 1, 2, Innamincka 1, Coongie 1 and Kalladeina 1 have many cores. Therefore, for those wells, the measurements near top of Warburton Basin strata have been chosen because they are more likely to trap Cooper Basin hydrocarbons. A difference of orientation with depth is prominent in Gidgealpa 1 (Fig. 22), probably due to footwall and hanging wall deformation differences in a compressive fault system.

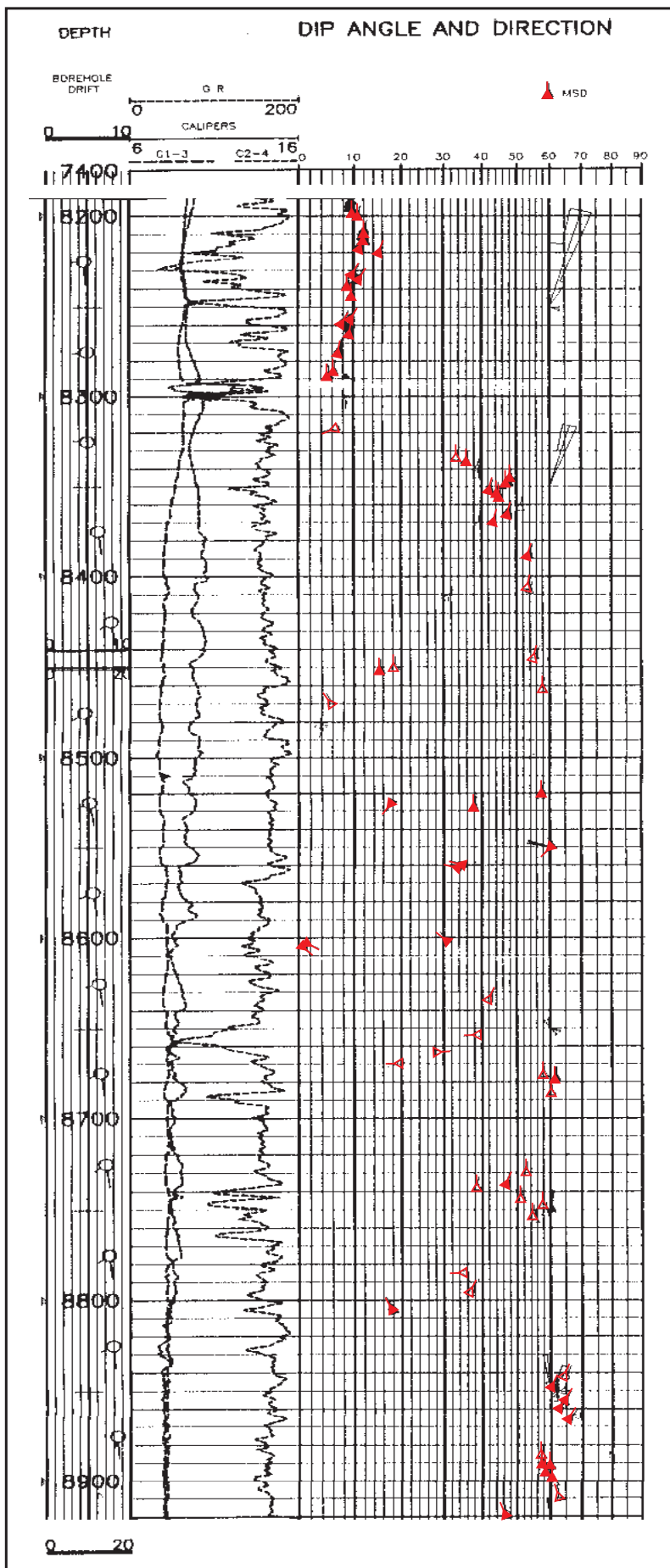


Fig. 17 Dipmeter in Lycosa 1.

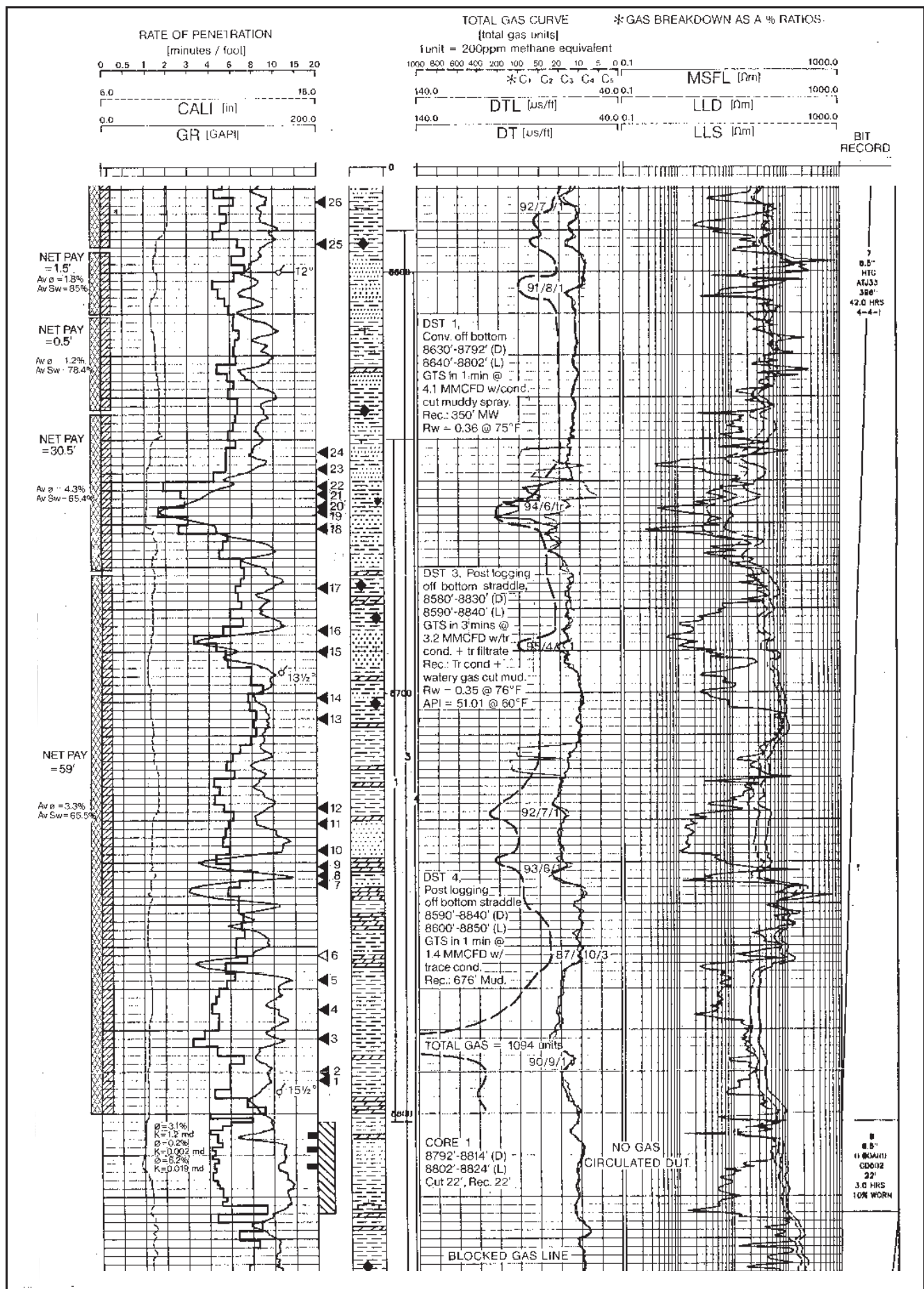
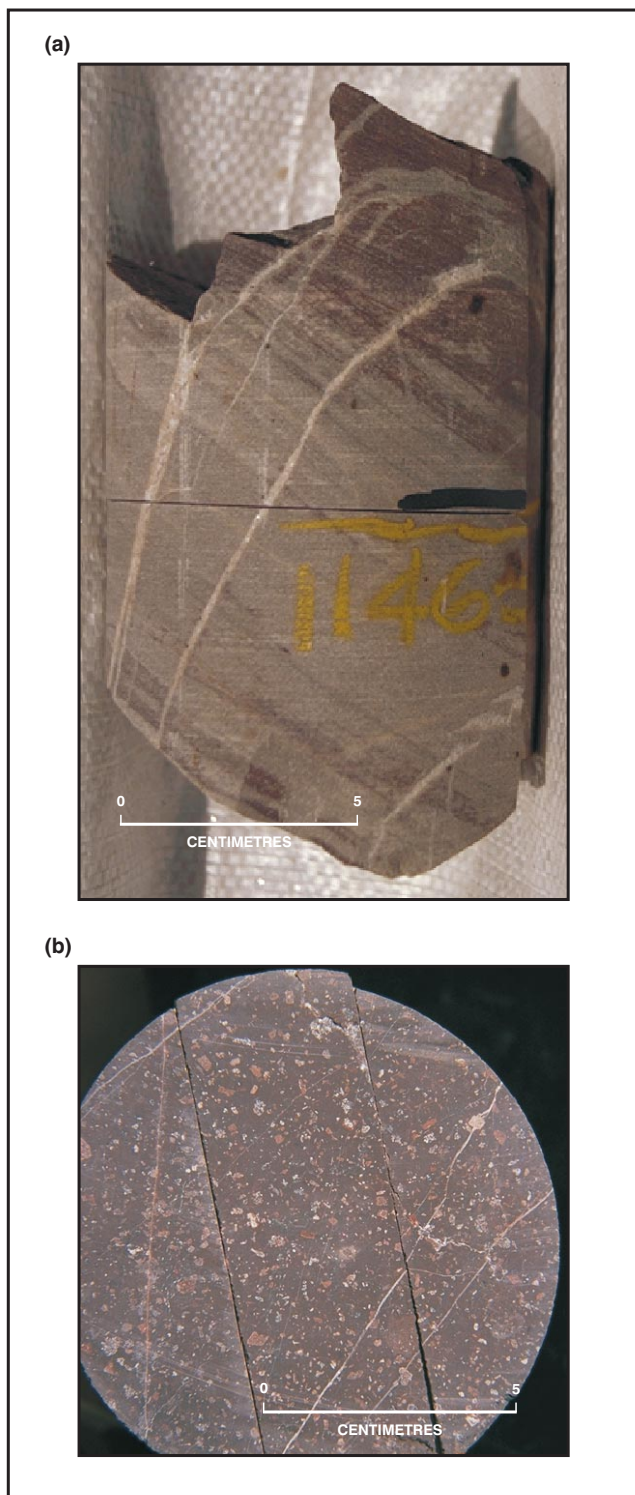


Fig. 18 Composite log in Lycosa 1



**Fig. 19** Fracture orientations in cores,  
 (a) circumferential surface in Innamincka 1,  
 (b) right angle to core axis, Gidgealpa 3. (Photos 046738,  
 046739)

Since major regional structural trends in the Cooper Basin are inherited from those which deformed the Warburton Basin (Sun, 1997 and references therein), Warburton Basin fracture systems are grouped in the five major structural domains which control Cooper Basin architecture. They are further partitioned into seven strike subdivisions to show similarity from well to well within a subdivision.

**Table 5** Absolute orientations of mean strike direction of fractures, including those interpreted from FMS by Hillis et al., 1997 (\*) and in (Rayner and Chin, 1990; Chin, 1991) (<sup>1</sup>) (o = open fractures, po = partially open fractures).

	STRIKE SUBDIVISION						
	1	2	3	4	5	6	7
<b>Sturt-Malgoona-Nealyon-Jennet Structural Domain</b>							
Malgoona 4 (o) <sup>1</sup>		018°		060°		150°	
<b>Gidgealpa-Merrimelia-Packsaddle-Innamincka Structural Domain</b>							
Gidgealpa 1	001°	018°	046°	060°	107°	150°	
Snake Hole 1	007°				104°		
					126°		
Gidgealpa 2				087°	120°	150°	
						162°	
Gidgealpa 3		026°	046°	074°	120°		176°
Gidgealpa 5		021°		054°			
				063°	133°		
Gidgealpa 7		025°		059°	136°	150°	
Merrimelia 6						147°	171°
Merrimelia 7		026°					173°
Mudrangie 1		030°	041°	060°		150°	
Wantana 1				079°	115°		
Packsaddle 3		021°		064°		150°	
						140°	
Innamincka 1				079°	135°	150°	
<b>Boxwood-Daralingie-Lycosa-Moomba Structural Domain</b>							
Boxwood 1	006°		050°	085°	102°		
Lycosa 1		020°		063°	110°(po); 140°(o) <sup>1</sup>		
					127°(o) <sup>1</sup> ;		
						162°(o) <sup>1</sup>	
Yalcumma 1			072°	082°			
Moomba 2		020°					
Moomba 73*							147°
<b>Della-Nappacoongee-Dullingari Structural Domain</b>							
Della 1					112°	141°	
Dullingari 1					117°	144°	
<b>Tilpatee-Pelketa-Toolachee-Munkarie Structural Domain</b>							
Murteree 1		021°				156°	
Munkarie 1	008°		068°		090°		
Pelketa 1			046°		108°		179°

The strike data in 23 wells (Table 5) chosen for final interpretation are from high angle fractures and averaged into 45 mean strike directions from many measurements. They are illustrated in Fig. 23. From these seven subdivisions, four groups of fractures can be further separated (Fig. 24; Appendix 4). The four groups have average strike azimuths of 22°, 61°, 114°, 148°, which can be approximated as four strike directions: 20°, 60°, 110°, 150°. As shown in Table 5, in the Gidgealpa-Merrimelia-Packsaddle-Innamincka domain, NW-SE strikes are dominated by azimuth 150-330°, subsidiary NW-SE strikes can be averaged as 110°. NNE strikes can be averaged as 020°. NE strikes can be averaged as 60°. These major strike directions can be seen in other domains as shown in Table 5 and Fig. 23. For example, in Lycosa 1, 020° and 110° are orthogonal directions, one dipping SW and the other dipping SE (Fig. 11k). I interpret the NE striking 060° and 150° pair as a second orthogonal set. These two sets are more or less found in all the structural domains although some fractures may not have been intersected during drilling or have no core or other logs to record them. These two systems are simplified and superimposed on the Z time structural map (Fig. 25). Relatively few wells, Munkarie 1, Pelketa 1, Wantana 1, Yalcumma 1, Boxwood 1 and Gidgealpa 2 have fractures close to E-W striking fractures.

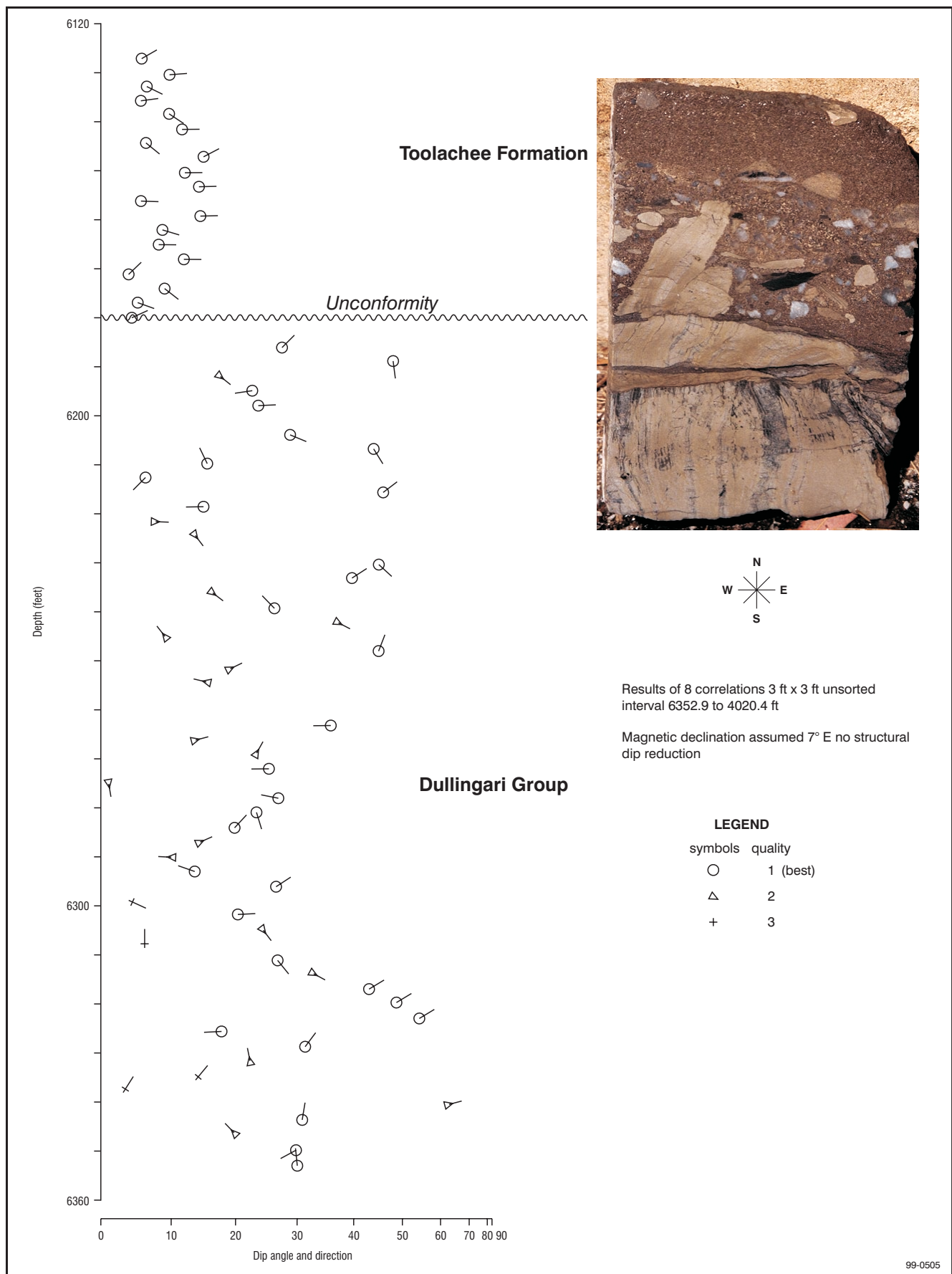


**Fig. 20** Strzelecki 3 dipmeter and core illustrations of angular unconformity between Toolachee Formation (Permian) and Dullingari Group (Ordovician). (Photo 046740)

**Table 6** Absolute dip azimuths and dip angles (e.g. 120/60) of steep fractures, including those interpreted from FMS by Hillis et al., 1997 (\*) and in (Rayner and Chin, 1990; Chin, 1991) (<sup>1</sup>)

<b>Sturt-Malgoona-Nealyon-Jennet Structural Domain</b>				
Malgoona 4(o) <sup>1</sup>	240/65(o) <sup>1</sup>	288/55(o) <sup>1</sup>	330/80(o) <sup>1</sup>	
<b>Gidgealpa-Merrimelia-Packsaddle-Innamincka Structural Domain</b>				
Gidgealpa 1	136/55	197/35	239/80	271/55
Snake Hole 1	14/89 or 194/89	36/80	277/83	
Gidgealpa 2	72/50, 177/80, 210/70, 240/68			
Gidgealpa 3	116/78, 136/73, 164/82, 210/85, 266/85			
Gidgealpa 5	144/55, 291/60, 333/50			
Gidgealpa 7	226/85, 240/78, 295/43, 329/73			
Merrimelia 6	237/87, 261/87			
Merrimelia 7	83/75, 296/80			
Mudrangie 1	120/48, 240/80, 311/45, 330/60			
Wantana 1	169/60, 205/50			
Packsaddle 3	63/70, 230/80, 291/61, 334/85			
Innamincka 1	45/70, 240/70, 349/68			
<b>Boxwood-Daralingie-Lycosa-Moomba Structural Domain</b>				
Boxwood 1	175/63, 192/55, 276/80, 320/60			
Lycosa 1	110/84, 200/78(op), 230/67(o) <sup>1</sup> , 333/65 <sup>1</sup> , 217/62(o) <sup>1</sup> , 252/67(o) <sup>1</sup>			
Yalcumma 1	172/70, 342/58			
Moomba 2	290/85			
Moomba 73 *	57 or 237			
<b>Della-Nappacoongee-Dullingari Structural Domain</b>				
Della 1	202/77, 231/80			
Dullingari 1	54/55			
<b>Tilpatee-Pelketa-Toolachee-Munkarie Structural Domain</b>				
Murteree 1	111/85, 246/70, 306/60			
Munkarie 1	98/72, 158/75, 180/80			
Pelketa 1	89/45, 136/52, 198/60			

Dip azimuths of absolute orientations are presented in Fig. 26 and listed in Table 6. Several major groups of dip azimuths include in order of decreasing frequency: SW, SE, NW and NE.

### Relative orientations

The majority of cores are from wells that are not orientated down-hole in the Warburton Basin. In 24 wells, bedding is arbitrarily assumed to dip north, with other fractures measured relative to the bedding (Appendix 1, 2). Because the two orthogonal fracture systems transcend local structures, and more or less have the same orientations as low frequency lineaments, they are interpreted as regional fractures. With guidance of the regional fracture pattern, relatively oriented high angle fractures can be rotated into sensible strike directions by their angular relationships. In this way the relatively-oriented high angle fractures from an additional 17 wells can fit within two orthogonal fracture systems. However, there are two possible solutions (Table 7, Figs. 27, 28 and 29).

A choice can be made between the two possibilities by considering the regional fracture patterns recognised in the nearby wells. Since the regional fractures in the Warburton Basin have been superposed by local tectonic fractures (see discussion), local structural features such as thrust faults, slickensided surfaces and lineation directions can constrain the more likely possibility on a case by case basis (Table 8). Absolute and relative orientations of fractures can then be combined to present a fracture strike map (Fig. 29).

### Orientations of open and partially open fractures

From FMS interpretation, Chin (1991) identified 181 natural fractures in the Mooracoochie Volcanics in Malgoona 4, of which 167 are open (or conductive). He also



**Fig. 21** Mudlalee 1 core, illustration of fracture sets. (Photo 046741)

found that the fractures have mean azimuth 288.6°, dip 55.9°, and the most intensely fractured intervals are 7225-7230 and 7278-7285 feet, in which fractures have aperture: max: 0.1 mm, mean: 0.063 mm; density of open fractures 7/foot. However, there are at least three dominant azimuths with 167 conductive fractures (Chin, 1991, Fig. 5), whose mean values are 290°/55, 240°/65, 330°/80. It is illogical to calculate a mean azimuth and dip for these fractures and hence Figure 29 displays all three directions for

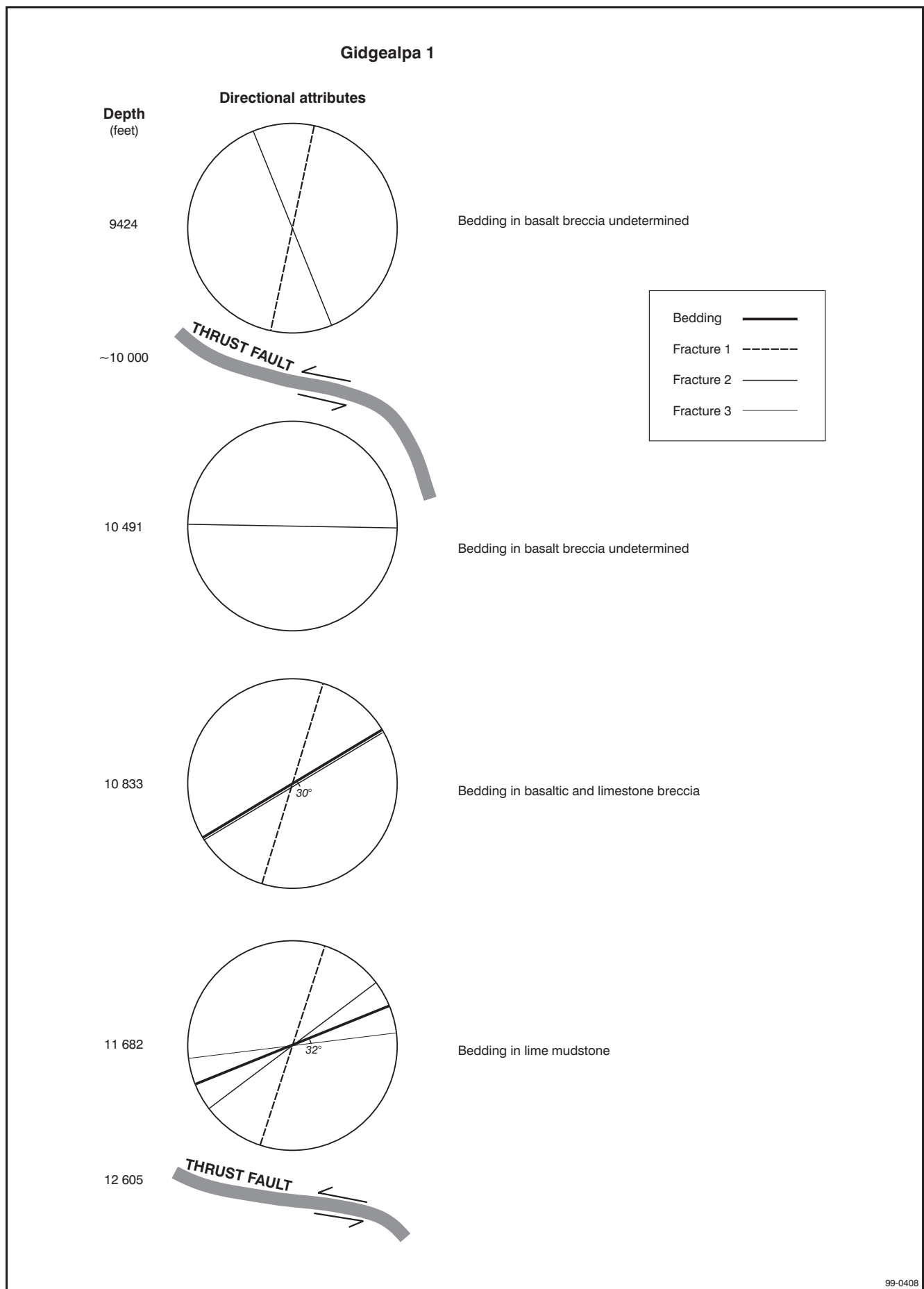


**Fig. 22** Variation of fracture orientation with depth in Gidgealpa 1

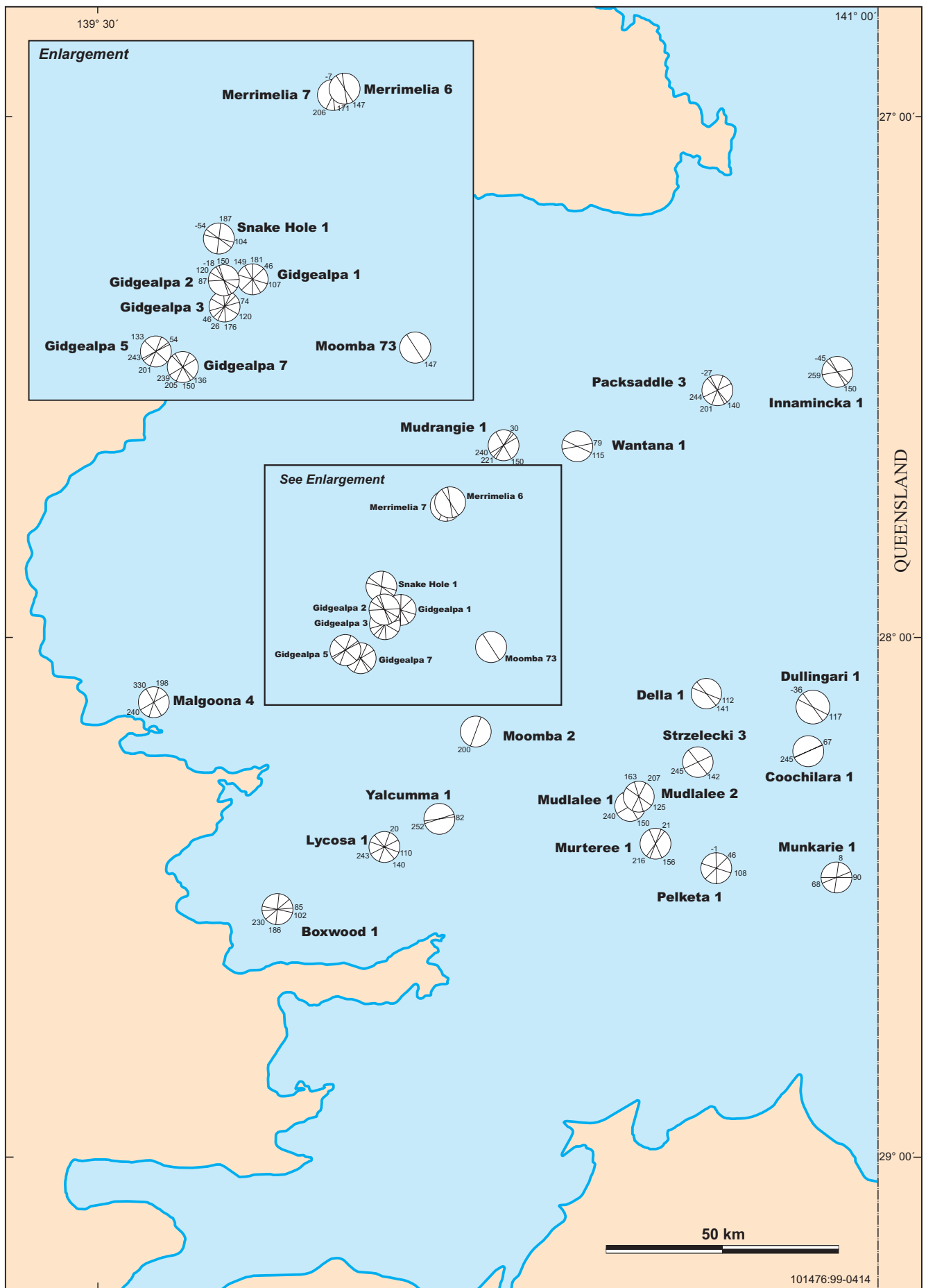
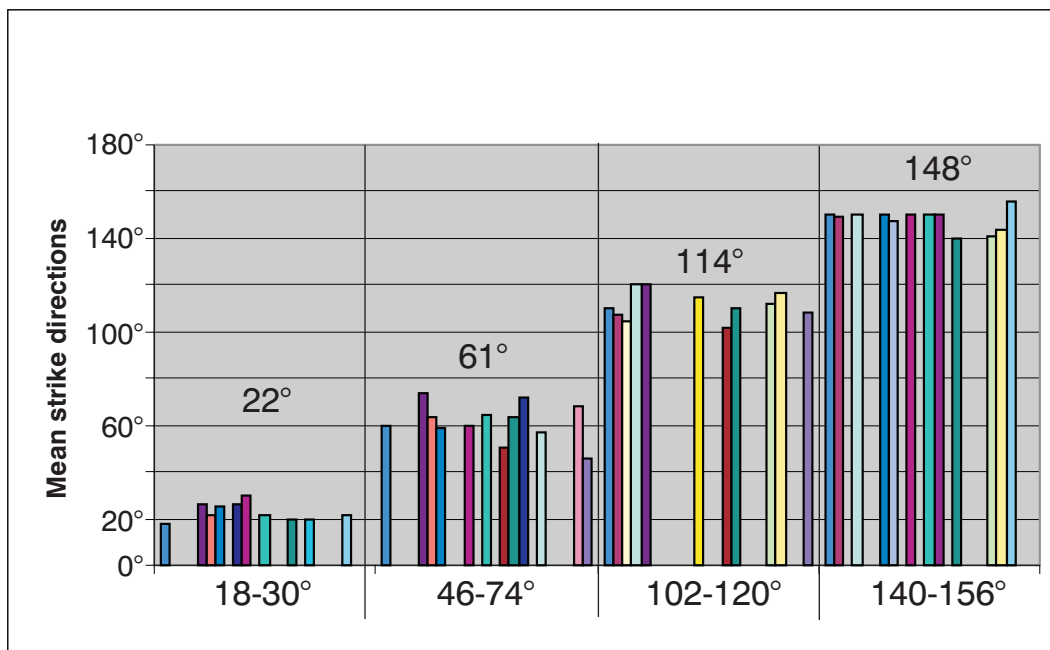
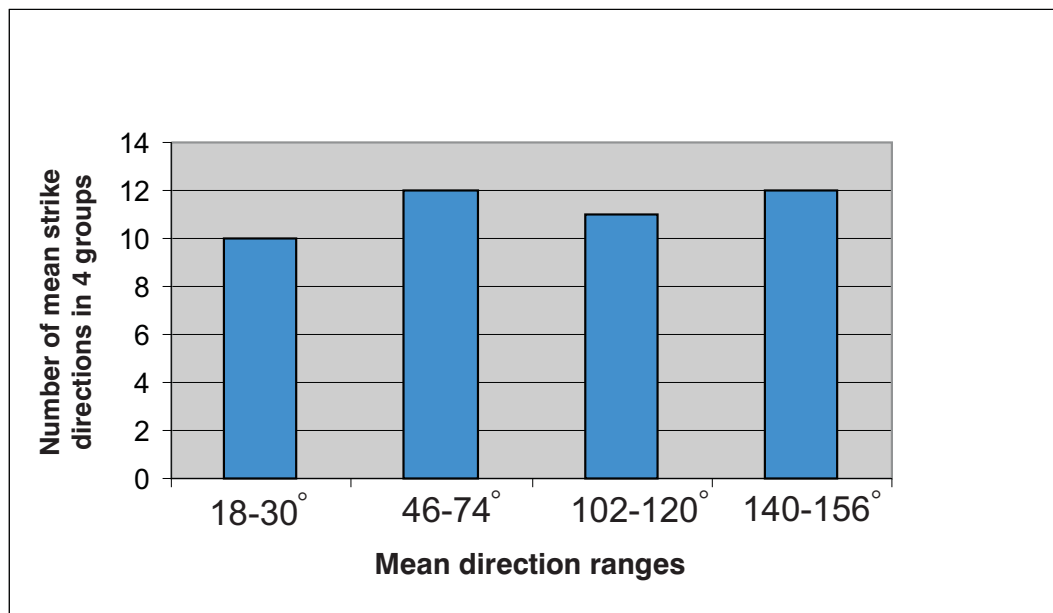


Fig. 23 Map of Cooper Basin showing absolute orientations of strike directions

(a)



(b)



99-0415

**Fig. 24** Four groups of strike direction stand out from mean high angle fracture strike direction as shown in two histograms ( $n=45$ ):  
(a) mean strike direction plot, with four average directions: 22°, 61°, 114°, 148°;  
(b) frequency of mean strike direction in four groups.

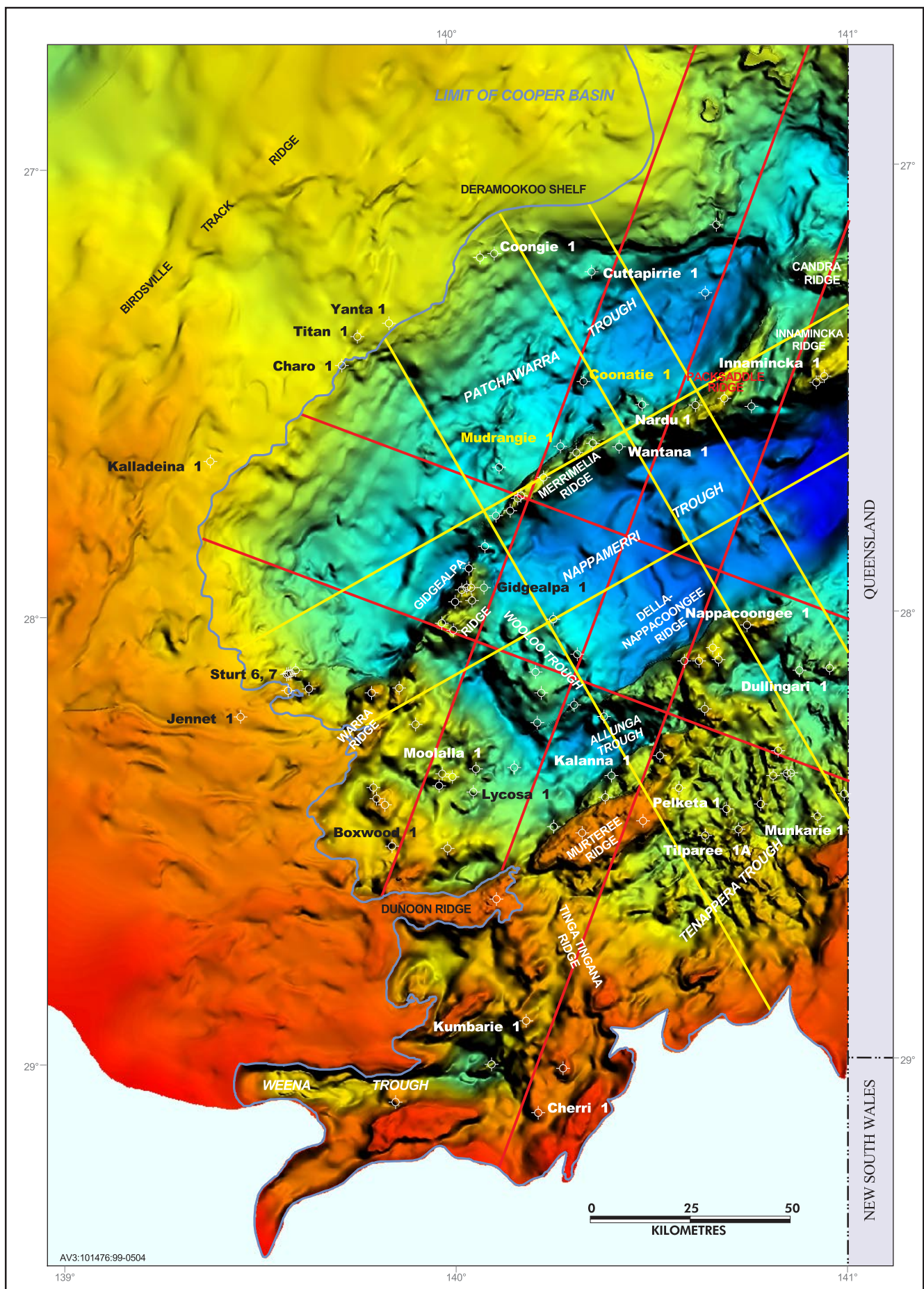


**Fig. 25** Map of Cooper Basin showing two sets of orthogonal fractures which are independent of local structure when laid over the 'Z' horizon structural map.

**Table 7** Strike orientations of fractures rotated in azimuth to fit within regional fracture systems

Well name	Possibility 1	Possibility 2
Big Lake 52	20°, 150°	60°, 110°
Brumby 1	20°, 110°	60°, 150°
Cherri 1	20°, 150°	60°, 110°
Coonatie 1	20°, 60°	110°, 150°
Daralingie 1	20°, 150°	60°, 110°
Della 2	20°, 60°	110°, 150°
Jennet 1	20°, 110°	60°, 150°
Kalanna 1	20°, 110°	60°, 150°
Kumbarie 1	20°, 60°	110°, 150°
Lowanna 1	20°, 150°	60°, 110°
Nappacoongee 1	20°, 60°	110°, 150°
Narcoonowie 1 (upper core)	20°, 60°	110°, 150°
Narcoonowie 1 (lower core)	20°, 150°	60°, 110°
Nealyon 1	20°, 60°	110°, 150°
Packsaddle 1	20°, 60°, 150°	60°, 110°, 150°
Tilparee A1	20°, 150°	60°, 110°
Toolachee 1	20°, 110°	60°, 150°
Toolachee 9	20°, 60°	110°, 150°

**Table 8** Case by case selection of more likely fracture strike orientation.

Well name	More likely fracture strike orientations	Brief reasons
Big Lake 52	20°, 150°	shear plane (~1500) due to strike slip faulting zone, also relate to those from Mudlaalee 1 and 2 and Moomba 2
Brumby 1	60°, 150°	NE trending anticline related fractures.
Cherri 1	20°, 150°	N-S aligned small anticline
Coonatie 1	20°, 60°	Similar to adjacent Mudrangie 1
Daralingie 1	60°, 110°	NE trending anticline related fractures. Similar to Lycosa 1.
Della 2	110°, 150°	Similar to adjacent Della 1
Jennet 1	60°, 150°	Slickenside lineation dipping NW (3400), high angle fault dipping NW or SE, more NW.
Kalanna 1	60°, 150°	NE-SW trending fault zone
Kumbarie 1	20°, 60°	NE trending anticline related fractures.
Lowanna 1	20°, 150°	Close to Big Lake 52
Nappacoongee 1	110°, 150°	Similar to Della 1
Narcoonowie 1	110°, 150°	NE-SW trending anticline, NW flank
6543' (10 differ.)	60°, 110°	Similar to Pelketa 1
Nealyon 1	20°, 60°	Similar to Malgoona 4 and Jennet 1
Packsaddle 1	20°, 60°, 150°	NE trending anticline related fractures, especially thrust faults (~150°).
Tilparee 1A	60°, 110°	E to NE trending small anticline
Toolachee 1	20°, 110°	Large N-S trending anticline
Toolachee 9	20°, 60°	N-S bounding fault

this well. There is insufficient material to determine whether or not all three fracture sets are open (no core was cut).

Four of the wells shown in Table 9 have open or partially open fractures with known absolute orientations. They represent three of the five structural domains. One of the remainder, Gidgealpa 4, has open fractures along a normal microfault. Although this well is not oriented down the hole, and also has fractures with a single orientation, we can assume that its bedding plane dips SE (i.e. 130°) like many other nearby wells in the Gidgealpa North Dome. If this is the case, then the open fracture will dip towards the SW (236°) whose strike will be NW-SE (nearly 150°) similar to common bedding strikes of several nearby wells such as Gidgealpa 2 and 3. Open fractures are also found in Beanbush 1 (Fig. 5e)

and Meranji 2 (Fig. 5d), with high angles ranging from 80° to subvertical. Unfortunately these wells lack dipmeters and have no fracture patterns to help find their orientations. If we assume the bedding in Meranji 2 dips NW (330°), the subvertical fracture (dip angle 85°) will dip towards SW (215°) as shown in Table 9 (Appendix 2).

There are some possibly induced open fractures, which need further examination to be certain of their nature. Numerous irregular open fractures are observed in Jennet 1 (Fig. 31), also at some depths in Merrimelia 2. In Jennet 1, possible open fractures are observed in coarse-grained sandstone. Because it is an unoriented well, the dip azimuth of the fractures will be 230° (average) if one assumes that they belong to System II regional fractures striking 60° and 150°.

## Fracture density

The productivity of a fractured zone is directly proportional to the number of fractures intersected by a wellbore. Where fracture distribution is even, I have recorded average distance or spacing between the fractures along the borehole; if not, I have measured both minimum and maximum distance between adjacent fractures along the borehole. I have used average distance to calculate the number of the fractures per foot along the borehole which is similar to raw fracture density (the number of fractures per foot or meter selected along the borehole, Schlumberger, 1997). Usually there are one or two fractures which intersect the circular face of a plane cut perpendicular to the core axis except in heavily fractured wells which can have more than 10 small fractures. Examples are cores from Murteree C1, Mureree A1, Pelketa 1, core 25 in Gidgealpa 5 and Kalanna 1 (Fig. 32). Therefore, for typical wells I calculate the number of fractures along the core axis. For heavily fractured cores, I take account of fractures which intersect a plane perpendicular to the core axis as well. These quantitative spacing data are recorded in excel format (Appendix 3). For mapping, I classified the fracture density of all the studied wells into five grades: very high (>25/1'), high (>=7/1'), moderate (>2/1'), low (<1/1'), nil (0 fractures, in normally about 10 feet of core). The five grades for 91 wells are listed in Table 10 together with their main lithologies. They are illustrated in Figs 32-35. For those wells which have long intersections such as Gidgealpa 1, Innamincka 1, I have taken an average and shown the main lithology especially near the top of the Warburton Basin for the density map (Fig. 36). In such wells with many cores, fracture density varies with depth and lithology, such as in Merrimelia 2 (Table 11). Fracture density is often unevenly distributed within a single 10 or 20 feet length of core, such as in Lycosa 1 (Fig. 13) and Wancoocha 1. Normally, very high fracture density occurs in brecciated zones which are probably caused by faulting. In Lycosa 1, a severely fractured and brecciated zone is observed over the interval of 8794'5". The low angle microfaults and mineralised breccia zone all indicate faulting. At this stage, I have not attempted to compare the fracture densities of the two separate orthogonal sets.

**Table 9** Orientations, aperture, lithology of open and partially open fractures

Well, Depth (feet)	open (o), partially open (po)	lithology	aperture (max. mm)	Azimuth (mean)	dip (average)
<b>Lycosa 1</b>					
8793	po	siltstone and shale	0.1	202°	78°
86271	o	as above	no data	217°	62°
<b>Malgoona 4<sup>+</sup></b>					
7278-7285	o	acid volcanics	0.1	288° 240° 330°	55° 65° 80°
<b>Merrimelia 6</b>					
7441.5-7442	po	sandstone	0.2	249°	87°
<b>Merrimelia 7</b>					
7445.33	po	sandstone	broken	83°	75°
7451	po	as above	0.2-0.3	296°	80°
<b>Gidgealpa 4*</b>					
7226.67	o and po	tuffaceous sandstone	0.2	236°	75°
<b>Meranji 2*</b>					
10920	o	fine sandstone	0.1	215°	85°
<b>Jennet 1*</b>					
5525	o	coarse sandstone	0.35	230°	65°
<b>Beanbush 1</b>					
	o	fine sandstone	0.1	no data	85°

\* assumed from relative orientation data,

+ from FMS interpretation

**Table 10** Fracture density and main lithology from 91 studied wells

Well	Fracture density	Main lithology
Beanbush 1	low	siltstone, fine-grained sandstone.
Big Lake 52	high	siltstone and shale
Bookabourdie 1	high	siltstone and fine-grained sandstone
Boxwood 1	moderate	ignimbrite; siltstone and shale
Brumby 1	high	siltstone and mudstone
Burke 1	moderate	siltstone, sandstone
Charo 1	nil	grainy limestone
Cherri 1	high vertically	slate
Coonatie 1	moderate to high (not even)	siltstone, fine-grained sandstone, shale
Coongie 1	low (siltstone and shale to high (grainy limestone)	shale, siltstone, sandstone, grainy limestone
Cuttapirrie 1	high	rhyodacite
Daer 1	low-moderate (not even)	grainy and minor marly limestone
Daralingie 1	moderate to high (not even)	sandstone and siltstone (low); quartzite (high)
Daralingie 2	high	fine-grained sandstone, siltstone, shale
Daralingie 10	moderate to partly high (breccia)	protoquartzite, breccia
Della 1	moderate, not even	siltstone
Della 2	very high	siltstone and shale (weathered)
Della 4	low	sandstone
Della 5A	very high	siltstone and shale (weathered)
Dullingari 1	moderate to high	siltstone and shale, minor fine-grained sandstone
Dunoon 1	nil	siltstone, fine-grained sandstone
Gidgealpa 1	moderate to partly high (breccia)	marly limestone, grainy limestone, dolomite
Gidgealpa 2	high	tuffaceous sandstone, tuff, rhyodacite
Gidgealpa 3	moderate to high	tuffaceous conglomerate, tuff, rhyodacite
Gidgealpa 4	high to very high (breccia)	tuffaceous sandstone, tuff, ?rhyodacite
Gidgealpa 5	very high to moderate	marly and grainy limestone, dolomite (veryhigh), tuffaceous sandstone and rhyodacite (moderate)
Gidgealpa 7	high to very high (breccia)	marley limestone, grainy limestone, dolomite, tuffaceous sandstone
Gidgealpa 8	very high (breccia) to partly high	fault breccia, tuff
Gidgealpa 11	low	ignimbrite, tuff
Gurra 1	high	phyllite
Innamincka 1	low (mudstone) moderate to high (sandstone)	green siltstone, vf sandstone; red mudstone and siltstone.
Innamincka 4	low	siltstone and very fine sandstone.
Jennet 1	high	sandstone and minor siltstone.
Kalanna 1	high to very high	mudstone and shale
Kalladeina 1	low to partly moderate	siltstone, shale, marly and grainy limestone, rhyodacite
Kumbarie 1	high	weathered mudstone; siltstone and shale
Lowanna 1	high	siltstone and shale
Lycosa 1	to very high	siltstone and shale
Malgoona 4	high and partly moderate	?ignimbrite
McKinlay 1	moderate, not even	siltstone and shale
Merrimelia 1	low (mudstone), moderate (sandstone)	
Merrimelia 2	low (mudstone), moderate (sandstone), high (breccia zone)	
Merrimelia 3	high at top (8210'), nil in lower part (8964-76')	sandstone, siltstone and mudstone
Merrimelia 5	nil	mudstone
Merrimelia 6	low to moderate	fine-grained sandstone
Merrimelia 7	moderate	fine-grained sandstone
Meranji 2	low	siltstone, fine-grained sandstone

Minkie 1	low	fine-grained sandstone
Moomba 2	high	weathered sandstone, siltstone
Moomba 3	low to moderate	hornfels
Moomba 7	low to moderate	sandstone
Moomba South 1	high to very high (breccia)	hornfels
Mudrangie 1	high to very high (breccia)	quartzite
Mudlalee 1	moderate	balsalt; siltstone and shale
Munkarie 1	high	grey mudstone and shale
Murteree 1	moderate to high	dk siltstone and shale
Murteree A1	veryhigh	basalt
Murteree C1	very high	weathered siltstone and mudstone
Nappacoongee 1	high to very high (breccia)	shale, f. sandstone
Narcoonowie 1	very high	weathered mudstone; mudstone and shale
Nealyon 1	high	siltstone and shale
Packsaddle 1	high	siltstone and f. sandstone, sandy limestone
Packsaddle 3	moderate to high	shale and f. sandstone
Pando 1	moderate to high	sandstone
Pando 2	high (breccia)	weathered shale; sandstone
Pando North 1	moderate	mudstone and siltstone
Pelketa 1	high to very high	weathered siltstone and shale
Pinna 1	low, partly moderate	mudstone and siltstone
Snake Hole 1	not even, moderate to high	siltstone, red mudstone
Spencer 1	nil to low	conglomerate of volcanics
Spencer 2	moderate to high	rhyolite
Strzelecki 1	high to very high (short fractures)	pyritic shale
Sturt 7	low but high partly	tuff (low); ignimbrite (moderate)
Stuart 8	low to moderate	tuff (low); ignimbrite (moderate)
Taloola 1	low	ignimbrite
Tilpatee A-1	high	pyritic shale
Tinga Tingana 1	moderate to partly high	quartzite; shale
Tirrawarra 1	nil to low	sandstone, siltstone
Titan 1	moderate to high (breccia)	siltstone and shale, grainy limestone
Toolachee 1	high and partly very high	pyritic shale and siltstone
Toolachee 2	moderate	sandstone; shale
Toolachee 4	moderate	arkosic sandstone
Toolachee 9	high	arkosic sandstone
Toolachee East 2	high	weathered siltstone and shale
Walkillie 1	moderate	rhyolite
Wancoocha 1	not even, high in upper part, (breccia), low in lower part (siltstone and shale)	weathered siltstone and shale
Wantana 1	moderate to high	siltstone and shale, grainy limestone
Weena 1	nil	pebbly sandstone
Wirrarie 1	nil	sandstone, siltstone
Yalumma 1	not even, moderate to partly high	siltstone and shale
Yanpurra 1	nil	siltstone and shale

**Table 11** Fracture density change with depth in Merrimelia 2. Core recovery is 100%, except core 11 (92%) and cores 7, 15, 17 (85%).

Top depth (feet)	Bottom depth (feet)	Core	Number of fractures	Main lithologies
7900.00	7916.70	2	26	Bioturbated red-brown, micaceous mudstone; x-laminated sandstone which is well fractured through along the core axis.
8339.00	8349.00	3	4	Similar lithology to the above, but more green pebbles.
8572.00	8603.00	4	>8	Similar to the above, sandstone with irregular lamination.
8630.00	8644.00	5	7	Cross-laminated sst, truncated bed. Green shale clasts.
8695.00	8715.00	6	5	Orthoquartzite and shale with vague low angle lamination. A possibly induced fracture (open).
9117.00	9127.00	7	18	Sandstone with thin soapy green shale layers, numerous fractures filled by quartz and calcite. Red sheet-like micaceous shale with fractures.
9627.00	9637.00	8	2	Low angle planar cross laminated sst. Red mudstone.
10139.00	10149.00	9	0	Bioturbated mudstone and siltstone, sandstone with. rip-up clasts.
10636.00	10646.00	10	1	Slightly silty, convolute bed; siltstone, cross lamination. Red brown mudstone.
11110.00	11119.50	11	0	Brown laminated siltstone and sandstone. Well-bioturbated mudstone.
11513.50	11523.50	12	2	Red micaceous shale, and fine sandstone, planar lamination; rip-up clasts of green mudstone.
12071.00	12081.00	13	0	Red bioturbated mudstone and siltstone.
12123.00	12138.00	14	1	Lateral accretion foreset, calcareous. Trough cross-lamination; flat-pebbles, some still fit. Red shale breccia.
12673.00	12680.00	15	1	Red-brown mudstone, bioturbation. Slightly laminated.
12765.00	12781.00	16	3	Bioturbated mudstone, rip-up intraclasts (green), minor x-laminated siltstone.
13004.00	13011.00	17	2	Brown to purple sandstone, granules along bedding; truncated "trough" cross-lamination.

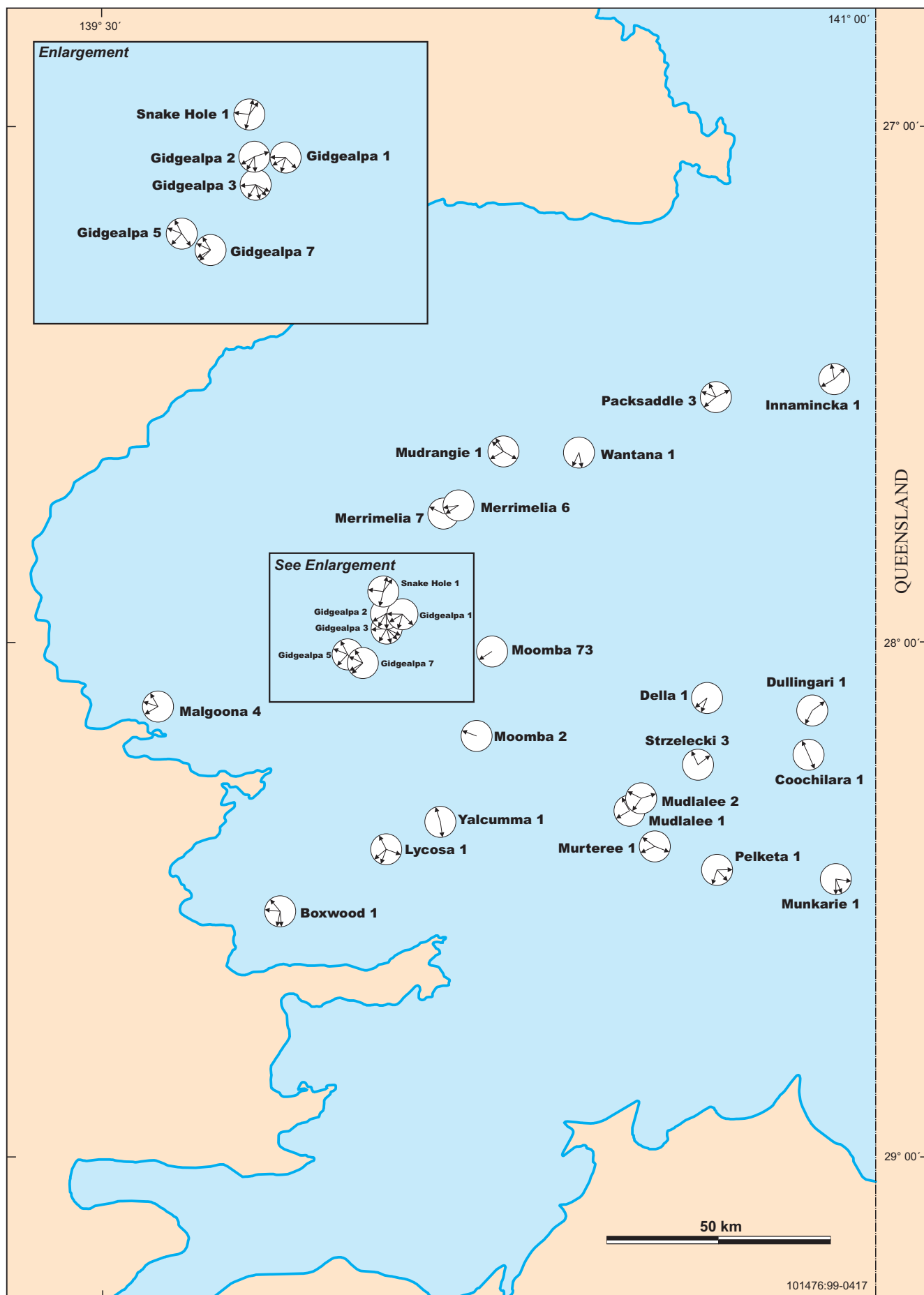


**Fig. 26** Map of Cooper Basin showing absolute orientations of dip azimuths.



**Fig. 27** Map of Cooper Basin showing those relative orientation data which fit within system I or II, or both orthogonal sets (possibility 1).



**Fig. 28** Map of Cooper Basin showing those relative orientation data which fit within system I or II, or both orthogonal sets (possibility 2).



Fig. 29 Map of Cooper Basin showing combination of absolute and relative data (strike only).



**Fig. 30** Map of Cooper Basin showing absolute strike orientations of steep fractures (circled) to low frequency lineaments (LFL), NNE8, WNW9 and NE1 identified by Boucher (1998).

A fracture density map with lithologies has been constructed (Fig. 36). The fracture density depends first on structural style and severity of deformation, secondly on lithology, thickness and pattern of interbeds. The density distribution is consistent with the severity of structural deformation. Fractures are most severely developed along fault zones, such as in Kalanna 1 which has high to very high fracture density. Kalanna 1 lies on a NE-SW fault zone, and is a fault dependent trap with the Merrimelia-Tirrawarra-Patchawarra section truncated against Warburton strata along the fault (Morgeneier, 1985). Most wells with grade 5 fracture density are associated with faulting and gouge fill fault zones such as Lycosa 1, Gidgealpa 4, 5, 8, some of Gidgealpa 1 and 7, Della 5A, Murteree C1. Fractures are also more severe on the crests of structural culminations such as in the vicinity of Strzelecki 1, Pelketa 1, Murteree A1 and the Gidgealpa area (Appendix 3). Most of these culminations are bounded by faults at Z horizon depth. Wells without fractures such as Dunoon 1, Weena 1, Wirrarie 1 and Charo 1 are situated away from fault zones and off the crests of fault-related anticlines. They are almost flat-lying, and probably only suffered uplift within a large block such as Dunoon 1 or mild and broad folding such as in Charo 1. In severely faulted and uplifted areas, fractures are well developed and independent of lithology, which ranges from siltstone and shale to carbonate, sandstone or volcanics.

Within the Gidgealpa-Merrimelia-Packsaddle-Innaminka structural domain, fracture density varies markedly for two reasons. The first is due to structural control, strata which have been overthrust have higher bedding dips and higher fracture density than those in underlying flat-lying and gently dipping beds. From seismic interpretation, we know that Gidgealpa 1, 7, Wantana 1 and Packsaddle 1 are located on overthrust slices, they are relatively steeply dipping and have high to very high fracture density. The second, is controlled by lithology, in the flat-lying or gently dipping thick Innaminka Red Beds as found in most Merrimelia wells, fracture density tends to be moderate to high in siltstone and sandstone, but nil to low in the interbedded bioturbated mudstone and micaceous shale. Generally speaking, steeply dipping strata have higher fracture density than flat-lying beds. Thicker beds have less fractures than thinner beds which have undergone the same structural history.

## DISCUSSION

### Major fracture types and orientations

Three main types of natural fractures are identified in the Warburton Basin, namely regional, tectonic and contractional. Possible contractional fractures have been recognised in the volcanics, varying from the acid Mooracoochie Volcanics such as in Gidgealpa 2 and 3 to basalt of Murteree A1. Since such fractures are sinuous, irregular and discontinuous, their orientations cannot be mapped.

Regional, high angle fractures are the most significant, forming two systems of orthogonal pairs. They cross local structures, and extend beneath the Cooper Basin in South Australia. They can be used as a guide to interpret fractures in cores from unoriented wells. System I has a pair of orthogonal fractures, striking NNE-SSW (20-200°) and ESE-WNW (110-290°). System II has a pair of orthogonal



**Fig. 31** Core photo in Jennet 1, showing possible open fractures in brittle coarse sandstone.

fracture sets, striking NE-SW (60-240°) and NW-SE (150-330°). System I is similar in direction to low frequency lineaments NNE8 (approximately 20°) and WNW9 (approximately 290°) referred to the Tethyan primary and orthogonal lineament network by Boucher (1998b). One of the system II fractures is similar in direction to low frequency lineament NE1 (approximately 60°), but the other is not recognised in lineament data (Fig. 30). The high degree of directional similarity indicates that these lineaments are basically related to deep-seated fracture systems in the Warburton Basin. According to Boucher (1998b), intersections of the WNW and NNE lineaments of the Tethyan primary and orthogonal lineament network are not prospective for petroleum but provide prospective mineral targets. He also found that most of the larger gas fields occur in 'shadow zones', 1-10 km from the NW and NE trending lineaments. However, in the Warburton Basin,

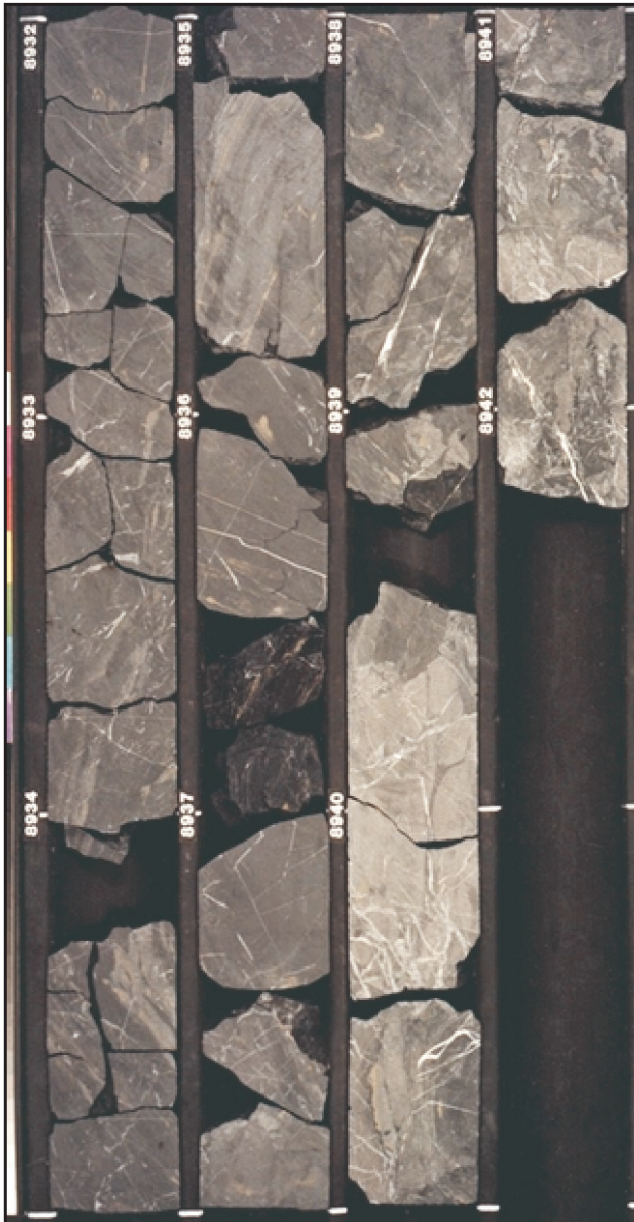


**Fig. 32** Core photo in Kalanna 1, showing high to very high grades of fracture density.

WNW 9 is parallel to the strike direction of productive open fractures in Lycosa 1.

Similarly oriented orthogonal natural fracture sets have been recognised independently from FMS data by Hillis *et al.* (1997, p.13) in the lower Patchawarra Formation of the Cooper Basin. However, in the Big Lake Suite granodiorite of Moomba 73, Hillis *et al.* (1997) interpreted only northwest striking fractures. Fractures in Big Lake Suite cores have not been studied here.

### Origin of fractures

In a recent publication on naturally fractured reservoirs, Aguilera (1997, p.26) stated that various reasons have been offered to explain the existence of regional fractures. These include: (1) Regional uplift (Price, 1966), (2) Fatigue due to low level cyclic stress differentials, (3) Formation of fractures soon after sedimentation, due to prolongation of fractures in the beds below. The first explanation is the best

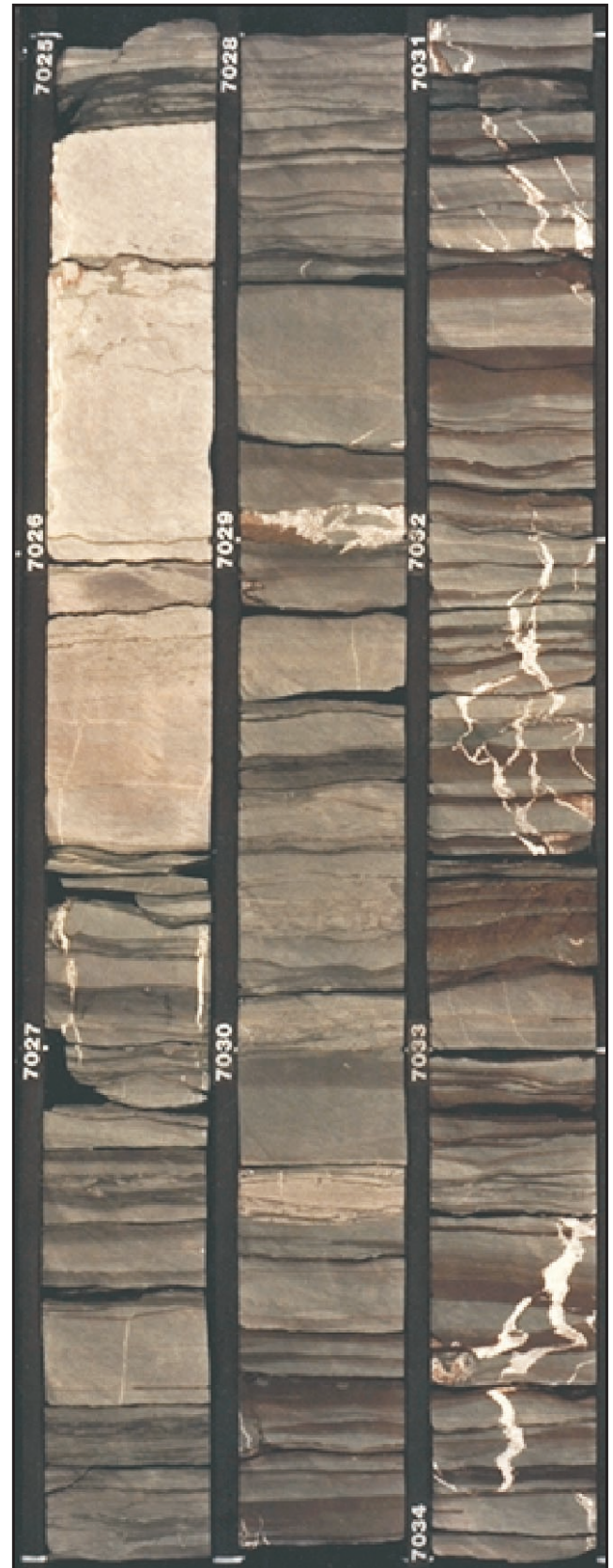


**Fig. 33** Core photo in Titan 1, showing moderate grade of fracture density.

but it cannot explain the occurrence of two superposed patterns (four fractures) (Stearns and Friedman, 1972). Although no single explanation has proven conclusive, regional fracture systems produce hydrocarbons in

numerous fields, they are second in importance only to tectonic fractures in hydrocarbon production. Excellent fractured reservoirs occur when tectonic fracture systems are superposed over a strong regional system (Nelson, 1985, p.19). Some of these reservoirs include the Austin chalk, the Big Sandy field of eastern Kentucky and West Virginia which produces from Devonian shale (Bagwal and Ryan, 1976), the Altamont-Blue Bell field of Utah which produces from fractured sandstone (Baker, 1972). Regional fracture systems have also been called "systematic joints" by many authors (see Nelson, 1985 for references) because they are consistently distributed over a large area with orientation variations of only 15-20°, and fracture spacing ranging from just under 1 ft to over 20 ft vertically along the borehole axis. Warburton Basin regional fractures have all these characteristics, thus have reservoir potential.

The regional fractures in the Warburton Basin may be caused by regional uplift, and the two systems may have been caused by two different regional stress fields, due possibly to the Benambran and Alice Springs Orogenies. The Bebrambran Orogeny was responsible for mid-Palaeozoic convergent tectonism on the eastern part of the Australian continent (E-W compression) while the Alice Springs Orogeny was responsible for convergent tectonism in Central Australia (N-S compression). Timing of system I and II is difficult to determine, it is possible that system I postdates II. As observed in Gidgealpa 5 (7942') regional fracture system I (200°) displaced system II (240°); a similar case exists in Lycosa 1. It is interesting that younger fractures have much finer apertures (about 0.1-0.3 mm) than older fractures (about 10-20 mm). One of the regional fracture systems, 20-200° and 110-290° in

the basin is almost parallel to NNE (G8, GD) and WNW (RD5, RD6) lineaments with less than 5° discrepancy. Sprigg (1961) believed that the lineaments were due to crustal fracture. They have been interpreted as fundamental lineaments controlling morphology of the Warburton Basin, which influenced distribution of oil and gas fields of the overlying Cooper and Eromanga Basins (Campbell and O'Driscoll, 1989). These authors also stated that the Warburton Basin was framed by the NNE and WNW continental lineaments. Interestingly, Price (1974) suggested that the two orthogonal orientations of most regional fracture sets parallel the long and short axes of any sedimentary basin due to the loading and unloading history of the rock. Supporting studies have been reported in Narr and Currie (1982) and Das Gupta and Currie (1983). If the regional fractures in the Warburton Basin are superposed over these crustal fracture lineaments, they are expected to be inherited by the Cooper Basin.

The tectonic fractures in the Warburton Basin include mainly fold and fault related fractures. Friedman (1969) used the orientation of microscopic fractures from oriented cores in the Saticoy Field of California to determine the orientation and dip of a nearby fault. There are not enough data to determine a relationship between faulting and fracturing. Only for those fractures along the fault planes or associated with small-scale thrust faults and reverse faults, can the orientation of fault movement be determined (Table 12). For other fractures associated with structural features, I can only decide their nature but not their orientations. The fractures related to folding include those associated with microfolds such as seen in Wantana 1 and Dullingari 1 (Figs. 11a, b). The fractures due to microfaults include reverse faults in Lycosa 1 (Fig. 11g) and

**Table 12** Orientations of fault-related tectonic fractures.

Well depth (feet)	Type	Dip azimuth (degree)	Dip angle (degree)	Slickensides, tension gashes	Slickensided lineation Direction (degree)
<b>Lycosa 1</b>					
8793	reverse fault	171	20	no	-
8802	fracture	32	26	yes	96 (older)
	fracture	129	80	yes	133
(younger)					
8810	reverse fault	158	84	yes	146
<b>Wantana 1</b>					
9634'3"	reverse fault	169	60	no	-
<b>Gidgealpa 1</b>					
12605'	thrust fault	67	32	yes	~67
~10000'	thrust fault	155	37	no core	no core
<b>Gidgealpa 19</b>					
7400'	thrust fault	150	20	no core	-
<b>Gidgealpa 7</b>					
9069	thrust fault, associated with fault breccia	SE	no data	no data	no data
<b>Packsaddle 1*</b>					
10386'	thrust fault, fracture	150	60	no	
<b>Gidgealpa 1</b>					
11682'	slickensided surface	233	50	yes	143
<b>Gidgealpa 5</b>					
8391'	slickensided surface	4	65	yes	no data
7946'	slickensided surface	193	25	yes	223
8793'	? fault plane, fracture	40	5	yes	no data
<b>Packsaddle 3</b>					
7217'4"	slickensided surface	63	70	yes	231
<b>Snake Hole 1</b>					
9315'6"	slickensided surface	277	80	yes	277
<b>Jennet 1*</b>					
5525	slickensided surface	330	65	yes	160
<b>Pelketa 1</b>					
7097'6"	slickensided surface	124	40	yes	108

\* assumed from relative orientation and seismic interpretation



**Fig. 34** Core photo in Meranji 2, showing low grade of fracture density.

Wantana 1 (Fig. 11f), thrust faults in Packsaddle 1 and Gidgealpa 1 (Figs. 11c, d); and normal faults in Gidgealpa 4 (Fig. 5c). A conjugate set of fractures in Lycosa 1 (Fig. 11i) possibly relates to faulting. The orientation of thrust faults and reverse faults can be determined from dipmeters and core measurement in several wells. (Table 12).

Slickensided fractures are common, and more or less superposed over regional fractures as indicated by associated thrust or reverse faults and fault breccias. Thrust faults and slickensided surfaces (Table 12) are dominantly SE dipping, and slickenside lineations are dominantly NW-SE. They indicate a NW-SE compressional regime. The GMI Ridge is believed to have overprinted the pre-existing Warburton Basin thrust belt. The GMI Ridge trends in a curve 50-60° (NE); thrust faults or reverse faults associated with it should dip 140°, 150°, 160°, depending on which compartment the faults are located in along the ridge. Amazingly, Gidgealpa 1,

5, 7, 19, fit about 140-150° dip angles; while Wantana 1 fit 169°, and Packsaddle should be 150°. Furthermore, 150° striking fractures have been measured from many wells around this domain. Therefore, the tectonic fractures are believed to overprint regional fracture system II by thrust and reverse faulting and slickensides.

The contractional fractures in the volcanics are probably due to thermal contraction, caused by volume reduction during cooling of lava. The classic example of natural thermally induced fractures is columnar jointing in fine-grained igneous rocks (Peck and Minakami, 1968). Sustained flow of oil and water of up to 1,000 bbl/day was achieved from such contractional fractures in the Tertiary basalt flows at West Rozel Field, Salt Lake, Utah (Nelson, 1985, p.24). The Jena Basalt in Murteree A1 is severely fractured, but the fractures have been mineral filled. If they were not filled, excellent fracture porosity and permeability would have had existed and may still be present at undiscovered locations.

### Fracture fairway

Steeply dipping regional fractures cross the Warburton Basin and are interpreted to constitute two orthogonal sets which strike NNE/WNW and NE/NW. These directions remain the same in different structural domains at least on the drilled anticlines. Based on FMS interpretation the gas-productive open fracture system in Lycosa 1 strikes WNW and NW (Fig. 37) which leads to a conclusion that all open fractures in the region will similarly strike these two directions. However, FMS interpretation in Malgoona 4 (approx. 53 km from Lycosa) indicates a NNE-SSW open fracture strike direction in addition to the above two strike directions. Three directions of open fractures in Malgoona 4 seem unlikely and needs further study to clarify if some of them are alternatively caused by conductive minerals.

Although the regional fracture pattern does not vary across different local structural zones, the choice of which fractures are open probably does. The preferred orientation of open fractures is controlled by several factors, which include:

- superposition by tectonic structures
- reactivation through geological history
- younger tectonic movements
- present day stress state

As mentioned in the discussion on the origin of fractures, tectonic fractures are believed to be superposed over regional fracture system II as a result of thrusting and reverse faulting, and also over regional fracture system I as evidenced by slickensides. Therefore, they have potential for fluid communication after tectonic movement.

Natural fractures found in the Cooper Basin may be caused by reactivation of the old Warburton Basin thrust belt, as old faults were propagated along the crests of the GMI Ridge as observed in seismic sections (Sun, 1997). Since compression has caused reactivation several times after the Late Carboniferous, filled fractures may be re-opened due to reactivation of relatively weak zones. Furthermore, the two sets of regional fractures in the Warburton Basin are very close to two lineament networks which occur within the Cooper Basin area and recognised by Campbell and O'Driscoll (1989) and Boucher (1998b). This

further supports the commonly held opinion that the Cooper Basin structures are inherited and reactivated from underlying Warburton Basin structures.

Mesozoic wrench fault activity and Tertiary east-west compression have generated large scale strike-slip faults and folds. These structures drape over the thrust belt and fault zones of the Warburton Basin. As a result, these deformations probably created new fractures, others may have re-opened previously filled fractures of the Warburton Basin. NW-SE striking fractures of system II may be related to strike-slip wrench faults along the GMI Ridge.

From borehole breakouts Hillis *et al.* (1997) interpreted the maximum horizontal stress to be oriented approximately east-west in the Nappamerri Trough area. Any steep-dipping, east-west striking, pre-existing fractures in the Trough should thus be open and potentially productive. It is possible that natural fractures can be re-opened if they are parallel to such maximum *in situ* stress direction. Relatively few wells, Munkarie 1, Pelketa 1, Wantana 1, Yalcumma 1, Boxwood 1 and Gidgealpa 2 have close to E-W striking fractures. It is worth knowing that the interpreted maximum horizontal stress is not exactly east-west, but slightly WNW (see Hillis *et al.*, 1997, Fig. 2.2). Furthermore, in Moomba and Wantana and other areas, it varies from WNW to NW. Therefore, it is possible that WNW (110-290°) striking regional fractures could re-open due to *in situ* stress. This is probably the case in Lycosa 1, in which the SW dipping fractures striking WNW (110-290°) were probably previously filled by calcite but re-opened later.

Considering all the factors, the preferred orientation of open fractures probably will include in decreasing order of likelihood order: WNW trending regional fractures of system I, NW oriented fractures of system II, and possibly NNE trending fractures of system I.

Although most fractures from the studied wells are either filled with minerals or deformed with gouge-fill or slickensides, some open fractures and many partially open fractures are observed both from cores and FMS. Although more than 90 wells in the Warburton Basin have hydrocarbon shows (Sun and Gravestock, 1999), they were not tested with fractures in mind, and were not optimally drilled. With few exceptions Cooper Basin wells are not designed to test naturally fractured reservoirs either. This is similar to the situation pointed out by Aguilera (1997) as a reason why many naturally fractured petroleum reservoirs around the world have not become profitable discoveries. Many have been abandoned because of 1) incorrect pressure extrapolations, 2) poor completions, and/or 3) failure to intersect the natural fractures. For example, three vertical wells were drilled in the Dilly field's Austin Chalk unsuccessfully. As a result the lease was dropped in 1979. More recently two horizontal wells were drilled in the same general area and were successful. Another example where a vertical and a second, slightly deviated well failed to yield commercial production is in the Palm Valley gas field, Amadeus Basin. A third well was drilled as a highly deviated well from the same borehole, it produced 137 MMSCFD from naturally fractured reservoir (Fig. 38). The successful gas producer Lycosa 1 is an unusual deviated well (max. 17.9°), and its success may be due in part to the unintentional deviation.

The Palm Valley gas field fracture systems are localised, mainly tectonic fractures related to a doubly plunging

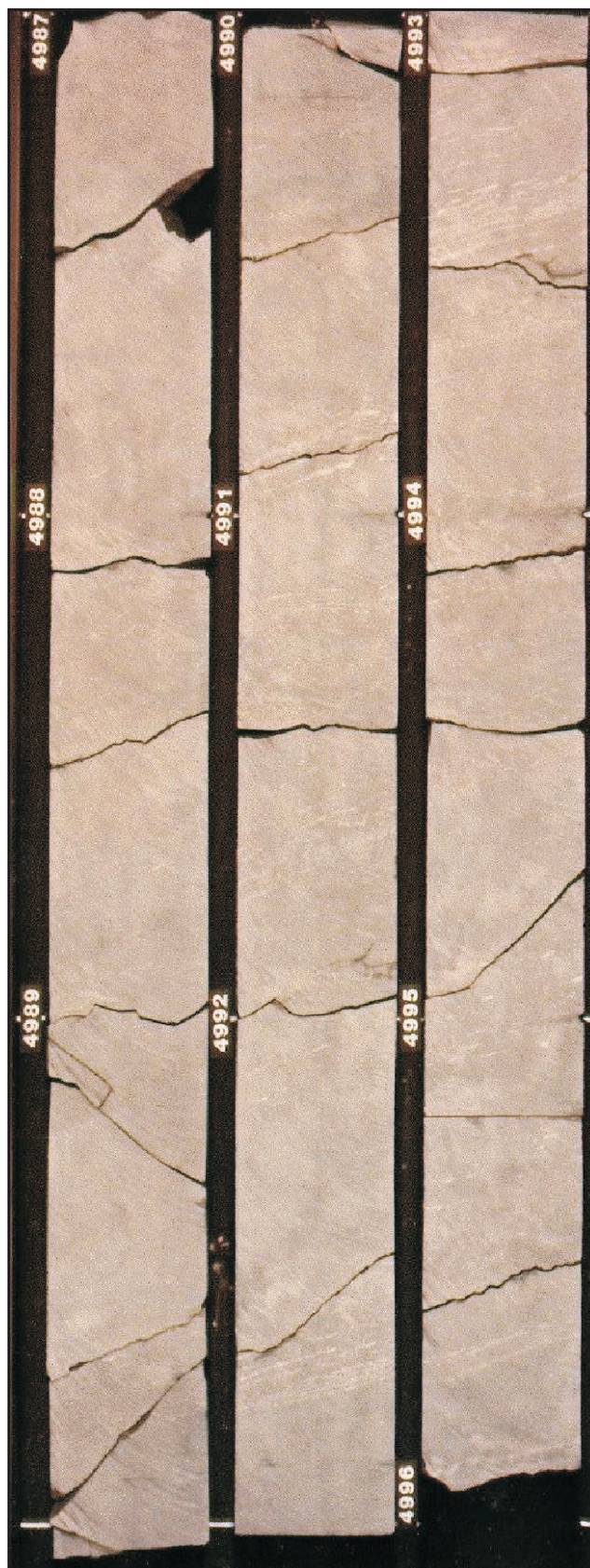


Fig. 35 Core photo in Dunoon 1, showing nil grade of fracture density.

anticline (Berry *et al.*, 1996) whereas the fracture systems in the Warburton Basin are regional, but superposed by tectonic fractures in many localised structures essentially related to thrust and reverse faults or fault-related anticlines.

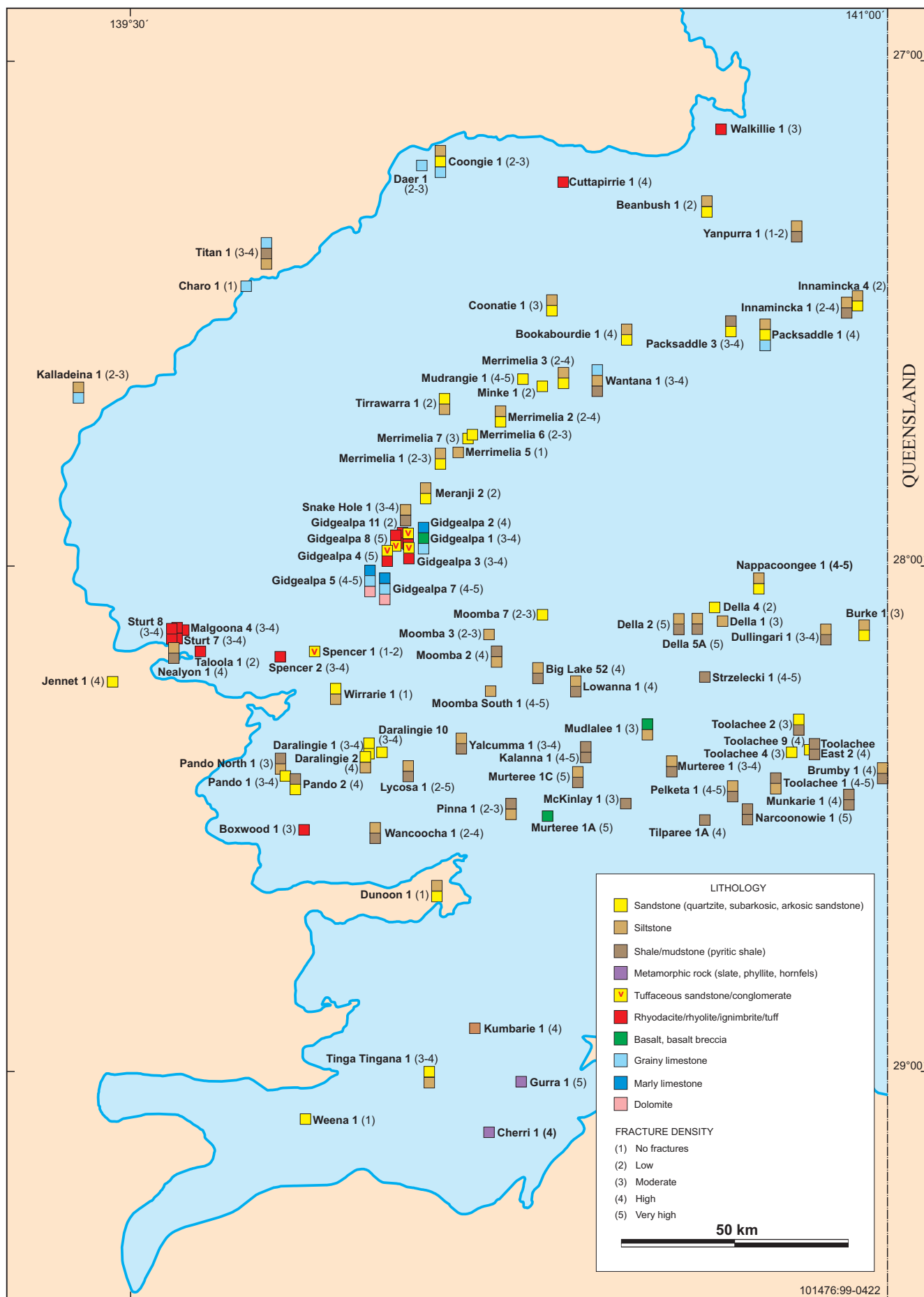
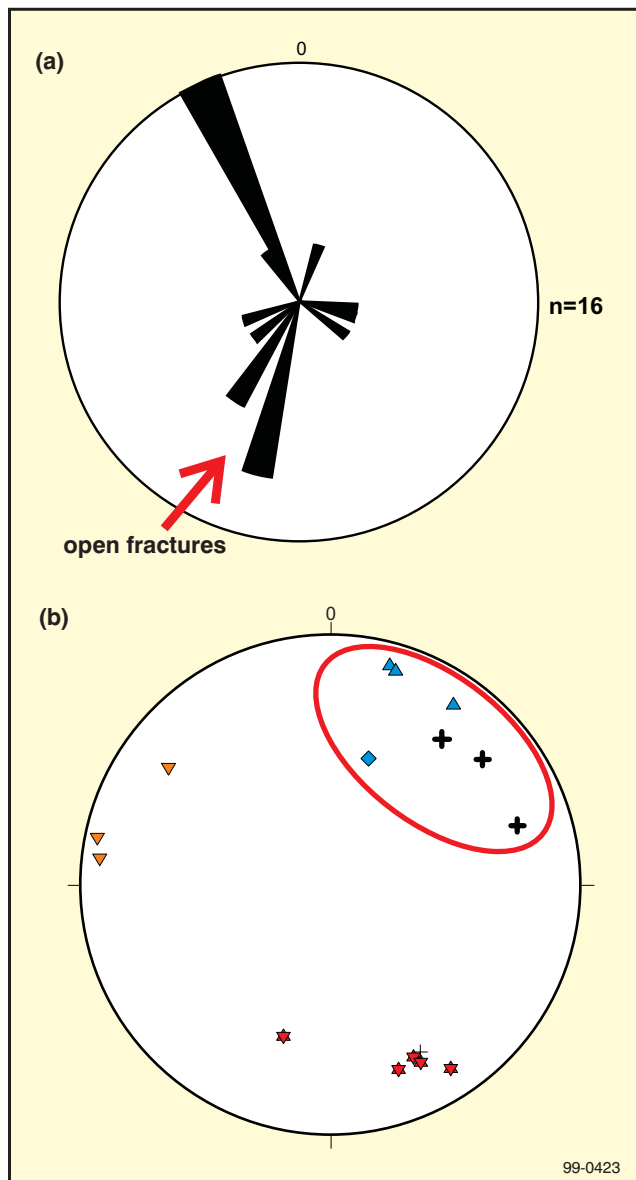
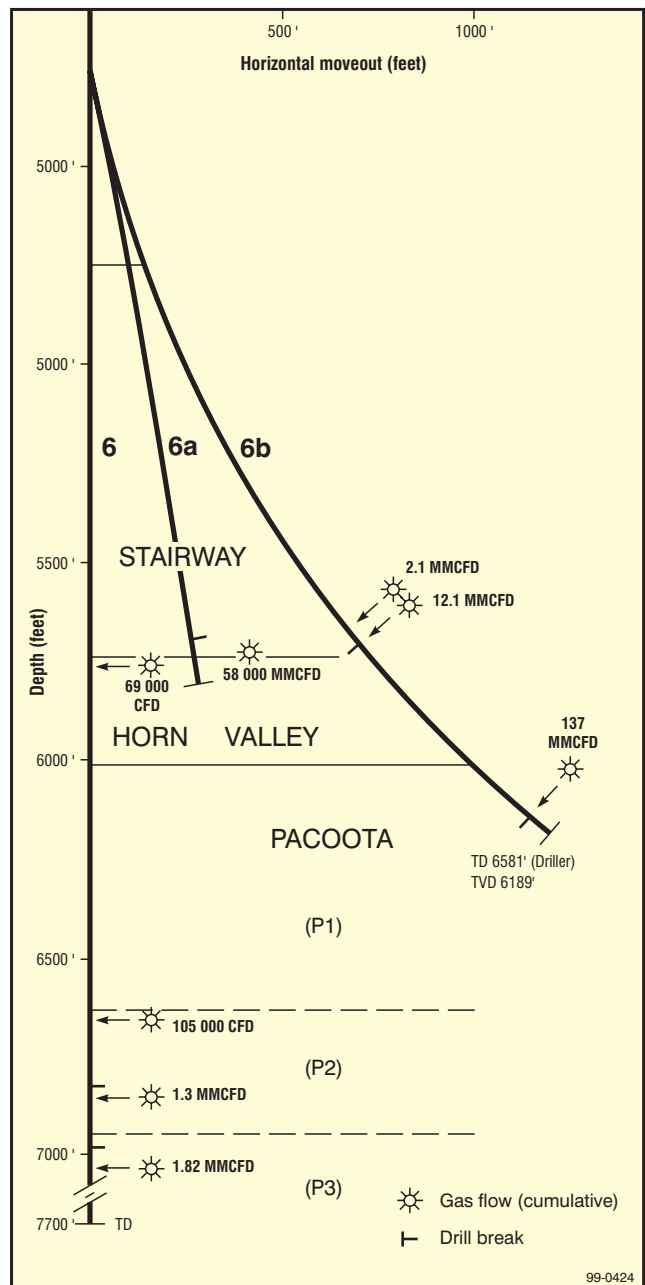


Fig. 36 Fracture density map of the Cooper Basin with main lithologies.



**Fig. 37** High angle fractures in Lycosa 1, including those interpreted from FMS (symbol +),  
 (a) rose diagram,  
 (b) lower hemisphere, stereographic projections of poles to, open fractures are within red circle and dip SW.



**Fig. 38** Well deviation plot – Palm Valley 6, 6a, 6b – showing location of drill breaks and cumulative gas flows. (from Aguilera, 1997).

## CONCLUSIONS AND RECOMMENDATIONS

This study is the first of its kind to characterise and analyse fracture systems in the Warburton Basin from 199 cores and wireline logs of 93 wells beneath the Cooper Basin in South Australia. Of the 93 wells, about 22 are oriented and 3 wells have FMS data, among them, Lycosa 1 has been studied intensively because it has produced gas from a fractured reservoir with the most complete data sets.

Natural fractures can be classified into contractional, regional and tectonic types. The Contractional fractures have been recognised in acid and basic volcanics. The regional high angle fractures comprise two systems of orthogonal pairs. They extend beneath and probably through the Cooper Basin in South Australia, and cross local structures. System I has a pair of orthogonal fractures, striking NNE-SSW and ESE-WNW. System II has a pair of orthogonal fracture sets, striking NE-SW and NW-SE. System I is similar in direction to low frequency lineaments NNE8 and WNW9 identified by Boucher (1998b). They are fairly close to NNE (G8, GD) and WNW (RDS, RD6) lineaments. The similarity of the regional fracture systems in the Warburton Basin and these lineaments suggests that the lineaments are related to the deep-seated fracture systems. The regional fracture pattern is useful for interpreting fractures measured from unoriented wells.

The tectonic fractures in the Warburton Basin include fractures related to mainly folds, thrust and reverse faults, and minor normal faults. From a few oriented wells, fault planes of thrust and reverse faults along the GMI Ridge dip SE, slickensides are very common and have majority orientation NW-SE. These features confirm a compressive tectonic regime interpreted from seismic and borehole breakout data. The tectonic fractures are superposed on the regional fractures.

Lithological control on fractures includes the following points. Thinly-interbedded siltstone and shale have more fractures than adjacent thick bedded sandstone mainly in the Dullingari Group. Thinly bedded brittle rocks of the Innamincka Formation including sandstone and siltstone are fractured whereas the adjacent thick ductile beds such as bioturbated micaceous mudstone are hardly fractured. Brittle dolomite and grainy limestone are also fractured and brecciated more than marly limestone of the Kalladeina Formation. Fine-grained tuff has fewer fractures than the adjacent welded ignimbrite of the Mooracoochie Volcanics.

Fracture density is not even in many wells, but varies with vertical depth. Density is controlled by structural style and structural intensity, less importantly by lithology. The greatest fracture density is associated with fault breccia, and located at fault zones or structural culminations. They are possibly caused by mainly thrust, reverse and strike-slip faults. Because this report mainly concentrates on hand specimens and some thin sections of about 20% of core specimens, it is possible that microfractures will be under-estimated. Further microscopic study is recommended.

More than 90 wells in the Warburton Basin have hydrocarbon shows, including some with drilling evidence indicating the existence of fractured reservoirs. This further encourages discovery at Warburton Basin depths. Future wells should be drilled at least 400 feet vertically into the Warburton Basin contacting Cooper Basin source rocks, and wells should be deviated approximately 30° from horizontal in the fracture zone to intersect open fractures. Proper testing for hydrocarbons in the Warburton Basin is recommended. Wireline logs should include dipmeter or FMS, especially where bedding dips are suspected to be significant.

## REFERENCES

- Aguilera, R., 1997. Naturally fractured reservoirs. Second edition. Pennwell Books. 515pp.
- Baker, D.A. and Lucas, P.T., 1972. Strat trap production may cover 280 plus square miles. *World Oil*, 65-68.
- Baily, T.A., 1991a. Lycosa 1 well completion report for Santos Ltd. *South Australia. Department of Primary Industries and Resources. Open file Envelope, 7290* (unpublished).
- Baily, T.A., 1991b. Sturt 6 well completion report for Santos Ltd. *South Australia. Department of Primary Industries and Resources. Open file Envelope, 7299* (unpublished).
- Baily, T.A., 1996. Gahnia 1 well completion report for Santos Ltd. *South Australia. Department of Primary Industries and Resources. Open file Envelope, 7518* (unpublished).
- Berry, M.D., Stearns, D.W. and Friedman, M., 1996. The development of a fractured reservoir model for the Palm Valley Gas Field. *The APPEA Journal*, 36:82-103.
- Boucher, R.K., 1998a. A beginner's guide to picking basement from wireline logs, Cooper Basin area. *South Australia. Department of Primary Industries and Resources. Report Book 97/37a*, p.1-16.
- Boucher, R.K., 1998b. Lineament associations in the Cooper Basin region, South Australia: basement controls on hydrocarbon distribution. *South Australia. Department of Primary Industries and Resources. Report Book 98/00030*. (unpublished).
- Campbell, I.B. and O'Driscoll, E.S.T., 1989. Lineament-hydrocarbon associations in the Cooper and Eromanga Basin. In: O'Neil, B.J. (ed.), *The Cooper and Eromanga Basins, Australia. Proceedings of the Petroleum Exploration Society of Australia, Society of Petroleum Engineers, Australian Society of Exploration Geophysicists (S.A. Branches), Adelaide*, p.295-313.
- Carroll, P.G., 1990. Pre-Permian structure and prospectivity at Gidgealpa, South Australia. *University of Adelaide, M. Sc. thesis* (unpublished).
- Chin, A., 1991. Santos Limited Malgoona 4 FMS Interpretation. In: Nugent, O.W., 1992. Malgoona 4 well completion report for Santos Ltd. *South Australia. Department of Mines and Energy. Open file Envelope, 7395* (unpublished).
- Crozier, P.N., 1999. Special core analysis final report of Cooper Basin Paleozoics for PIRSA. *South Australia. Department of Mines and Energy. Open file Envelope 9267* (unpublished).
- Daily, B., 1964. Appendix 3 part B and Addendum to Appendix 3 part B. In: Harrison, J. and Higginbotham, G.T., 1964. Delhi-Santos Gidgealpa No. 1 South Australia, Well Completion Report. *South Australia. Department of Mines and Energy. Open file Envelope 363* (unpublished).

- Das Gupta, U. and Currie, J.B., 1983. An application of photoelastic models to explain microfractures and joints in carbonate strata. *Can. Jour. Earth Sci.*, 20:1682-1693.
- Delhi-Santos, 1964. Gidgealpa 5 well completion report. *South Australia. Department of Mines and Energy. Open file Envelope*, 449 (unpublished).
- Friedman, M., 1969. Structural analysis of fractures in cores from the Saticoy field, Ventura County, California. *AAPG Bulletin*, 53(2):367-389.
- Gatehouse, C.G., 1986. The geology of the Warburton Basin in South Australia. *Australian Journal of Earth Sciences*, 33:161-180.
- Gravestock, D.I., Alexander, E.M., Morton, J.G.G. and Sun, Xiaowen, 1998. Reservoirs and seals. In: Gravestock, D.I., Hibburt, J.E. and Drexel, J.F., 1998. The petroleum geology of South Australia Volume 4: Cooper Basin. *South Australia. Department of Primary Industries and Resources. Report Book 98/9, p.159-181.*
- Gravestock, D.I. and Flint, R.B., 1995. Post-Delamerian compressive deformation. In: Drexel, J.F. and Preiss, W.V. (eds.). *Geology of South Australia. Vol.2, The Phanerozoic. South Australia. Department of Primary Industries and Resources. Geological Survey Bulletin*, 54:80-81.
- Hillis, R.R., Meyer, J.J. and Magee, M.E., 1997. The contemporary stress field of the Nappamerri Trough and its implications for tight gas resources. *Confidential Report for PIRSA* (unpublished).
- Kulander, B.R., Dean, S.L. and Ward, B.J. Jr., 1990. Fractured core analysis: interpretation, logging, and use of natural and induced fractures in core. *AAPG Methods in Exploration Series*, No.8, 88pp.
- Kuang, K.S., 1985. History and style of the Cooper-Eromanga Basin structures. *Australian Society of Exploration Geophysicists, Bulletin*, 16(2/3): 245-248.
- Morgeneier, C., 1985. Kalanna 1 well completion report for Delhi Petroleum Pty. Ltd., *South Australia. Department of Mines and Energy. Open file Envelope*, 6041 (unpublished).
- Nelson, R. A., 1985. *Geologic analysis of naturally fractured reservoirs. Contributions in Petroleum Geology and Engineering 1.* Gulf Publishing Company Book Division Houston, London, Paris, Tokyo, p. 320pp.
- Narr, W. and Currie, J.B., 1982. Origin of fracture porosity – example from Altamont field, Utah. *AAPG Bulletin*, 66(9):1231-1247.
- Nugent, O.W., 1991. Sturt 7 well completion report for Santos Ltd. *South Australia. Department of Primary Industries and Resources. Open file Envelope*, 7303 (unpublished).
- Ostler, S., 1996. Toolachee 51 well completion report for Santos Ltd. *South Australia. Department of Primary Industries and Resources. Confidential Envelope*, 7517 (unpublished).
- Peck, D.L. and Minakami, T., 1968. The formation of columnar joints in the upper part of Kilauean Lava Lakes, Hawaii. *Geol. Soc. Amer. Bull.*, 79(9):1151-1166.
- Pemberton, R.L., 1970, Coongie No.1 well completion report. Flinders Petroleum No Liability. *South Australia. Department of Mines and Energy. Open file Envelope* 1388 (unpublished).
- Pexa Oil, N.L., 1970. Final Report on Cherri No. 1 Well, South Australia. *South Australia. Department of Mines and Energy. Open file Envelope* 1340 (unpublished).
- Phillips, S.E., 1997. Petrology report Narcoonowie 1 and Putamurdie 1, Warburton Basin. *Report to PIRSA. Open file Envelope* 9267 (unpublished).
- Price, N.J., 1966. *Fault and joint development in brittle and semi-brittle rock*, Pergamon Press, London, 176p.
- Price, N.J., 1974. The development of stress system and fracture patterns in undeformed sediments. *Proc. Third Cong. Intern. Rock Mech.*, TA 487-496.
- Rayner, B.L. and Chin, A., 1990. Lycosa-1 Formation MicroScanner image examiner interpretation. In: Baily, T.A., 1991. Lycosa-1 well completion report for Santos Ltd. *South Australia. Department of Mines and Energy. Open file Envelope*, 7290 (unpublished).
- Rezaee, M., 1997. Timing of fracture-filling cements in the Warburton Basin. *South Australia. Department of Mines and Energy. Open file Envelope*, 9267 (unpublished).
- Roberts, D.C., Carroll, P.G. and Sayers, J. 1990. The Kalladeina Formation - A Warburton Basin Cambrian carbonate play. *The APEA Journal*, 30(1):166-184.
- Schlumberger Well Services, 1997. Fractures in geological applications of dipmeter and borehole electrical images. Schlumberger Oilfield Services.
- Sprigg, R.C., 1961. On the structural evolution of the Great Artesian Basin. *The APEA Journal*, 1:37-56.
- Stearns, D.W. and Friedman, M., 1972. Reservoirs in fractured rock. *AAPG Memoir*, 16:82-100.
- Sun, Xiaowen, 1996. Sequence stratigraphy, sedimentology, biostratigraphy and palaeontology of the eastern Warburton Basin (Palaeozoic), South Australia. *University of Adelaide. Ph.D. thesis* (unpublished).
- Sun, Xiaowen, 1997. Structural style of the Warburton Basin and control in the Cooper and Eromanga Basins, South Australia. *Exploration Geophysics*, 28, p.333-339.
- Sun, Xiaowen, 1998. Prediction of carbonate reservoirs and traps by applying sequence stratigraphy in the eastern Warburton Basin, South Australia, 1998 *The APPEA Journal*, 38(1), 380-398.
- Sun, Xiaowen and Gravestock, D.I., 1999. Potential hydrocarbon reservoirs in upper levels of the eastern Warburton Basin, South Australia. *South Australia. Primary Industries and Resources. Report Book* (in prep).
- Taylor, S., Solomon, G., Tupper, N., Evanochko, J., Horton, G., Waldeck, R., and Phillips, S., 1991. Flank plays and faulted basement: new directions for the Cooper Basin. *The APEA Journal*, 31(1):56-73.
- Wopfner, H., 1985. Some thoughts on the post-orogenic development of northeastern South Australia and adjoining regions. *Spec. Publ. South Australia. Dept Mines and Energy*, 5:365-372.

## ACKNOWLEDGMENTS

I am grateful for receiving a Postdoctoral Fellowship from the Petroleum Group, PIRSA for this comprehensive study. I appreciate constant encouragement and supervision from Dr Dave Gravestock at the Petroleum Group. I would like to thank Messrs Brian Logan, Michael Pate, Kevin Braithwaite with excellent service of core inspection. Thanks also go to Les Tucker for his assistance with microphotographs, to Dragan Ivic for generating maps, and to Gayle Bruggemann, Jeff Weber, Ann Young and Adrian Francis for excellent drafting and desktop publishing skills.

# FRACTURE ANALYSIS OF THE EASTERN WARBURTON BASIN (EARLY PALAEOZOIC), SOUTH AUSTRALIA

Disk contains data files for Appendix 1, 2, 3 and 4

## Appendix 1

Stereon1.xls is an Excel file containing measurement data

## Appendix 2

Contains StereoNett TXT files.

Nodmeter directory contains 61 files for Stereonet, rose, density and text data files for those without dipmeters.

Dipmeter directory contains 185 files for Stereonet, rose, density and text data files for those with dipmeters.

The software required to view these files is free for non-commercial use and available from the following website

<http://homepage.ruhr-uni-bochum.de/Johannes.P.Duyster/stereo>

## Appendix 3

Fracture 1 : Excel file - basic data for wells with dipmeters

Fracture 2 : Excel file - basic data for wells without dipmeters

## Appendix 4

Excel file : 45 mean high angle fracture strike data of absolute measurement and plots

	A	B	C	D	E	F	G	H	I	J	K	L	M	N	O	P	Q	R
1	Well	depth	KIND	No.	Marks	Azimu		Dip	assumed dip azi.	reasons	dipmeter log	Comment	chronology	fill	Deviation	Dev Azi	Dipmeter picks (WCR)	file names
2	Boxwood 1	6332	bedding	1	green	0	63	60-65			6220-6250	bedding						
3			frac(1)	2	red	170	60				24-30NW326	fracture						
4			frac(2)	3	blue	126	80				? fractures, fault	fracture						
5			frac(3)	4	green	42	55	50-60			6280-6326	fracture						
6			frac(4)	5	green	25	63	60-65			20-32SE137-170	fracture						
7																		
8																		
9	6339	bedding			green	0	47	45-50				bedding						
10					purple	105		low				low angle fracture						
11			fault plane		no plastic			70			?bedding	fault plane, can be discontinuous						
12			fracture				12	10-15			36 SWS195	oblique to the fault plane, low angle fracture		brownish, ?				
13			bedding		no plastic		47	45-50			? Fracture							
14			fault plane				80	70-90				similar fault, but steeper,						
15			slickenside				30					along fault plane, crosscut bedding plane		calcite + chlorite?				
16	6155-61546"	bedding			no plastic		63	60-70				ignimbrite, possible bedding 10-15dg						
17			fault plane		no plastic							60 dg to 70, shear plane?		filled by kaolinite				
18																		
19																		
20																		
21																		
22																		
23	Daralingie 1	c2, 7420'	bedding	1	green	0	67	65-70			missing	bedding, quartzose sandstone						
24			frac(1)	2	blue	224		65				high angle fracture		brownish, ?				
25			frac(2)	3	red	285		70				high angle fracture		0.1-0.2mm, yellow, ? still open				
26			frac(3)	4	red	315		25										
27																		
28																		
29																		
30	Della 1	7123	bedding	1	green	0	42				CDM							
31			frac(1)	2	yellow	60	80				SE 20dg							
32			frac(2)	3	yellow	60	72					high angle fracture		0.05mm, black?				
33			bedding	1	green	0	55					high angle fracture						
34			frac(1)	2	yellow	88	88					lineation of bedding, not sure						
35			frac(2)	3	yellow	90	82					high angle fracture						
36																		
37	Dullingari 1	9210'6"	bedding	1	green	0	60	60	27	should be opposite		bedding						
38			frac(1)	2	blue	46	81	81		deviated direction		high angle fracture,		0.2mm, ? Dolo.				
39			frac(2)	3	purple	236-56	87	85-90		S27W, 1dg.		? Induced curved, open frac, changing dip						
40			bedding	1	green	0	60	60	27	should be opposite								
41			frac(1)	2	brown	180	20	20		deviated direction				0.2-1mm, ? Dol.				
42			frac(2)	3	black	27	55	55		S27W, 1dg.		? Induced,		< 0.1mm				
43			bedding	1	green	0		?										
44	9198'-2"	bedding	frac(1)	2	blue	162		?										
45			frac(2)	3	blue	162		?										
46			bedding	1	blue	0	85	80-90				sandstone, bedding, not sure						
47			frac(1)	2	yellow	163	62	62										
48			frac(2)	3	purple	122	61	60-62				? stylolite, possible bedding						
49			frac(3)	4	orange	113	43	43										
50			frac(4)	5	yellow	326		30-35				veinlet						
51	9802'4	not exact	bedding	1	green	0						not apparent						
52			frac(1)	2	brown	90		83						pyrite				
53			frac(2)	3	orange	297		30										
54			bedding	1	green	0		?				not recorded						
55			frac(1)	2	orange	334		?				not recorded						
56			frac(2)	3	blue	190		60										
57																		
58	Gidgealpa 1	12605	bedding	1	no plastic	0		25				bedding						
59			thrust fault	2				30-35				thrust fault plane						
60			fracture	3				60				fracture		0.2-0.5mm, calcite	7 max			
61			bedding	1	green	0	32	30-35										
62			frac(1)	2	purple	173		55				important		3mm, calcite				
63			frac(2)	3	red	210		70				not important						
64			frac(3)	4	red	195		50				hairline, 0.2mm		0.2mm, calcite				
65	-10491	bedding	frac(4)	5	yellow	130		45				very fine, vague fracture						
66			frac(1)	2	purple	180		80				fracture, displaced bedding		0.8mm, calcite				
67			frac(2)	3	brown	138		35				microfault replacement		0.2mm, calcite				
68																		
69																		
70																		
71																		
72	9424'8"	bedding	frac(1)	2	purple	280		65				bedding not sure;		2mm, calcite				
73			frac(2)	3	blue	246		60				coarse fracture		1mm, calcite				
74												fracture						
75																		
76																		
77																		
78																		
79	Gidgealpa 2	6890'3"	bedding	1	green	0		25				bedding?						
80			frac(1)	2	blue	138		70				fracture,		0.1mm; hematite?				
81			frac(2)	3	blue	105		80				fracture,						
82																		
83																		
84																		
85																		
86	6898' 3/4"	bedding	frac(1)	2	green	not sure		low angle				bedding?						
87			frac(1)	2	brown	0	50	40-60				fracture,		? Brown , hematite				
88			frac(2)	3	orange	211	40	40				fracture,		lining, hematite,				
89			frac(3)	4	red	120	21	20-22				fracture,		sider or hemat.				
90																		
91																		
92																		
93	6910'	bedding	frac(1)	2	blue	168		68				bedding?						
94			frac(2)	3	blue	162		70				fracture,		0.5mm; ? Kaolinite				
95			frac(3)	4	blue	162		70				fracture,						
96			frac(4)	5	blue	178		60				fracture,		0.2mm; brown, ? Clay				
97																		
98																		
99																		
100	7275'	bedding	frac(1)	2	blue	157		60				bedding?		calcite				
101			frac(2)	3	blue	157		60				fracture,		calcite				
102																		
103																		
104																		
105																		
106																		
107	7276	bedding	frac(1)	2	blue	238		65				? Bedding						
108			frac(2)	3	blue	219		70				fracture,		0.5-0.8mm;calcite				
109			frac(3)	4	blue	51		60				fracture,		0.2-0.3mm;calcite				
110			frac(4)	5	red	234		60				fracture,		0.2mm; calcite				
111			frac(5)	6	red	234		60				fracture,		calcite				</

	A	B	C	D	E	F	G	H	I	J	K	L	M	N	O	P	Q	R
185	Gidgealpa 7	10573	bedding	1	green	0	23	20-25				bedding, not exact (cut not 90 to axis)						
186			fract	2	red	233		40				fracture		0.2mm, calcite				
187		9995	bedding	1	green	0		20				bedding						
188	S31E		fract	2	red	85		85				fracture		1mm, calcite				
189		8074 (a)	bedding (b)	1	green	0		10				bedding (a)						
190			fract(1a)	2	red	90	45	40-50				?hair line fracture						
191			fract(2a)	3	blue	123		70				hairline fracture		calcite				
192		8074(b)	bedding (a)	1	green	0		10				bedding (b)						
193			fract(1b)	2	red	155	43	40-50				?hair line fracture						
194			fract(2b)	3	blue	180		70				hairline fract, up 3cm becomes 80		calcite				
195		7709	bedding	1	green	0		107										
196			fract	2	red	160	73	70-75				calcite filled fracture		0.1-0.2mm, cal				
197	Inammincka 1	71993"	bedding	1	green	0	17	15-20										
198			fract(1)	2	blue	107		85				bedding						
199												fracture						
200																		
201		11424"	bedding	1	green	0		730				bedding						
202			fract(1)	2	blue	73		76				fracture		1.5mm				
203			fract(1)?	3	blue	68		80				fracture		1mm				
204			fract(2)	4	blue	105		80				fracture		1.4mm				
205																		
206		11444"	bedding	1	green	0	31	30-32				bedding						
207			fract(1)	2	blue	218		50				fracture						
208			fract(2)	3	blue	180		68				fracture						
209			fract(3)	4	blue	150		30				fracture						
210		11458	bedding	1	green	0		31				bedding? With heavies lining up						
211			fract(1)	1	blue	235		80				fracture		2mm; calcite				
212																		
213		11462	bedding	1	green	0		30				bedding						
214			fract(1)	2	blue	108		60				fracture		calcite: 0.6mm				
215			fract(2)	3	blue	90		88				fracture		Calcite; 0.2mm				
216																		
217		11465	bedding	1	green	0		33				bedding,						
218			fract(1)	2	blue	220		60				fracture		1.2mm, calcite				
219			fract(2)	3	blue	260		60				fracture		5-7mm, calcite				
220																		
221		11467"6"	bedding	1	green	0		30				bedding,						
222			fract(1)	2	blue	256		86				fracture		1.5mm,				
223			fract(2)	2	brown	141		55				fracture		1mm, calcite				
224																		
225		11553	bedding	1	green	0		36				bedding,						
226			fract(1)	2	blue	70		69				fracture		0.7mm				
227			fract(2)	3	blue	72		65				fracture		0.4mm				
228																		
229		11561"2"	bedding	1	green	0		22				bedding						
230			fract(1)	2	blue	133		78				fracture		0.5mm, calcite				
231																		
232		12070"7"	bedding	1	green	0		38				bedding						
233			fract(1)	2	blue	223		45				fracture		0.6-0.7mm, calcite				
234			fract(2)	3	blue	104		54				fracture		1mm, calcite + catac.				
235																		
236	Lycosa 1	8793'	bedding	1	green	0		35	339	8803.54		bedding, siltstone and shale						
237			fract(1)	2	orange	217		67		339 / 17.5		fracture		calcite			15.4	176
238			fract(2)	3	blue	115		115		dev. 176 / 15.4		fracture		partially calcite				
239	than drillers so core measurements should add 10'	second measure	fract(1)	4	blue	220	65	65				fracture		partially calcite				
240			fract(2)	5	yellow	240	65	60-70	65			should = fract(1), blue		? dolom, pyrite				
241			fract(3)	6	orange	120	80					= red, fine fract., open; cut blue.		calcite				
242			fault plane	7	red	180	5					fracture or fault pla., + slicken.						
243		8798	bedding	1	green	0	57	55-60		8811		bedding, siltstone and shale					15.4	176
244			fract(1)	2	black	207	12	10-15		10 / 41.8		fine, low-angled calcite veinlet	1	calcite				
245			fract(2)	3	black	0 to 6	67	60-70		dev. 177 / 15.6		coarse, high angle, calcite and ?siderite vein	2	2-5mm				
246																		
247		8799' - 4"	bedding	1	no plastic	0		60		as above		bedding, siltstone and shale					15.4	176
248			fract(1)	1	no plastic	~ 0	77	75-80				open fracture, ? induced, disconti.						
249																		
250		8801	bedding	1	green	0	52	50-55		as above		bedding, siltstone and shale					15.6	177
251			fract(1)	2	purple	180	17	15-20				v. fine, low-angled, cut fract(1)		? siderite				
252			fract(2)	3	purple	302		?				v line, 0.1mm		? siderite				
253			fract(3)	4	red	110		60				displace bedding; 0.1-0.8mm,		calcite				
254																		
255		8802 - 3"	bedding	1	simple	0		55		as above		bedding, siltstone and shale					15.6	177
256			fract(1)	2	plastic	116		70				slickenside and calcite, up to 1cm		calcite				
257		slickenside	3			100-280						up to 1mm						
258			fract(2)	4		10		40				up to 1mm						
259		8803	bedding	1	no plastic	0		not mesure	as above			bedding, siltstone and shale					15.7	177
260			fract(1)	2	no plastic	~ 0		not mesure				calcite vein, up to 2.5cm, intercrystal. Pore		calcite				
261			slickenside	3	no plastic	not measure		not measure										
262																		
263																		
264		8805	fract(1)	1	no plastic	120		80				high angle fracture		calcite			15.7	177
265		8806	bedding	1	no plastic	0	57	55-60		as above		bedding, siltstone and shale					15.8	177
266			fract(1)	2	no plastic	~ 0		~90				up to 1mm		calcite				
267			fract(2)	3	no plastic	~ 180						low-angle fracture, filled by up to 0.5mm		? siderite				
268																		
269		8806' 5"	bedding	1	green	0		55		8816.31		bedding					15.8	177
270			fract(1)	2	yellow	37	12	10-20		6 / 61.9		fracture	1					
271			fract(2)	3	blue	330		80		dev. 177 / 15.8		fracture	2					
272			fract(3)	4	red	197	15	10-20				slickenside surface	3					
273			lineation	5	purple	65-248						slickenside lineation						
274																		
275		8806' 5"	bedding	1	green	0		60		8816.31		bedding, siltstone and shale					15.8	177
276			fract(1)	2	blue	335	82	80-85		6 / 61.9		fracture	2					
277			fract(2)	3	yellow	42		15		dev. 177 / 15.8		low-angle, fracture filled by yellow, ? dolo.	1					
278			fract(3)	4	purple	200		30				open						
279																		
280		8807' 6"	bedding	1	no plastic	0		60				bedding, siltstone and shale					15.8	177
281			fract(1)	2	no plastic	~ 180		40				low-angle fracture						
282		8808' 7"	bedding	1	no plastic	0		60				bedding, siltstone and shale						
283			fract(1)	2	no plastic	~ 180		25				low-angle fracture						
284		8809' 5"	bedding	1	no plastic	0		50				bedding, siltstone and shale					15.9	176
285			fract(1)	2	no plastic	~ 180		25				low-angle fracture						
286																		
287		8810	bedding	1	green	0		60		8819.81		bedding, siltstone and shale					15.9	176
288		correct	fract(1)	2	red	338		40		357 / 70.4		x-cut tension gashes						
289			fract(2)	3	green	160	69	68-70		dev. 176 / 15.9		slickenside surface						
290			lineation		green	310-130						lineation of slickenside						
291																		
292		8810'2"	bedding	1	green	0	63	60-65		as above		bedding, siltstone and shale					15.9	176
293			fract(1)	2	red	322		7 20-30				tension gashes						
294			fract(2)	3	blue	155	77	75-80				?slickenside surface						
295			fract(3)	4	purple	321	22	20-30				slickenside cut by blue slickenside						
296			fract(4)	5</														

	A	B	C	D	E	F	G	H	I	J	K	L	M	N	O	P	Q	R
433												after filled with white ? minerals.						

	A	B	C	D	E	F	G	H	I	J	K	L	M	N	O	P	Q	R
434																		
435	No dipmeters Big Lake 52																	
436		9487'8"	bedding	1	green	0		70				bedding, siltstone						
437			frac(1)	2	purple	180		50				hair line, shear quartz vein		brown, ?				
438			frac(2)	3	orange			90				strike parallel to bedding						
439			frac(3)	4								155-335 strike, dip not sure; displace bedding						
440			frac(4)	5								18-198 strike, same as frac(3), both displaced by frac(1) and (2)						
441																		
442	Brumby 1	7710	bedding	1	green	0		25										
443			frac(1)	2	blue	265		55										
444			frac(2)	3	blue	0		45										
445		7709	bedding	1	green	0		25										
446			frac(1)	2	blue	343		40										
447	Cherri 1		frac(2)	3	blue	180		60										
448		4592	bedding	1	green	0	47	45-50										
449			frac(1)	2	purple	175	83	80-85				reliable		0.2mm				
450		4588	bedding	1	green	0		50										
451			frac(1)	2	purple	260	79	78-80										
452			frac(2)	3	brown	210		65										
453		4582	bedding	1	green	0		50										
454			frac(1)	2	red	160		75										
455			frac(2)	3	red	160		65				veinlet, coarser than the above						
456												slowly acid reactive						
457	Daer 1	10634'4"	bedding	1	green	0		20				bedding, grainstone						
458			frac(1)	2	blue	314		80				high angle fracture		0.8mm, calcite				
459			frac(1)	3	blue	304		72				high angle fracture		0.2mm, calcite				
460			frac(1)	4	blue	300		60				high angle fracture		0.6mm, calcite				
461																		
462		10636'8"-10637	bedding	1	green	0		25				bedding, grainstone						
463			frac(1)	2	blue	272		10				low angle fracture		2mm, calcite				
464			slickenside	3	blue	318		31				slickenside surface		0.8mm, calcite				
465			lineation		brown	95-275						slickenside lineation						
466																		
467	Della 2	7219	bedding						270	domal, flanking W		not measured						
468		2cm	frac(1)	1	purple	0		40				assume to N		0.2mm				
469		below	frac (2)	2	yellow	340		85				meshwork		0.1mm				
470		the next	frac(3)	3	orange	227		65				fracture		0.1mm				
471		measurement	frac(4)	4	brown	168		80				veinlet		2mm				
472		7219	frac(1)	1	purple	0		50				assume to N						
473			frac (2)	2	yellow	120		85				fracture						
474			frac(3)	3	brown	163		70				fracture						
475																		
476		7117'5"	frac(1)	1	brown	0		40				fracture assumed to N		0.8mm, siderite				
477			frac (2)	2	brown	18		60				fracture		2mm, siderite				
478																		
479		7117'10"-7118'	frac(1)	1	brown	0		60				fracture assumed to N		1-5mm, calcite				
480			frac (2)	2	brown	24		55				fracture		0.3mm, siderite?				
481																		
482		7151	frac(1)	1	blue	0		80				dominated fracture assumed to N, breccia		> 2mm, calcite				
483			frac (2)	2	brown	39-219		90				almost vertical fracture		> 1mm, calcite				
484												below which, v. broad calcite veinlet (4cm)						
485												tut siderite filled fracture.						
486																		
487																		
488	Inammincka 4	6976	bedding	1	green	0		20										
489			frac(1)	2	blue	286		85										
490												0.6mm						
491	Jennet 1	c1, 5525'	bedding	1	green	0		65				bedding						
492			frac(1)	2	blue	90	67	65-70				high angle fracture		open, fine frac, predate slickenside?				
493			frac(2)	3	yellow	70		60				possibly equal blue		open, fine frac, predate slickenside?				
494		2" below	slickenside	4	orange	0		65				slickenside strike on the bedding surf.						
495			lineation	5	orange	10-190		65				slickenside lineation						
496																		
497		5232'2-7"										vuggy fractures						
498																		
499	Kalanna 1	8937'3"	bedding	1	green	0		70	315	W. flank of major		possible bedding, muds.		pyrite lam.	4			
500			frac(1)	2	blue	274		65		NE-SW Kal. Fault		fracture, subpara to 300° (blue)		calcite, 0.3mm				
501			frac(2)	3	orange	355		50		Coaxial P-Z dome/fault trap		fracture, displaced fra(1)		clay seam, v. fine, 0.08mm				
502																		
503	Kumbarie 1	5400'4"	bedding	1	green	0		60				bedding						
504			frac(1)	2	blue	356		78				high angle fracture		0.5mm, open, siderite "stitches"				
505			frac(2)	3	brown	200		33				fracture		0.2mm, transparent crystal, non- calcite, further by siderite				
506																		
507			frac(3)	4	orange	346		25				fracture, conjugate with frac(2)?		0.1mm, transparent crystal, non- calcite, further by siderite				
508			frac(4)	5								abundant, small, fine fractures, branched?						
509																		
510																		
511		5524'10"	bedding	1	green	0		70				bedding						
512			frac(1)	2	red	170		65				fracture		1.3mm, dolomite				
513			frac(2)	3	blue	200		35				fracture		0.6mm, ?				
514		5534	bedding	1	green	0		55				possible bedding between sst and shale.						
515			frac(1)	2	blue	33		30				fracture		2.1mm, ?				
516			frac(2)	3	blue	172		35				fine fracture, cut by the above		0.1mm				
517	Lowanna 1	9802'3"	bedding	1	green	0	53	50-55										
518			frac(1)	2	red	210		25				veinlet fill		2-3mm, calcite				
519			frac(2)	3	purple	240	57	55-58						0.1, calcite				
520			frac(3)	4	orange	120		60						.1-<1mm, calcite				
521		9801'3"	bedding	1	green	0		55										
522			frac(1)	2	purple	280		50										
523			frac(1)	3	purple	290		65				dominated fracture		calcite				
524			frac(1)	4	purple	284	80	75-90						calcite				
525			frac(2)	5	orange	230		70						calcite				
526			frac(3)	6	red	170		18				calcite and breccia zone		calcite				
527			frac(4)	7	purple	134		70				hairline, minor fault displacement						
528												? branch from frac(1)						
529	Meranji 2	10920	bedding	1	green	0		20				bedding						
530			fracture	2	black	245		85				open fracture						
531																		
532																		
533																		
534	Narcoonowie 1	6542'5"	bedding	1	green	0	43	42-45	330	NW flank of anticline		bedding, siltstone and shale						
535			fra(1)	2	blue	335	67	65-70				fracture	1	siderite or dolomite				
536			fra(2)	3	yellow	horizontal		0				fracture	after 1?	siderite or dolomite				
537			fra(3)	4	black	260		80				fracture	3	siderite or dolomite				
538	opposite side		frac(4)	5	brown	205		40				coarse frac, or vein	2	siderite or dolomite				
539			fra(1)		blue	30	67	65-70					1					
540			fra(3)		black	310		80					3					
541																		
542		6540	bedding	1	green	0		40	330			bedding, siltstone and shale						
543			fra(1)	2	blue	57		70				high angle fracture						
544			fra(2)	3	brown	150	43	45-50				? Conjugate, coarser fract.						
545			frac(3)	4	yellow	horizontal		0				horizontal fracture						
546																		
547		6543	bedding	1	green	0	43	40-50	330			bedding, siltstone and shale						

# Appendix 2

## Text files on CD









Well	Formation	core round?	depth (t) m	ft	depth (b) m	ft	Rec ft	?deviation	bedding dip angle	Sedi. structure	slickenside	stylolite	vein (1)	filled by	vein (2)	filled by	fractures (1)	filled?	fractures (2)	filled?	fractures (3)	filled?	chronology	fracture intensity	Comments	Structure (WCR)	WCR		
Beanbush 1	IRB	5	y	12126.0	3696.0	12138.0	3698.7	11.7		Laminated and cross-laminated siltstone, fine sandstone, minor red mudstone.														3 / 12	Open subvertical fracture at 12130'6", aperture: 0.1mm 80-85 degree				
Big Lake 52 > 12" than driller	Dulligari	2	y	9462.0	2884.0	9520.0	2901.7	428"		Thin-bedded, grey, siltstone and shale. Steeply dipping bedding below almost horizontally bedded Cooper conglomerate (Merrimella Fm).	para. bedding at 2892.5m 75dg		quartz vein	4mm, qtz			35 dg (1mm) displace 7mm	?	Siderite					qtz vein cut by siderite	high 10 / 7"	strongly fractured and sheared, slickenside 65-70. see plastics; dip: 50-55, siderite cemented veinlet (2.5mm) (fault displacement); liner (0.5mm) also displaced. Quartz vein (3mm) twisted at 9491', ? right-lateral. Fracture breccia.	domal anticline	Steeply dipping slate and quartzite with quartz veins.	
Bookabourdie 1 6237	Innam. Red	4	Y	9700.0	2956.6	9710.0	2959.6	6"	subhorizontal but deformed at 9705'6"-9706', slump or folding	light brown, grey, greenish siltstone/sst, below 9710'; cross lamination & bioturbation at 9706' some part calcite rich; above 9710': red ms							85-90" at 9707'	grey to white 40"	conjugate at 9702'6"	light grey			fractures in differer intervals, not possible to decide.	high, 5 1/1" or 1-2" not even fault zone?	fracturing and brecciation, slickenside, ? Fault zone. To fragile to measure. 85-90" at 9707 conjugate, 40 at 9702'6"	anticlinal dome striking NE. Basement uplifted along NW-trending Permian faults as compressional and wrench tectonics.	High angle fracture, NW-trending Permian faults as compressional and wrench tectonics.		
Brumby	Dulligari	4	y	7703.0	2347.9	7713.0	2350.9	10.0	3/02/2004 7703	Dark grey, thin-bedded, siltstone, with abundant spicules.	common bedding plane													5"	Fractures, 20 (5) - 30 (1)	drilled close to the crest of a broad anticline, trends NE	Banded siltstone (phyllite), low-grade metamorphic. Fracture planes at 50 dg structural dip: 30.		
Burke 1	Dulligari	7	y	8375.0	2552.7	8385.0	2555.7	10.0	2 3/4	Light grey siltstone, sandstone, slumping. ? weathered zone														3-5"	Weathered former sandstone to siltstone, shale. Patches of siderite within sericite shale, fractures. Fra(1): nearly horizontal to 20dg; Fra(2) 60 to 90.	Burke feature is closure adjacent to the Dulligari structure. Burkes 1 just off the crest of the Burke feature, which is part of a larger closure which forms the Dulligari-Burke feature.	Siltstone and shale, light grey, slightly fossiliferous (sponges? Spicules).		
Charo 1	Kalladeina	1	y	7309.0	2227.8	7319.0	2230.8	4.95		Oncolitic packstone, grainstone, thin beds, storm beds (thin).		abundant												nil no fractures	No fractures. Abundant stylolites, every 4-6cm. 5 dg bedding and emphasised by stylolite.	NW flank of the Patchawarra Trough. N-S elongated, low relief anticline, prevailing SE regional dip. A. fault in Cambrian sequence.	Massive limestone with minor siltstone Lithic fragments (<1cm) meta sandstone within limestone at 7313.8'		
Cherri 1	Dulligari	3	y	4581.0	1396.3	4596.0	1400.9	14.00	2 max.	Laminated mudstone / shale, marked by white (?) and pyrite, possible due to metamorphism (DiG). Very black, graphite or carbon. ? schist or slate	minor		75; 2mm	minor calcite ? Kaolinite			80-85; 0.2mm	pyrite	65; 0.2-3mm				?	Siderite	bedding (white) cut by 2, by coarser pyrite (parallel to bedding then by 3 (65).	almost across through all core vertically, but half horizontally across core (8cm) in diameter.	Possible bedding alignment possibly emphasised or pure due to metamorphism. at least two or three sets of fractures and veinlets.	locates flank of westerly culmination of N-S aligned small anticline, located also at the southern extremity of a magnetic and gravity high. Cycle skipping on sonic over 4569-79' indicates fracturing. Marked decrease in sonic travel time indicates considerable movement prior to the deposition of the Permian.	45 bedding, shale and minor siltstone; rare white siliceous vein approx. 80dg, micromicaceous, fissile, finely carbonaceous
Coonatie 1 1697	"Mudr. Sst"	8	Y	10395.0	3168.4	10405.0	3171.4		0-5°	light grey fine sst. with cross-bed, cross-lamina, rounded green shale pebbles; interbedded with dark greenish siltstone / shale.			at 10401': 2-4cm 80-85 dg	brownish breccia			85-90"	auth. Qtz, min. calcite	para. Bedding Fe- clay? 4mm	brownish Fe- clay? 4mm	60-65"	1mm-1cm brownish Fe+ clay	3 cut 2	not even 4 / 1" in fractured zone and vuggy moderate in other	some faint fractures: more or less parallel to bedding and also connect vertically, dish-structure like, not cross-cut whole core, 5-25" discontinuous. High angle cut by horizontal or low angle	North of GMI, a Permian downwarp, this low is bounded to the South by normal down to north faulting	numerous small faults & joints in core		
Daer 1	Kalladeina	1	y	10630.0	3240.0	10640.0	3243.1	8.00		nodular skeletal wackestone, thin bedded packstone, oncolitic grainstone, dolomitised														low to moderate 2 / 1' 1 / 1-2'	Bedding measured: 15, 20, 25, fractures: 10, 2mm, calcite filled; 75, calcite, 0.4mm second phase fracture, 80, calcite, fill, fract. 0.15mm; stopped below slickenside. High amplitude stylolites, > 25 dg. At 106377': 1cm calcite vein + catac. slickenside along surface, similar to thermal fluid. Stopped at slickenside.	The structure located on NW flank of Pat. Trough. NE -SW aligned folding with W.B. sequ. But extensive NW-NSE normal faulting on EW sides of structure. Changing of structural style. W of Daer structure, the western flank of the Patchawarra Trough trends N-E; to the east, the margin defined by an EW fault system 4km WSW of Coongie 1.	Bedded dolomitic limestone, intrasparite. The core to bedding angle averages 70 dg. Minor calcite veining. Most prominent set of calcite veins averages 60 dg to core axis. Calcite veinlets form stockworks at 106317"-106311" and 10630-10636'5". Also good porosity equivalent to Coongie 1, but water wet.		
Della 2	Dulligari	7	y	7212.0	2198.2	7222.0	2201.3	10.00	1 1/4 at 7212	weathered, slightly deformed rock, originally siltsh. no bedding; well fractured and brecciated partially.			1-3mm; 70-80 gauge up to 3mm	Fe? Siderite kaolinite			1, 25-35; 0.1-0.3mm	Fe, or siderite = lining vein 1	2 meshwork 80-90; 0.1mm irregular				Fe clay	Vein 1displace frac(1) which repli frac (2)	3-5mm : < 1cm wide	thoroughly fractured: weathered, altered 3 phases of fracture, vein, veinlet displaced frac 1-displac frac2. Weathered crust (Dr Luo, per. comm.) Filled by siderite or arkerite in this section.	Angular u/c with overlying Merrim. Fm at 7148'	low meta, fractures 40-50, filled by silica, pyrite, distinct parting at 40, bedding pos. 70.	
Della 4	Dulligari	6	y	7063.00	2152.8	7073.00	2155.9	4.50		relatively well-sorted sandstone (0.1-1mm), no bedding. A mud clast about 2cm long.							50-60 not regular	?	Siderite					30cm	Irregular fractures, siderite patches (2-3cm interv) at 7065', possible induced fracture, open to be filled by brownish clay, grey mud(drilling?)	near axis of N-E trending Della structure, north of Della 1 structurally equal to Della, higher than Della 2 and 3.			
Della 5A	Dulligari	4	y	6409.0	1953.5	6446.0	1964.7	37.00	3 1/2 above core interv.	light grey siltstone, but it is badly weathered and altered zone, fractured and brecciated. slightly foliated; common slickensides similar to Della 2, but more strongly deformed, more brecciation, broken core at bottom, u/c Cooper at top	abundant high angle 85-90 very polished lineation new mineral formed on curved surfa.						gauge, 2mm 25dg, lining + filling	Fe + trace dol. (reactive)	meshwork high angle +low angle connected breccias			Fe clay or siderite	5mm (length) < 1cm (width)	Weathered, altered zone, brecciation, slightly foliation: angular unconformity below horizontal ? Merrimella Fm. Veinlet cut meshwork (2), some shining surface has sericite a few low angle gauge	Crest of the Della structure, between productive Della 1, 2, and SW of Della 4. It is development well to test if gas was escaping from Della 5.	Dip horizontal at 6407', below it, badly broken core 4, mudstone breccia, high angle foliation slickensides. Minor crystalline fracture filling. Trace calcite on fractures.			
Dunoon 1 6047 > 7" driller	? Dulligari	1	Y	4987.0	1520.0	4997.0	1523.1		1 to 1+1/4	grey, mm to cm laminated siltstone and v. f. sst. 271 feet thick of W.B.													nil no fractures	No fractures at all.	58 km SSW of Moomba; on an E-W trending anticline located in SW of the Munterree Horst.	Metasandstone, grey green, very fine, well sorted, angularity, quartzitic, chloritic, v. hard, horizontal beds.			
Gurra 1	W. GP	2	y half	4684.0	1427.7	4686.0	1428.3	1.3	Max: 2 at TD	Phyllite, possibly originally shale and siltstone crenulation, vertical graphite alignment. Horizontal and vertical calcite veinlet, brecciation, formal shale, shining lineation.			0; upto 7mm	calcite			80-85; 1mm	calcite						5cm	Well-fractured, horizontal and vertical, filled by calcite.	SW margin of Cooper, small anticline -fracture and indurated WB succession, recovered low salinity water. Similar to Chern 1, with low grade dg of metamorphism	Core 1 phyllite shale, between 4529-4533'; numerous fractures from very fine to 1.5", filled by milky quartz, slightly vuggy. core 2, dip 20, core 1, 10-15 dg.		
Gidgealpa 4	Mooracoochie	9		7190.0	2191.5	7257.0	2211.9			tuffaceous sandstone, breccia of porphyritic latite? ignimbrite in core 11.														4-15 /1'	severely fractured, brecciated	Western flank of gentle NE-SW anticline, u/c on crest	tuff, green-yellowish. Small veins of apparently of carbonate in the upper section.		
		10		7402.0	2256.1	7494.0	2284.2	11.00																				tuff, varicoloured, with abundant green specks, unreliable traces of bedding, 15dg.	
		11		7773.0	2369.2	7703.0	2347.9	9.66																				tuff, varicoloured, buff-brown, sandy in places.	
Gidgealpa 8	Mooracoochie		y						3 3/4	tuff, fault breccia, still jig-saw fit. Warburton Basin top at about 7089'.															not even		Western flank of gentle NE-SW anticline, slightly higher than Gidgealpa 4. Volcanics with ? 20 dip angle.	tuff, extensive veining. Fractures with slickensides, dip over the upper nine feet is irregular within 20dg.	
		6		7079.0 7089 WB	2157.7	7145.0	2177.8	46.0																	1-5cm	highly fractured, brecciated.			
		7		7149.0	2179.0	7157.0	2181.5	8.0																	1-2cm /vert. 2-5cm / hor.	highly fractured, brecciated. highly fractured, brecciated.			
Gidgealpa 11	Mooracoochie	3		6852.0	2086.5	6885.0	2096.5	30.5		ignimbrite, tuff.															low	sparse fractures, due to ? Contractional	norther part of Gidgealpa structure.		
Jennet 1 7028	metasst, silt	1	y	5525.0	1684.0	5535.0	1687.1		1°	Coarse to fine porous sst with brownish ms layer, cross lamination at 5525-5526'. (phyllite WCR) most porous at cross-lamination portion.	many such as 5525 5528' (WCR).							3 / 1' vertically 3.4cm						brittle fracturing, some open, ? induced fractures at 5232'2"-5' slcenside at 5525'9", fracture displ. bedding.	crest of a domal anticline developed upon a major NE-SW trending horst block plunging basinward towards the NE. Pre-2, high angle fault along its NW & SE displacement along NW more significant	Steeply dipping metasandstone, minor metasilstone. Common fracturing, nil visual porosity, no shows. Slickensides, phyllite at 5525'6".			
Kalamna 1	Dulligari	1		8933.0	2722.8	8943.0	2725.8		4° 8930'	dark grey to black mudstone, bedding unrecognisable, because of folding. Some sandy layers sheared in between mudstone, e.g. at 8940'.	N		40-50" 1-3mm	calcite			70"	calcite	20, 30" ? Para bedding	calcite					high 2-5 cm or 2 / 1"	Possible fault plane (40-50") subparallel intersecting and anastomosing faults that cut the scarp into a number of wedge slices of varying throw.	At 2, NE-SW Kalamna fault zone is defined by a series of subparallel intersecting and anastomosing faults that cut the scarp into a number of wedge slices of varying throw.	silt, sst, fractures filled by calcitic brecciated;	
Innamincka 4	IRB	1	y	6976.0	2126.3	6986.0	2129.3	7.50	1 3/4	Green to red siltstone, mudstone, v.f. sst. thin beds, flat pebbles of rip-up greeb shale clasts. minor x-lamination. Skolithos.			6976' - 5" see measured	calcite	6977'9" fracture	not calcite ?	6982'1-8", 2 frac 1. 0.1mm; 2. 0.6mm	calcite	6976'-3": 80 0.6mm	calcite	6981'6"-6983'	calcite	low	6978'2"-6978'8"-9" fracture filled by calcite.	on the upthrown side of the basement fault, Patchawarra Fm pinched out at the flanks.	Interbedded sandstone and siltstone.			
																													Vertical fracture with quartz infill at 5981 to 5982. no obvious bedding dip.
Kumbarie 1	? Dulligari	2								weathered, light grey mudstone, whole core broken															1-2cm, hor/ver. or > 10 / 1'	N-E trending antinical accumulation, on a N-S trending ridge.	N-E trending antinical accumulation, on a N-S trending ridge.	Light grey sandstone, siltstone with shary lustre very siliceous with common slickensides highly fractured with healed fractures, cleavage planes, shale with minor siltstone. Fractures healed partly by white anhydrite or gypsum. Siltstone band: 70-80 dg dip.	
		3	y	5376.0		5392.0		7.9		dark siltstone and shale, 5526' has sandstone layer.															2-3cm				
Lowanna 1	Dulligari	1	y	9800.0	2987.0	9803.0	2988.0	2 7"	3 1/2 at 9800'	Green-grey siltstone, shale, laminæ. cm laminated very fine sandstone, shale.															1-2cm	Well fractured, filled by calcite. 0.1mm-4mm at bottom. Dip: 50-65? Measured, see plastics.	N margin of the Allunga Trough, SE of Big Lake trend. Dormal form is caused by prominent NE-SW folds extending SW from Della-Nagapacoonjee trends with less prominent - folds oriented NW-SE. The Permian and Mesozoic Fms are simply draped over the underlying Pre-Permian bed, with minor crestal thinning.	Very small flame structure.	
Logger > driller 16'																									3 / 10' low	high angle open fractures, aperture 0.15mm	metasandstone and metasilstone.		
Meranj 2	IRB	1	y	10912.0		10922.0				x-laminated fine sandstone, siltstone and minor red shale.															nil		NE-SW anticline, southern flank of this structure.	Red shale, ss/b-fissile, silty, slightly micaceous. Red sandstone, very siliceous. Dip: 10.	
Merrimella 5 ENV 1525	Innamincka	5	y	8969.0	2733.8	8989.0	2739.8	20.00	4 1/2	Red mudstone and minor fine-grained sandstone, siltstone, x-lamination, slump, nodular structures. Faint bioturbation																		Sandstone with shale clasts; laminated siltstone. Shale clasts generally angular, smooth texture, fissile, commonly aligned parallel to bedding.	
Minkie 1 8 > driller	Innamincka	1	y	7840.0	2399.6	7847.0	2391.8	7.00	3	Light grey x-laminated fine-grained sandstone, with green shale pebbles, siderite nodules and patches.															3 / 7"	No obvious fractures.	NE of Merrimella structure (NE trending uplifted horst block. Located in the Merrimella North high, irregular and plays east from normal NE trend. 2" seismic mapping, basement has been faulted by major NE trending faults on the sides of Merrimella High, throws up to 900'. Reactivation bounding faults in Pre-Toolachee caused uplift, erosion Permian in crest.		
												40-50"														3 fractures and a meshwork.			
Moomba 3	?	8	slab	9506.0	2897.4	9508.0	2898.0	2.0	No data	Green, ? hornfel, pyrite-rich.																a few fractures	5.6km NNW of Moomba 2, correlated with Moomba 2. Moomba structure, it 119' lower than Moomba 1.	x-ray core shows 18dg, fractures 20-30dg; pyrite fill. Sandstone, siltstone, shale.	
Moomba South 1 5487	?	2	y	9858.0	3004.7	9876.5	3010.4	17.80	3 1/2	massive metasst, siltstone, ? hornfel. Bedding not recognisable, well fracture but irregular network. dk brown to grey. Contact with granite?															1-10 mm	a few horzional fractures filled by brown (?) clay.	to the south of the Moomba structure, a broad, low relief composite antinical structure with subsidiary culminations at the P' horizon. The Moomba South prospect is a NE-SW trending elongate dome.	Meta sst, siltstone, sst.	
Mudrangie 1 1577	"Mudr. Sst"	11	Y	10455.0	3166.7	10452.0	3185.8		40-60°	light grey, medium to fine, well sorted quartzite, lamination, greenish muddy siltstone and mud. Greenish pebbles of shale or mudstone are lined up along the bedding plane of quartzite, some visible fragments of black ? lithics along the bedding of the sst.			45-50" at 10450; 5mm	brownish ?			50-52°	brownish ? Fe clay	50-60°	brownish ? Fe clay	90°	brownish ? Fe clay	1 and 2 cut by 3 in some core not st	high > 4 1/1"	severely fractured, brecciated, thick vein filled by breccia and brownish ? Fe rich clay.	northern (downthrown) side of the fault of Merrimella stru southmost of 3 en echelon structures, trending NE-SW.	Bedding: 40° southmost of 3 en echelon structures, trending NE-SW.		
Murterree A1 2156	? Kalladeina	2	2/3 top 1/3 missing	5155.0	1571.2	5165.0	1574.3		1/4° 5051'	amygdalites in basalt, brecciation called original basalt in water, displaced by later (frac(1)).							50c seems cut f(2)	brownish, ?		60.0					f(1) cut f(2)	1 cm or 8 / 1"	Numerous fractures, series of displacement surfaces. fine fractures, several phases (> 2). Fill of amygdale & veinlets are white silica and ? carbonate and ? Kaolinite	large antinical feature.	andesite, 70-75" fracture planes abundant rare bedding 30-35" suggesting a tuffaceous nature in part.
Murterree C1 2186	Dulligari "altered"	2	2/3 missing outside	7427.0	2263.7	7437.0	2266.8		3-1/4° at 7344'	Light grey, siltstone and mudstone, cm's layering. ? = bedding, 60"; because of alteration, hard to decide.	6x4cm".		breccia of mother rock & qtz (vein qtz?) = brownish clay.				80°	brownish	20°		60° = slickenside				need work out	1cm or > 10 1/1"	Down thrown side of SW-NE trending fault, forming N flank of the horst.	Low grade metamorphic (phyllite). Occasional thin layers of quartz pebbles up to two inches delineating bedding at approx. 70°	
																													Fracture planes frequent at approximately 70°, along bedding and at 80° opposite to bedding planes. Dental andesite highly fractured, metasilstone or phyllite.
McKinlay 1	Dulligari	3	Y	5130.0	1563.6	5140.0	1566.7		1°	Dark grey to black siltstone/shale, mm's lamination (brecciation / veinlet), pyrite lamination and nodules (1x5cm) along bedding.			50-55 (6), 1-5mm branches of 1-20 "				fine, 2-20" (6) 40" (1)	calcite or kaolinite						2 1/1" not even	microfaulting & veining of at least two phases of filling, brown ? dolo or siderite, calcite or kaolinite.	subsidiary structure on the larger Murterree Horst.	Prominent NE-SW trending Horst flanked by major faults. Basement structure is one of a network of faults. Domed anticline of McKinlay. Phylitic metasilstone, foliation, possibly represent bedding.		
Narcoonoowie 1 Env 4 > driller	? Dulligari	2	Y	6540.0	1993.4	6550.0	1996.4		N/R not recorded	grey, dark grey mudstone, shale, siltstone from 6545' downwards; light grey, medium to coarse sandstone with slumps, thin interbeds of mudstone and siltstone.			brown: 40-70°	dolomite			blue: 65-70°	dolomite	yellow: horizon? asso. stylolite	black: fine: 80° to vertical	?			fra (blue) by fra (brown) by fra (fine, ?black).	2cm or less	bedding: 45°, fra (blue): 70°; fra (brown): 40-70°, two direction; (yellow): nearly horizontal and associated with stylolites; fra (black)	NE-SW trending anticline, fault bounded on the NW flank. Narcoonoowie 1 was drilled on the apex of 60 to core, 45 to core, filled by thin quartz veins. structure or very close to the highest closing contour.	Dark grey phylitic siltstone, dip: 45 to core. Fractures: 65-65' and downwards; metasst. V fine veins of pyrite and quartz filled thin fractures.	
		1	y	6106.0	1861.1	6116.0	1864.2		N/R 2.5 above 6000'	6112 & below: pale grey to creamy claystone, brecciated, patches of siderite after silica. ? Burrowed at 6112'E at 6112' 10" contact with Permian conglomerate ? Merrimella Fm, with reworked angular these claystones or other.																			



Well	mean strike azimuths				range	frequency
Malgoona 4	18	60	110	150	18-30	10
Gidgealpa 1			107	149	46-74	12
Snake Hole 1			104		102-120	11
Gidgealpa 2			120	150	140-156	12
Gidgealpa 3	26	74	120		total: 45	
Gidgealpa 5	21	63				
Gidgealpa 7	25	59		150		
Merrimelia 6				147		
Merrimelia 7	26					
Mudrangie 1	30	60		150		
Wantana 1			115			
Packsaddle 3	21	64		150		
Innamincka 1				150		
Boxwood 1		50	102			
Lycosa 1	20	63	110	140		
Yulcumma 1		72				
Moomba 2	20					
Moomba 73		57				
Della 1			112	141		
Dullingari 1			117	144		
Murteree 1	21			156		
Munkarie 1		68				
Pelketa 1		46	108			
sum	228		1225	1777		
aver.	22	61	114	148		
min	18	46	102	140		
max	30	74	135	156		

